THE GEOCHEMISTRY, PETROLOGY, AND PROVENANCE OF THE PINAL SCHIST

By

John P. De Melas

Submitted in Partial Fulfillment
of the requirements for the Degree of
Master of Science in Geology

New Mexico Institute of Mining and Technology
Socorro, New Mexico
May 1983

ABSTRACT

The Pinal Schist is a supracrustal assemblage of metasedimentary and meta-igneous rocks of middle-Proterozoic age occurring in southeastern Arizona. The age of the schist is approximately 1700 my, and it is the oldest know unit in this area. The study area is located west of Globe, within the area of the Pinal Ranch quadrangle.

Original sedimentary characteristics are preserved including graded beds; erosional contacts; relict crossbedding; and relict grains of quartz, feldspar, lithic fragments, tourmaline, zircon, and epidote.

The Pinal Schist can be divided into four lithologic types that occur in the study area. These include meta-sedimentary schist, phyllite, and quartzite; and tonalite. The schists occur as massive or graded beds; the phyllites are massive or interbedded with the graded schists; the quartzites are lenticular beds of massive or graded pebble to medium-sized sand; and the tonalite occurs as a concordant sill having a deformational style similar to the surrounding meta-sedimentary schist. Intergradation of the meta-sedimentary schists is common.

Petrographic analysis of the meta-sedimentary schists suggests two primary sediment sources: felsic plutonic (granitic) and felsic volcanic (rhyolitic?). Modal analysis of the meta-sedimentary schists indicates they are quartz wacke, arkosic wacke, lithic graywacke, and pelite. Tectonic provenance is continental craton and/or recycled-uplift.

Chemical analyses of the Pinal Schist sediments indicate they are immature clastic sediments similar to arkose, sub-arkose, or sub-graywacke. Sediment source composition is similar to granite, quartz monzonite, and granodiorite. Minor mafic sediment input is also possible. Mixing ratios of sediment types are from 20 to 60 % orthoquartzite, 40 to 80 % granite, and up to 10 % percent mafic rock.

Tectonic environment indicated is passive or rifted continental margin. A tectonic interpretation of the Pinal Schist can be accommodated by either continental rift or back-arc basin models. In either case a continental margin must be established in order to deposit the sediments as wackes by turbidity currents, grain-flow, traction, and pelagic sedimentation.

ACKNOWLEDGMENTS

I would like to acknowledge the following persons. Dr. Kent C. Condie offered suggestions and criticisms, helped in the field, and assisted with petrographic and geochemical studies. The Head Ranger at Tonto National Forest made facilities available at the ranger station. Phillip Allen instructed the author in the use of the NAA facilities at Tech and assisted in preparation and analysis of samples. K. B. Farris instructed the author in and assisted in preparation and analysis of samples by XRF. Dr. Antonius J. Budding assisted in petrographic analysis. Dr. James Robertson provided photomicrographic facilities. Dr. David Johnson advised the author on the use of sedimentary classification schemes and also provided photomicrographic facilities. Terry Jensen advised in selection and repair of my field vehicle. Stephen Blodgett of the New Mexico Bur. of Mines helped with editing. I would particularly like to thank my parents; without their help and encouragement this project would never have been attempted.

This research was supported in part by National Science Foundation grant number EAR - 7918911, by teaching and research assistantships from NMIMT, and by a New Mexico State Guaranteed Loan.

TABLE OF CONTENTS

LIST OF TABLES

LIST OF FIGURES

LIST OF PLATES

INTRODUCTION

The origin and tectonic history of Precambrian rocks in the southwestern United States is a subject of current interest (Condie, 1982a; Condie and Budding, 1979; Silver, et al.,1977; McLemore, 1980; Livingston and Damon, 1967; Lanphere, 1967; Damon, et al., 1962; Livingston, 1969; Silver, 1978; Schmidt, 1967; Peterson, 1961, 1963; Brown, et al., 1979). Most rocks of Proterozoic age in the Southwest are metamorphosed to greenschist grade, or higher, making interpretation of the origins of these rocks difficult. Exposure of sedimentary rocks of Proterozoic age, and relatively low metamorphic grade provides the opportunity for investigation into the Proterozoic history of the southwest.

The Pinal Schist is one of the oldest rock sequences in southeastern Arizona. Understanding the origin and conditions of formation of the Pinal Schist can lead to some useful deductions about the rocks from which the schist was derived, the regional paleogeography and tectonic setting of southeast Arizona in the mid-Proterozoic, and, possibly, the tectonic history of the southwestern U.S.

Purpose

The purpose of this study is to evaluate the geologic and tectonic significance of the Pinal Schist which occurs in the Pinal Ranch 7 1/2' quadrangle near Globe, Arizona.

Field, petrographic, and geochemical methods were used in the study. Gross effects and extent of metamorphism and deformation in the schist are described. Sedimentary features preserved in the schist, and geochemical characteristics of the Pinal Schist are described and compared to those of modern sediments. Igneous bodies within the schist are noted and described.

Precambrian rocks of Arizona

Precambrian rocks exposed in Arizona include the middle Proterozoic Pinal Schist in south-central and southeastern Arizona, the middle proterozoic Yavapai Series in the central part of the state, the later Proterozoic Apache Group and Grand Canyon Series that overlies both the Pinal and Yavapai (Figure 1). Relict sedimentary textures in the Pinal Schist suggest that it is composed chiefly, if not entirely, of metamorphosed clastic sedimentary rocks. The Pinal Schist and Yavapai Series appear to be of equivalent age (Livingston and Damon, 1968, Lanphere, 1968), but stratigraphic correlation between them has not been established (Lanphere, 1967). The Pinal Schist is included in the 1650 - 1730 m.y. crustal-age province (Condie, 1982b).

Location

The Pinal Ranch 7 1/2' quadrangle (Figure 2) is located in the southeast part of central Arizona, about 25 miles west of Globe, and 15 miles south of Miami. Approximate boundaries of the quadrangle are latitudes 33 degrees 15' - 33 degrees 22' 30" N and longitude 110 degrees 52' 30" - 111 degrees W. Samples were collected from 130 locations (overlay, Figure 2). A part of the study area is on land under the jurisdiction of the Tonto National Forest. Access to the area is by dirt roads from the north, northeast, east, and the south.

Methods

Methods used in this study include field examination of primary sedimentary structures, laboratory analyses of chemical characteristics of rock samples, petrographic analyses of thin sections, and modal analyses of detrital-framework grains in thin section. The exact techniques used are discussed in detail in the Appendices.

Previous work

The Pinal Ranch 7 1/2-minute quadrangle was originaly mapped as part of the Globe 15-minute quadrangle by the U. S. Geological Survey in 1901.

The Pinal Schist was first described by F. L. Ransome (1903, 1904, 1919) in the Globe area. He recognized the sedimentary and igneous origins of the rocks, and described the petrography, and field relations. Ransome (1919) concluded that the Pinal Schist is at least in part a series of meta-sediments that includes sandstones and pelites. He also recognized one metarhyolite in the schist near Granite Peak (Ransome, 1919).

As part of a comprehensive study of the Globe-Miami mining district, the geology of the Pinal Ranch quadrangle was mapped on a scale of 1:12,000 by Peterson (1954, 1963). He described the general geology of the area, with emphasis on economic geology. His geologic map is used in this study as the basic geologic reference map.

Geology of the Pinal Schist

The name "Pinal Schist" has also been used to describe similar rock sequences in southeastern Arizona, as far west as Ray, Arizona (Ransome, 1919), and as far south as the Johnny Lyon Hills and Little Dragoon Mountains (Silver, 1978). Current usage (Peterson, 1963; Schmidt, 1967; Silver, 1978) refers to the schist at Pinal Ranch as the type section of the Pinal Schist, althougn Ransome (1903, 1904, 1919) did not in fact describe a type section there. Lithology, appearance, description, and relative proportions of the rock units within the schist are variable. In some locations, contact metamorphism has progressed to such a

degree that it is impossible to ascertain the original rock.

Regionally, the Pinal Schist is dominanted by immature clastic sedimentary rocks with subordinate mafic to felsic volcanic flows and shallow intrusives. Quartzites are locally present, but are volumetrically insignificant. Carbonates are conspicuous by their absence. Well preserved sedimentary sections are characterized by turbidite textures and structures, suggesting deep-water accumulation. The regional extent and thickness (in excess of 6 km) of the Pinal Schist suggest deposition in a major geosyncline of regional extent (Cooper and Silver, 1954).

The Pinal Schist is part of a geosynclinal and magmatic arc, 1610 - 1700 m. y. old, in southern Arizona and southern and central New Mexico (Silver, et al., 1977).

The Pinal Schist appears to be the basement upon which all younger rocks rest, or into which younger rocks are intruded. Livingston and Damon (1968) speculate on the existence of an older gneiss upon which the Pinal Schist rests; however, as yet no evidence supporting the existence of this hypothetical basement exists.

Local Geology

Pinal Schist occurs as a series of schists, phyllites, and quartzites. Compositional layering of the rock is well defined, with steep dips from 40 to 90 degrees N 50 to 35 West, striking N 40 to 55 E. There is approximately 20

square miles of outcrop.

Madera Diorite (Precambrian) intrudes the Pinal Schist on the East. The schist is metamorphosed to hornfels near the Madera Diorite. Younger Precambrian conglomerates of the Apache group and Quaternary Gila copnglomerate overlie the Pinal Schist on the south. The schist is intruded by a series of Cretaceous or Tertiary dike-like diabase intrusions that become prominent toward the south. To the north, Schultze Granite (Cretaceous) intrudes the Schist, on the west the schist is in contact with a welded dacite tuff of Tertiary age. The tuff overlies, and is in fault contact with the schist. A number of small felsic dikes and sills of Tertiary age intrude the schist in scattered locations. Felsic sills at the southern end of the area are intrusive into the Pinal Schist and are defined as part of the schist.

Geochronology

Livingston (1969) used the Rb-Sr, whole-rock, and K-Ar mineral isochron dating methods to date the earliest intrusion of Madera Diorite into the Pinal Schist at 1693 +/- 30 m.y.; a second intrusive and/or metamorphic event occurred at 1507 +/- 50 m.y., and a third event reset the fine-grained micas of the Pinal Schist at 1365 m.y. Livingston's isochrons appear to be accurate. Dates used in this report were recalculated from Livingston's data using the 87Rb decay constant from Steiger and Jager, 1977). Livingston's date of 1356 m.y. for a sample of Pinal Schist

from just southeast of the Pinal Ranch Quadrangle is considerably younger than the age of the Madera Diorite. Livingston (1969) attributes this age discrepancy to the event that reset the micas approximately 1370 m.y. ago, which he relates to the emplacement of the Ruin Granite. Silver (1968) dated the Ruin Granite to be from 1430 to 1460 m.y. by using the U-Pb isotopic dating technique on zircons from the granite.

A rhyolite included in the Pinal Schist of the Tortilla Mountains by Ransome (1919) and dated by Livingston (1969) using the K-Ar method indicates an age of 1615 +/- 100 m.y. This age may suggest that the Pinal Schist contains material both older and younger than the Madera Diorite (Livingston, 1969).

FIELD REPORT

Pinal Schist

The Pinal Schist in the Globe-Miami district is primarily a sequence of phyllites, schists, and quartzites with rare volcanic or hypabyssal felsic members. The phyllites are dominantly blue-gray to gray-green with a shiny luster. The schists range in color from gray-green through blue-gray to white, with a sandy appearence due to their high content of clear to cloudy-blue clasts of rounded sand-sized quartz. The schists and phyllites often show color banding, textural layering, mineral laminations, and size-grading of quartz clasts. The quartzites are gray to white in color and are coarse-sand to pebble sized quartz with scattered pink, white, and black grains of chert and lithics. The quartzites also show grading.

Compositional layering

The Pinal Schist shows well-defined compositional layering of the rock types mentioned. The prevailing strike of the compositional layering parallels the major foliation of the Pinal Schist: dip 50 - 70 NW, strike N. 30 - 60 E.

Compositional layering is inferred to represent original sedimentary bedding because of the continuous nature of the layering and the existence of sedimentary structures within the layers.

Weathering

Weathering is most pronounced in the more mica rich phyllites and coarse-grained quartzites, while fine-grained, quartz-rich units are more resistant. The less porous nature of the fine-grained schists may make them less subject to the action of meteoric water.

Outcrops

Peterson (1961) found Pinal Schist "outcrops...not sufficiently characteristic to permit correlation from one outcrop to another." I concur with this, but feel that small-scale mapping may be able to provide correlation in future studies. Outcrops are discontinuous and there are no distinctive marker horizons.

The best outcrops of the Pinal Schist occur in the steep gulches that characterize the topography. Freshest samples and the most continuous outcrops are found in these areas. Orientation of Mead and Pinto Creek Canyons approximately perpendicular to strike in the northern section made it simple to sample across strike in that area.

Primary sedimentary textures

Primary sedimentary textures noted include graded bedding, erosional contacts of beds, possible trough-set crossbedding, and cyclic bedding expressed in turbidite-style bedding cycles, i. e. Bouma cycles (Bouma,

1962). The appearance of bedding is parallel and continuous, but some beds, particularly coarse-grained quartzites, pinch out.

Sedimentary indicators of stratigraphic "up" direction are recorded because their occurrence can be used to define areas that show a consistent stratigraphic "up" direction. This allows definition of areas representing outcrops of opposing fold limbs. Indicators used in order of assumed dependability are: Bouma cycles, graded bedding, (i. e. fining-upward sequences), and erosional contacts defining the tops and bottoms of beds. In most cases, suspected turbidite sequences contain one or more graded beds. Occasional beds show grading that is either reverse grading or overturned normal grading.

Metamorphic deformation

Deformation of the schist is characterized by small-scale (mm to m) similar folding, isolated small-scale (cm to m) isoclinal folds, and possible large scale (km) isoclinal folding. Minor boudinage of competent layers, and elongation of clastic grains form a lineation at an angle to original bedding. There is strong cleavage parallel to foliation. Local deformation, folding, and contact metamorphism occur near contacts with the intrusive bodies to the north, east, and south, and along the fault contact with Tertiary dacite tuff on the west.

Primary foliation is defined by compositional layering, which is inferred to represent original sedimentary bedding. Metamorphic deformation has superimposed a strong secondary foliation parallel to sedimentary bedding. In addition, a third intermittent foliation is seen at an angle to compositional layering that often strongly resembles sedimentary crossbedding. This third foliation is 30-45 degrees more steeply inclined toward the northwest than the secondary foliation but has the same strike. The third foliation is defined by platy minerals, is limited to fine-grained sediments, and is most pronounced in the more highly deformed rocks at the extreme northern exposure of the schist. Considering the limited occurrence of the foliation, a metamorphic origin rather than a relict sedimentary texture is indicated.

Occasional lineation is visible in coarse-grained layers. This lineation shows as elongated clastic grains and usually occurs at an angle to primary bedding, with dips 50 - 80 degrees toward N. 30 - 50 W. At times the lineation is suggestive of relict sedimentary features such as imbrication and crossbedding.

Local deformation has caused some small scale boudinage of more competent layers, but boudinage is not extensive and does not appear to effect large-scale changes.

An important question that this study attempts to address is the nature, extent, and evidence of isoclinal folding within the Pinal Schist. In lieu of a detailed structural study of the area, sedimentary indicators of stratigraphic "up" directions are used to determine the extent of isoclinal folding in the area.

Observations of sedimentary indicators lead to the following deductions concerning isoclinal folding of the schist. At least five fairly well-defined reversals of stratigraphic up-section indicators occur from northwest to southeast, i. e. across strike between NW and SE. These reversals define the approximate outcrops of the limbs of possible folds. Bedding is parallel across these planes, which indicates that if the regions of reversal are the limbs of folds then the folds must be isoclinal. Axial planes of the folds dip parallel or sub-parallel to the bedding of the schist. Minor folds support this interpretation, indicating that the fold axes may plunge 40 degrees N 60 E. with axial planes parallel to bedding. Small scale folds, stratigraphic up indicators, and locations of hypothetical fold axial planes are shown on the sample location map, (overlay, Figure 2).

Large scale isoclinal folding probably has taken place. presence of both proximal- and distal- turbidite facies indicates tectonic foreshortening like that produced by isoclinal folding. Evidence of small scale vergence that

could corroborate the existence of large scale isoclinal folding is not definitive.

Lack of evidence for transposition of bedding on microscopic, hand-sample, and outcrop scales indicates that this phenomena has not occurred on a larger regional scale. However, transposition of bedding is frequently associated with isoclinal folding, and as explained above, evidence of sedimentary indicators shows that the Pinal Schist has probably been isoclinally folded.

Faulting

Faults in the area have been mapped by Peterson (1963). Peterson concentrated his efforts on areas that were already under development as mines and prospects. I noted one fault that shows evidence of major displacement after the emplacement of the Madera Diorite. Fault breccia within this fault contains fragments of the younger Madera Diorite, which at this location is about one mile to the east. This fault is shown on the sample location map, (overlay, Figure 2). Movement appears parallel to compositional layering on the fault, because it does not cross-cut the compositional layering.

Alteration and mineralization

Hydrothermal fluids percolating along faults and near intrusions have caused local alteration and mineralization. Mineralization is primarily secondary copper (malachite, azurite, etc.). Silver and gold have been reported from the Red Rock mine, and the Samsel mine has produced small amounts of tungsten as wolframite. The Cole-Goodwin mine has produced significant amounts of copper. Peterson (1963) covers the history and mineralogy of this mine and other mines in the area.

LITHOLOGY

META-SEDIMENTARY ROCKS

Three basic categories of meta-sedimentary rock types can be distinguished in the field. The most common is chlorite/biotite-sericite-quartz schist that has fine to coarse (0.6mm to 4mm) clasts of quartz sand surrounded by a fine-grained matrix of sericite and chlorite. The next most common is chlorite-biotite-quartz-sericite phyllite in which sand fragments are rare and all other clastic fragments are less than sand sized (< 0.0625mm). The third and least common category is quartzite. Quartzite is rich in quartz, feldspar, and lithic clasts; grain size is medium sand to pebble (2.0 mm to 6.0mm in circular cross section).

Biotite (or Chlorite)-Sericite-Quartz Schist

Field description

The typical chlorite/biotite-sericite-quartz schist is tan to gray-green or pale gray. It is massive to friable, breaks into angular chunks, and has fine to coarse quartz sand grains surrounded by a fine-grained matrix of sericite, quartz, and chlorite and/or biotite. Graded beds are common in the schist, as are ungraded beds of uniform grain size. Elongated grains rarely define a lineation that gives the rock the appearance of sedimentary imbrication or crossbedding. The apparent imbrication could represent relict crossbedding. Rarely, apparent trough-set crossbedding

is observed; however, this "crossbedding" appears to be a metamorphic structure.

Graded bedding occurs in the schist as a well-defined decrease in sand size within layers. Graded schists are commonly succeeded by fine grain pelitic layers; these form lithologic couplets that include a coarser grained lower portion and a finer grained or pelitic upper portion. Grading represents a primary sedimentary texture. Beds grade from coarse to fine sand and from fine sand to silt, with variations between these extremes.

Classification of the schists using a sedimentary rock scheme after Pettijohn, et al. (1973) (Figure 3), shows a range from lithic graywackes and quartz wackes to pelites. The schists occur in well-defined, continuous beds that are 0.1 to 0.5 m thick. Beds can be traced as far as individual outcrops (m to 100m) and rarely show lateral pinching.

Petrographic description

Bimodal grain size and poor sorting are characteristic of this rock type, with detrital clasts averaging 0.4 to 1.25 mm in a supporting matrix of 0.01 mm average size (Plates 1 and 2). Nearly all clasts are quartz. Quartz clasts are monocrystalline and polycrystalline, blocky to lenticular, sub-angular to sub-rounded, sub-spherical to elliptical, and often show recrystallized margins, this is evidence that quartz clasts are of clastic detrital origin.

Most quartz grains show elongation parallel to the primary and secondary foliation, and undulose extinction. Some clastic grains are fractured into smaller fragments, that show optical continuity. Pressure fringes of quartz, sericite, and chlorite and/or biotite occur (flaser) and give the appearance of micro-augen texture. Ransome (1919) referred to these as "quartz eyes". Matrix is fine granoblastic quartz mixed with tabular idioblastic sericite, biotite and/or chlorite, opaques, epidote and granoblastic feldspar. Sericite is idioblastic, tabular, and colorless. Biotite is idioblastic, tabular, and pleochroic pale tan to pale brown. Chlorite is pleochroic pale-green to apple-green, is idioblastic, and tabular; it also occurs in vermicular habit characteristic of hydrothermal origin, (Blatt, et al., 1972).

Opaque minerals occur as equant porphyroblasts and clasts and in the matrix; they appear to be pyrite, magnetite, ilmenite, and hematite. In some cases, these opaques are associated with chlorite, epidote, and calcite.

Tourmaline that occurs mostly in the matrix and also as porphyroblasts is prismatic to blocky, pleochroic, poikiloblastic, and commonly zoned. Tourmaline crystals occasionally show orientation parallel to the primary foliation of the schist. In some cases, tourmaline exhibits evidence of metamorphic overgrowth on detrital grains (Plates 3 and 4). The persistence of detrital tourmaline in

the metamorphic environment has been documented (Henry, 1983). Overgrowth on the brown detrital core has added blue-green to olive green poikilitic tourmaline. Metamorphic source for the spherical core is indicated by its brown color (Deer, et al., 1966). Metasomatic origin for the overgrowth is indicated by the blue to green color and poikilitic texture (Deer, et al., 1966).

Zircon, which is usually slightly larger than the matrix (up to 0.1 mm across), is blocky to equant and zoned. Crystals frequently show rounding of crystal outlines indicating detrital origin. Zircon is dark brown, pale brown, or colorless. The brown color appears to be the result of radiation damage, (Deer, et al., 1966). Zircon shows no other evidence to indicate that it is metamict.

Apatite occurs in the matrix as colorless granoblastic grains. No particular origin for apatite is preferred.

Garnet, up to 0.05 mm across, is colorless, isotropic, equant to blocky, xenoblastic, and shows metamorphic overgrowths (Plate 5). Overgrowth occurs on rounded silt sized cores that appear to have detrital origin.

Epidote is common as sub-spherical to blocky, idioblastic grains, up to 0.5 mm across, associated with clots of chlorite, calcite, and opaque minerals. It also occurs as xenoblastic porphyroblasts up to 1.0 mm across. Epidote ranges from colorless to pale-green to brown-green.

Both metamorphic and detrital origins for epidote are indicated. The majority of epidote is of the idioblastic type and is approximately equivalent in size to the matrix. This epidote appears to be metamorphic and is colorless to pale-green. Rare xenoblastic grains of epidote, which are pale-green and larger than the matrix, may be of detrital origin. There is minor development of snowball-epidote.

Calcite occurs as micro-viens in pressure fractures, in the matrix, and as an alteration product of detrital plagioclase grains.

Plagioclase and potassium feldspar (Plates 2 and 6) occur as detrital clasts up to medium-sand size. Feldspar grains often show excellent development of micrographitic and myrmeckitic textures (Plate 2). Most feldspars are poikiloblastic, probably due to alteration of the crystals rather than metamorphic regrowth. Feldspar grains appear to be rounded to subrounded, which is indicative of detrital origin. All detrital feldspars are highly altered and show sericitization and recrystallization. Most show patches of water-clear metamorphic albite.

Ransome (1919) made note of rutile and fibrolite in a sample of Pinal Schist from 2 miles northwest of Pinal Peak and within a few hundred (sic) feet of Madera diorite.

Biotite (or Chlorite)-Quartz-Sericite Phyllite

Field description

The typical chlorite-biotite-quartz-sericite phyllite is blue-gray to pale gray-green. The phyllite is fissile and cleaves into flattened fragments having pronounced shimmer on cleavage faces. Phyllite occurs as laminated layers of fine-grained material in which infrequent fine-sand-sized clasts occur (Plate 7). Grading is occasionally observed. Using the Pettijohn, et al., (1973) sedimentary classification scheme (Figure 3), the phyllites classify as pelite. Phyllite frequently occurs interbedded with sandy schists, invariably on the fine side of grading. Phyllite also occurs as isolated thin beds on top of graded layers of coarser grained schists and quartzites.

Bedding in the massive phyllites is difficult to identify due to metamorphic deformation. Beds are not always distinct, and often grade into one another without well defined boundaries. Compositional layering that may represent original sedimentary bedding is often indistinct. Layers of massive phyllite are up to 10m in thickness while individual beds may be only centimeters to tens of centimeters thick. Where the phyllite is interbedded with layers of coarse-grained chlorite-biotite-sericite-quartz schist the phyllite strongly resembles the occurrence of the upper layers, e. g. Bouma sequence D - E, of turbidite successions (Bouma, 1964).

Petrographic descripition

Phyllite is characterized by uniform, very-fine grain size with rare, fine-sand-sized to silt-sized porphyroblasts of quartz and opaque minerals (Plate 8). Quartz is granoblastic and monocrystalline. Sericite is idioblastic and tabular. Biotite is idioblastic, tabular to equant, and shows undulose extinction typical of pressure-deformed biotite. Biotite is pleochroic (pale brown to tan). Chlorite is idioblastic and tabular to equant, and shows characteristic pale-green to apple-green pleochroism and anomalous birefringence. Opaque minerals that are blocky to equant are probably pyrite, magnetite, and ilmenite, and may be of secondary origin. Clastic textures are partly to completely obliterated, grain size is reduced, and there is well developed schistosity. Grains show mortar texture. Accessory minerals are plagioclase, epidote-clinozoisite, tourmaline, apatite, zircon, magnetite, ilmenite, hematite, and pyrite. A secondary foliation that occurs at an angle of 30 to 45 degrees to the primary and secondary foliation, is defined by sericite, biotite, and chlorite.

Quartzite

Field description

The least common of the sedimentary rocks types of the Pinal Schist is quartzite. Quartzite is used here as a metamorphic rock term meaning that the rock breaks across

grains rather than around them. The rock occurs as isolated beds of coarse clastic material in the size range of medium-sand to pebble size. Most quartzites are massive, having uniform grain size; occasional grading is observed. Quartzite beds range from 0.25 m to 2.0 m thick. In some cases, quartzites seem to represent the lowermost (A - C) units of Bouma cycles. In other cases, they may represent grain-flow deposits. Quartzites which pinch out appear to represent channel deposits.

Quartzite is primarily composed of distinct grains of quartz, feldspar, and varicolored lithic fragments. Grains are often elongated to give the appearance of imbrication. This could to be due to metamorphic deformation and elongation of grains to form a lineation that resembles imbrication; the observed phenomenon may be an original sedimentary texture.

About 50% less matrix surrounds clasts in the quartzite than clasts in the schists. The quartzite appears to be the best representation of a grain supported sandstone occurring in the Pinal Schist study area. Using modal analyses and the Pettijonn, et al., (1973) (Figure 3) sedimentary terminology I classify the quartzite as arkosic wacke and quartz wacke.

Petrographic descripition

Quartz occurs as subangular to well-rounded grains from 1mm to 14mm in size. Most grains are monocrystalline and show strain and moderate recrystallization (Plate 9 and 10). Some are polycrystalline (Plate 11 and 12) and show inclusions of plagioclase, muscovite (Plates 13 and 14), and rutile (Plates 15 and 16). Rarely, elongated quartz grains show phyllosilicates along their margins; phyllosilicates are thickest at the center of the grain and thinnest at the ends of the grains. The phyllosilicates appear be a relict coating of clay minerals, now metamorphosed to sericite, on the grains, (A. J. Budding, personal communication, 1982). Quartz occasionally shows pressure fringes of fine-grained matrix, recrystallization, and broken grains.

Plagioclase occurs as rounded, sub-spherical, fine sand-sized detrital grains (Plate 17), and shows albite and deformation twinning. It also occurs in the matrix. Composition of favorably oriented grains was determined by using optical methods (extinction angle of sections perpendicular to the a-axis). Composition of the detrital plagioclase is albite, An0-An10.

Potassium feldspar occurs as medium sand-sized, rounded, elongate to sub-spherical detrital grains (Plate 18). They are strongly altered and appear to be poikilitic; relict exsolution textures are visible.

Lithic grains (Plates 18 to 25) are present as large elongated grains, with grain boundaries poorly to well defined. Grain boundaries are better defined under plane-polar light than under crossed-polar light (Plates 18 to 23). Lithic grains are prolate (Plates 18 and 19) and up to 16mm long by 5mm wide. They are composed of varying proportions of small (0.006 mm) crystallites of quartz, K-feldspar, chlorite, sericite, plagioclase, hematite and opaque minerals. A fine-grained groundmass surrounds phenocrysts (0.004 to 1 mm in size) of plagioclase (Plates 20, 22, and 23) and quartz (Plates 24 and 25). Lithic fragments are deformed where they contact detrital quartz grains. Lithic fragments took staining for potassium indicating felsic composition.

The matrix of the quartzite consists of fine-grained (0.01 mm.) quartz, feldspar, sericite, rare chlorite and biotite, and very rare tourmaline. In some cases, lithic fragments grade into recrystallized quartz matrix without a well-defined boundary.

META-IGNEOUS ROCKS

Tonalitic sills

Field description

A tonalitic felsic rock occurs near the southern boundry of the area (PS-124, Figure 2, overlay). This felsic rock occurs as a pair of sill-like bodies that appear

to be intrusive into the surrounding schist. The tonalitic rock does not crosscut the schist. The two units are each 0.3m thick and are separated by 0.5m of fine-grained schist. Strike length is at least 2 km.

The felsic rock appears white, with black speckling on weathered surfaces; fresh fractures are pale green to pink, with pink crystals of feldspar, green platy clots of chlorite, and colorless rounded grains of quartz. Euhedral phenocrysts of quartz and feldspar are up to 6mm in diameter. Plates of chlorite in the felsic rock are parallel to the schistosity and foliation of the surrounding meta-sedimentary schist. The foliation of the chlorite is evidence that the felsic rock has undergone compressive deformation like that which produced the secondary foliation of the surrounding meta-sedimentary schist. Although there is no evidence of shards or vacuoles, this is as might be expected of a deformed volcanic rock. No indication of lineation is found in the felsic rock. No obvious evidence of a chilled margin exists on the edges of the felsic units, nor is there evidence that the schist was metamorphosed by heat or fluids from the felsic units.

The concordant nature of the units, lack of a crosscutting relationship with the schist, and lack of evidence for any sort of alteration of the surrounding schist by heat or magmatic fluids support the inference that these units represent a shallow intrusion. The possibility

remains that tight isoclinal folding may have folded one unit to appear as two, but no stratigraphic evidence exists to support this hypothesis.

This felsic rock was analysed and found to have affinity with tonalite-trondjhemite as shown by CaO-Al2O3-MgO (Figure 4) and by CaO-Na2O-K2O (Figure 5).

The tonalitic sills offer the opportunity to place better constraints on the age of the Pinal Schist.

Petrographic descripition

Relict quartz and plagioclase phenocrysts are supported by a matrix of quartz, sericite, chlorite, epidote, carbonate, and opaques. Foliation is defined by prolate clots of chlorite, epidote, calcite and opaques. Plagioclase and quartz phenocrysts are aligned parallel to the foliation of the felsic rock.

Feldspar phenocrysts, up to 2mm square, show albite, Carlsbad, and deformation twinning. The feldspars are poikilitic and intensely altered to sericite, epidote, calcite, and apatite. Some feldspar grains show mortar texture; most are equant and idiomorphic (euhedral). Many appear to have been fractured, due to deformation. The feldspar phenocrysts are surrounded by well-developed pressure fringes of chlorite, sericite and quartz, which could be taken as evidence for a metamorphic origin for the phenocrysts; however, the fractured appearance of the

feldspar contradicts this interpretation. Composition of plagioclase feldspars taken from a section cut perpendicular to the a-axis gives An-20.

Quartz occurs as broken, elliptical grains. The broken grains show optical continuity. Quartz grains, up to 1.5mm in cross section, are monocrystalline, show strain, and lack vesicles or inclusions.

Allanite occurs as oriented grains that show single cleavage, 2V=45 degrees, twinning, zoning, pleochroic red-brown to yellow-brown color, and epidote halos. The allanite is not metamict. Grains are up to 0.6mm in size, and are euhedral.

METAMORPHIC PETROLOGY

Metamorphic-mineral assemblages

The following are metamorphic minerals found in each rock type:

Phyllite: biotite-chlorite-epidote-albite-muscovite

Schist: biotite-chlorite-epidote-albite-garnet-muscovite

Quartzite: biotite-chlorite-epidote-albite-garnet-muscovite

Tonalite: plagioclase(?)-epidote-chlorite-muscovite

Maximum metamorphic grade

Metamorphic-mineral assemblages of the various Precambrian rock types indicate that the maximum metamorphic grade is upper-greenschist facies. This interpretation is supported by the pale-brown color of biotite and the limited occurrence of metamorphic overgrowth on detrital garnets.

Microscopic metamorphic deformation

Metamorphic deformation occurs on the microscopic scale. Most feldspar grains, some lithic grains, and occasional quartz grains show the effects of metamorphic-pressure deformation. These effects include fracturing and recrystallization. On the whole, fine-grained rocks show more metamorphic effects than coarse-grained rocks; monocrystalline quartz grains appear to be most resistant to metamorphic deformation and recrystallization, while feldspar grains are least so. Pressure fringes occur frequently around resistant grains, especially quartz. Rare snowball-epidote indicates shear-stress.

MODAL ANALYSES

Purpose

Modal analyses of detrital framework grains in the coarse-grained varieties of schist and quartzite were made in order to identify provenance and tectonic setting. Dickinson and Suczek (1980) demonstrated, by plotting frequencies of types of detrital framework grains, that it is possible to distinguish modern sandstones and graywackes according to the tectonic provenance in which these rocks occur (Appendix D). Results of modal analyses of selected Pinal Schist thin sections are given in Table 1.

Tectonic provenance

Diagrams from Dickinson (1983) and Dickinson and Suczek (1980) indicate a mix of craton-continental block and recycled orogen provenance (Figures 6, 7, and 8). These diagrams indicate a cratonic or recycled orogen setting, either collision orogen or foreland uplift. Cratonic and recycled orogenic provenance are indicated. Magmatic arc sources are excluded. The Pinal Schist shows no correlation with turbidite graywackes that occur in Pacific margin trenchs (Dickinson, 1982). The QmFLt (Figure 9) diagram only indicates recycled collision orogenic provenance.

Sedimentary rock classification

Matrix ranges from 40 to 80 percent of the Pinal Schist. The Pettijohn sedimentary rock classification method (Pettijohn, et al., 1973, Figure 3) categorizes the schist as quartz wacke, lithic graywacke, and pelite.

The QFR diagram (Figure 10) is a sandstone classification diagram used by Folk (1974). Sandstones plotted on this diagram fall into one of five sandstone categories. The Pinal Schist samples fall into the categories of quartz arenite, subarkose, sublithic arenite, feldspathic lithic arenite, and lithic arenite.

Folk's (1974) sandstone classification scheme ignores the presence of matrix in the rock and, therefore, classification of the Pinal Schist on this diagram may be questionable.

Metamorphic effects on detrital grains

If metamorphism has increased the matrix content of a rock at the expense of detrital framework grains, then feldspar and lithic grains will be preferentially destroyed before quartz. This occurs because, of the three grain types, quartz, especially monocrystalline quartz, is the least reactive, and therefore most likely to survive metamorphism (Bond and Devay, 1980). If there has been extensive metamorphism, the proportion of matrix derived

from feldspar and lithic grains should increase more rapidly than that derived from quartz. The proportion of matrix derived from feldspar and lithic fragments also increases as grain size decreases, and as matrix content of sandstones increases, grain size decreases, (Pettijohn, et al., 1973). To summarize, if altered detrital feldspar was the principal source of secondary matrix, then an inverse relation should exist between feldspar and matrix content. No clearcut relationship between feldspar content and matrix content is observed in the Pinal Schist. From the evidence, no conclusion can be drawn regarding preferential metamorphic destruction of detrital feldspar grains.

GEOCHEMISTRY

Purpose

The chemical characteristics of the Pinal Schist are determined in order to compare it to modern sedimentary rocks, to determine the most likly composition of sources, to indicate the relative proportions of igneous and sedimentary sediment sources, to suggest the sedimentary provenance and tectonic environment of deposition of the schist, and to classify the schist into sedimentary rock types. The methods applied use graphical plots of oxides, major elements, and minor elements. These plots are used to distinguish characteristics, origins, and types of sedimentary rocks.

The question of elemental mobility in the Pinal Schist is discussed first. The following section compares the Pinal Schist to modern sediments and sedimentary rocks and discusses the results of applying graphical analyses to the Pinal Schist.

Results of chemical analyses of the Pinal Schist are given as Table 2.

Evaluation of elemental mobility

The highly variable nature of clastic sedimentary rocks makes accurate evaluation of the existence, effects, and extent of elemental mobility, or alteration, difficult in

sediments.

As grain size increases in clastic sandstones, quartz content also increases (Pettijohn, et al, 1973). This causes an inverse relation to exist between silica content and content of other oxides in clastic sedimentary rocks. Assuming that the samples collected represent the range of grain size variation within the Pinal Schist, these samples must also represent the range in variation of silica. Therefore, in its pre-metamorphic state, the Pinal Schist would have shown a smooth inverse relation between silica content and other oxides. Based on this deduction, simple graphs of the content of silica versus other oxides in the Pinal Schist serve as tests of the relative stability of those oxides during metamorphism. If the plot of an oxide displays a smooth relationship between the oxide and silica then the preexisting inverse relationship has not been significantly altered by metasomatic processes. This is observed in the cases of Al_2O_3, MgO, K_2O, TiO_2, and Fe_2O_3T. In the cases of Na_2O and CaO, these trends occur but are not as distinct. This indicates that the elements Al, Mg, K, Ti, and Fe are relatively stable, while Na and Ca are more mobile. In the case of CaO, this mobility is not unlikely as seen by anomalous levels of this oxide in the APS compared to modern sediments and sedimentary rocks.

Only minor mobility of elements may occur, in which case the characteristics in question would reflect the original rock characteristics.

Sedimentary origin of the Pinal Schist

Leyreloup, et al (1977) use the plot of CaO - Al2O3 - MgO (Figure 11) to distinguish meta-igneous (ortho-metamorphic) rocks from meta-sedimentary (para-metamorphic) rocks. By applying their method, I conclude that the Pinal Schist has the overall characteristics of meta-sedimentary as opposed to meta-igneous rock, and is therefore of para-metamorphic origin.

Moore and Dennen (1970) employ the diagram Al-Si-Fe (Figure 12) to classify the sedimentary rock types ortho quartzite, sandstone, arkose, subgraywacke, graywacke, and pelite. The Pinal Schist is interpreted as a mixture of sandstone, subgraywacke, and graywacke because the analysed samples plot most frequently as sandstone and subgraywacke. Moore and Dennen's use of the term "sandstone" implies a rock with less mineralogical maturity than ortho quartzite, but more maturity than subgraywacke; Moore and Dennen apparently include the rock category lithic arenite under the term sandstone. Moore and Dennen use the term "ortho quartzite" to describe "quartz arenite" as used herein; the term "subgraywacke" as used by Moore and Dennen includes rocks described as subgraywacke and as protoquartzite in

Pettijohn (1963) uses the binary diagram of log(Na2O/K2O)-log(SiO2/Al2O3) (Figure 13) to chemically distinguish compositional maturity of sediments, and to differentiate sandstone rock types. Use of this diagram indicates that the Pinal Schist represents a collection of immature sediments differentiated into subarkose, arkose, and lithic arenite. Coarse-grained quartzites and the schists rich in silica plot with regularity in the subarkose field.

Pinal Schist compared to modern sedimentary rocks

Geochemical characteristics of the Pinal Schist are compared to those of modern clastic sediments and sedimentary rocks in Tables 3 and 4. The average Pinal Schist (APS) rock has about the same SiO2 content as average arkoses and sandstones. Al2O3 in the APS is closest to that in average modern graywacke. In the APS, the content of Fe2O3T falls between those of average modern graywacke and average modern lithic arenite. MgO in the APS compares best to average modern arkose. Both Na2O and K2O in the APS fall between modern arkose and graywacke, most closely approaching the percentages of modern average arkose. CaO in the APS is substantially lower than in average modern sediments and sedimentary rocks.

Pettijohn (1963) and McLemore (1980) use the binary diagram K2O-Na2O (Figure 14) to distinguish arkose from graywacke using the chemical characteristics of modern sedimentary rocks. The Pinal Schist samples plot on and near the border of the arkose and graywacke fields. The majority of the samples plot within the field of arkose. This reinforces the Geochemical evidence above that shows the Pinal Schist to be arkosic rather than graywacke-like.

Arkoses show a characteristic positive correlation between (K2O + Na2O) and Al2O3. This occurs because the alkalies and alumina in arkoses are present in feldspars. The Pinal Schist samples show a distinct positive trend (Figure 15) and plot within the limits of arkose compositions (Pettijohn, 1963).

Depositional environment and provenance

Schwab (1973) uses the plot (SiO2/10)-K2O-Na2O (Figure 16) to identify various geosynclinal environments of deposition of sandstones. The Pinal Schist samples plot dominantly in Schwab's miogeosynclinal field. The samples show some scatter with overlap into the eugeosynclinal field and into the continental-rift field. Schwab relates the terms "miogeosynclinal" and "eugeosynclinal" to modern continental margins. The Pinal Schist samples exhibit the "miogeosynclinal" characteristics of rift valley or Atlantic-margin type sediments.

Bathia and Taylor (1981) document the effect of provenance on Th, U, Hf, La, and on the Th/U and La/Th ratios in modern Austrialian flysch-type sedimentary rocks. They also discuss the relationship between tectonic settings and geochemical characteristics of sedimentary basins. Their work shows that Th and U abundances in graywackes and pelites increase in response to change of provenance from andesite, through dacite, to granites and mature sedimentary rocks. Also, coexisting high La/Th and low Th/U ratios in graywackes and pelites indicate substantial contributions from volcanic source areas. When evaluated using Bathia and Taylor's (1981) graphical methods, the Pinal Schist appears to have granitic and/or mature sedimentary terrane provenance ((La/Th) - Hf, Figure 17). This implies the original sediments were deposited in a marginal basin or rifted continental margin (Figure 17), and are dominantly mature sedimentary detritus rather than dominantly felsic volcanic detritus, because the samples do not show high La/Th ratios and low Th/U ratios.

Sediment source characteristics and proportions

Bavinton and Taylor (1980) use the triangular plot of CaO-Al2O3-MgO (Figure 4) to identify igneous sources. Location of the Pinal Schist samples on the diagram allows inferences to be made concerning mixing of granitic and mafic sediment sources. Mixing of less than 10% basalt or less than 4% mixing of ultramafics with granite is inferred.

This means that the Pinal Schist sediment had the characteristics of granitic bulk chemical composition, but does not necessarily mean that the sediment source itself was granite.

Condie (1979) uses the ternary diagram %CaO - Na2O - K2O (Figure 5) to identify the composition of sediment sources. In this diagram, the bulk-chemical characteristics of the Pinal Schist fall within the felsic rock categories of granodiorite, quartz-monzonite, and granite. This plot indicates that the bulk-chemical characteristics of the sediment sources of the Pinal Schist match the bulk-chemical characteristics of granitic through granodioritic rocks, but not those of tonalite-trondjhemite. It is possible using this geochemical approach to constrain the chemical composition of a source area but impossible to identify actual lithologies.

Bathia and Taylor (1981) use the graph of (La/Th)-Hf (Figure 17) to characterize sediment sources of flysch sediments. "Graywackes deposited on passive continental margins and marginal basins ... derive material from granites, gneisses and older sedimentary rocks of the recycled orogen and tectonic highlands, and are highly mature (Bathia and Taylor, 1981)." The distribution of points on the graph suggests that the Pinal Schist is similar to modern graywacke.

Martell (1982) uses binary-element/oxide diagrams to estimate the relative contributions of various sources to sediment. To use these diagrams "each individual ... sample point serves as a pivot point for mixing lines connecting two or more rock types (Martell, 1982)." This allows rough calculations of approximate sediment source proportions. Petrographic evidence shows that all samples may have had some proportion of quartzitic-sediment input; therefore the quartzite composition fields are used as end points to construct mixing lines so as to estimate the contributions of granitic and mafic sources. End points for mixing lines can exist anywhere within the fields of the contributing rock-type fields; this makes it impossible to obtain exact numbers; instead, mixing proportions are given in ranges of minimum to maximum allowable amounts. A mixing line can only indicate, and not prove, that an end member has contributed to the composition of a sample. In using this approach it must be assumed that chemical compositions have not been significantly changed by metamorphic processes; petrologic evidence indicates that there has probably been no drastic mineralogic change in the Pinal Schist samples.

Results of plotting the Pinal Schist samples onto binary element/oxide diagrams show that these diagrams do not always agree. For example K_2O-Na_2O (Figure 14), Al_2O_3-K_2O (Figure 18), Rb-Sr (Figure 19), and Fe_2O_3T-MgO (Figure 20) all indicate that mafic sediments should be

excluded from consideration, while Al2O3-Fe2O3T (Figure 21), Fe-Sc (Figure 22), and Ca-Sr (Figure 23) all allow some mixing of mafic sediments. Those diagrams that show mafic sediment contributions indicate that mafic contributions could be from 10 up to 40 percent of the Pinal Schist. The plot of Ca-Sr (Figure 23) limits the mafic contribution to 10 percent and constrains the mafic source to be similar to mid ocean-ridge basalt (MORB). All of the diagrams allow mixing of quartzitic material with granitic material in proportions ranging from 10 to 90 percent of either end member. The plots of Al2O3-Fe2O3T (Figure 21), Fe-Sc (Figure 22), and Ca-Sr (Figure 23) all allow contributions from quartzitic, granitic, and mafic sources. The plots Al2O3-K2O (Figure 18), Al2O3-Fe2O3T (Figure 21), and Rb-Sr (Figure 19) all exclude tonalite-trondjhemite as a felsic sediment source; they also indicate that the most important felsic source is granodioritic in composition.

In summary, binary-element/oxide diagrams indicate that mafic-source components were small or nonexistent. There is a wide range of contributions from quartzitic and felsic sources. Multiple felsic sources may have contributed sediment. Granodioritic rocks may have been the major felsic source. Ultramafics, tonalite-trondjhemite, rift tholeiites, and continental alkali basalts should all be excluded from consideration as major sediment sources.

Rare - earth element (REE) plots (Figure 26) show strong light-REE enrichment as shown by the high La/Sm ratios, strong heavy-REE depletion as shown by high Tb/Yb ratios, and pronounced negative Eu anomalies. This is characteristic of post-Archean REE patterns (McLennan and Taylor, 1980) derived from terriginous sediments, especially sandstone, siltstone and pelite, and indicates a granitic crustal sediment source.

DISCUSSION

Sediment characteristics

The overall sedimentary characteristics of the Pinal Schist samples compare in petrographic and geochemical classifications. Petrologic classification shows that the Pinal Schist includes lithic graywacke, quartz wacke, arkosic wacke, and pelite, while geochemical classification shows the sediments to be sandstone, subgraywacke, graywacke, and possibly pelite.

Matrix feldspar correction

In order to correct for the possible effects of preferential metamorphic destruction of detrital feldspar, modal quartz is subtracted from percent silica, and excess silica is then combined with available K2O and Na2O to make feldspar. The resulting matrix-corrected feldspar is added to modal feldspar and replotted. This brings the petrographic sedimentary characteristics of the Pinal Schist more in line with the schist's geochemical characteristics. Sandstone modal classification of the schist is then arkose, subarkose, and lithic arenite; This agrees with the geochemical sandstone classification. One problem with this approach is that most K2O is tied up in sericite and biotite, thus invalidating the assumption that all K2O can be used to make orthoclase.

Field evidence supports the general interpretation of the petrographic and geochemical classifications; rounded gravels, poorly sorted sands, pelites, and siltstones occur as might be expected.

Sediment transport and deposition

Field evidence provides the best constraints on sediment transport and deposition of the Pinal Schist. Features observed in the Pinal Schist include strata that compare with Bouma sequences (e.g., graded schists interbedded with phyllites), sequences of fine-grained pelite, possible flame structures, and isolated channel-like beds of coarse-grained quartz wackes and lithic wackes. These features are analogous to features in modern turbidites. Pelitic sequences appear to represent deposition by distal turbidite flows. Coarse graywackes can be deposited by grain flow confined to proximal turbidite flows. By analogy in the Pinal Schist, isolated coarse-grained beds of lithic graywackes and quartz wackes may have been deposited in channels. Sequences of fine grained wackes and pelites were deposited distal on the fan or in interchannel areas. Isolated sandy beds scattered through much finer grained material can be submarine overbank deposits formed by escape of coarse-grained material from channels.

Petrography provides one constraint on mechanisms of sediment transport. Quartzite grains that show remnants of clay coatings indicate that detrital quartz grains were subject to more than one cycle of transport and deposition. This suggests that drainage of a continental interior by a river system temporarily deposited sedimentary detritus on a continental shelf, possibly in a delta, and that this sediment was remobilized by grain flow and turbidity currents that deposited it in a submarine fan.

Rounded, sub-spherical detrital grains imply abrasion during sediment transport, perhaps in the swash-zone of a beach environment, or during transport by grainflow or creep down a submarine canyon.

An alternative explanation might be a fluvial system. Many of the individual observations made on meta-sediments in the Pinal Schist are consistent with either fluvial or turbidite deposition. Features which would be expected in a fluvial system but which are not observed in the Pinal Schist include: desiccation features (mud cracks, salt casts, etc.); channel lags; crevasse splays; levee deposits; and asymmetrical channel deposits. The lack of these features leads me to believe that the Pinal Schist is best explained by a turbidite depositional model.

Depositional environment

Field evidence provides constraints on the depositional environment. No evidence exists for tectonic imbrication, mafic bodies, or melange that occurs in accretionary prisms today. This indicates that the depositional environment was not a trench or fore-arc basin. Turbidite facies present indicate the depositional environment was middle-fan, distal-fan, and abyssal-plane.

Geochemical evidence is consistent with deposition of the Pinal sediments in an ocean basin along a rifted margin, or possibly in a back-arc basin, but not in a trench. A rifted margin is supported by the arkosic geochemistry of the sediments, and possibly by the feldspar-corrected petrography. Modal analyses that show the dissimilarity of the Pinal sediments from those of modern magmatic-arc trenches also do not favor forearc-basin and trench settings. The evidence shows that arc related subduction, volcanism, and tectonism are not necessary to explain the characteristics of the Pinal Schist. This is not unusual for lower Proterozoic successions as shown by Kroner, (1980).

Paleo sea level

Deep sea sedimentation is controlled by global changes in sea level, primarily due to tectonism and glaciation. The frequency of turbidity currents is greatly increased

during periods of low sea level; the occurrence of a thick sequence of turbidites should thus correspond to a global lowstand of sealevel (Shanmugam and Moiola, 1982). The presence of turbidites in the Pinal Schist indicates deposition during a global lowstand of sea level. This in turn suggests a period of low spreading-ridge volume or of glaciation about 1.7 b.y.

Sedimentary facies

Field evidence provides the chief constraint on sedimentary facies. The Pinal Schist fits Kuenen's (1958) "universal" definition of flysch: "A thick sequence of pre-paroxysmal marine geosynclinal sediments, consisting of an alternation of evenly stratified shale and muddy sandstone (graywacke, etc.) and showing at least a moderate amount of graded bedding. The maximum grain size in the graded beds is 5 to 10 cm diameter. Coarser material is not graded and subordinate in amount. Transitions to or alternations with calcareous types also occur. Geologic age is ignored." Characteristic mixed sequences of turbidites, channel sands, and pelagic pelites occurring in peripheral basins and oceanic basins are termed flysch by Dickinson, (1974).

Using the terminology developed by Mutti and Ricci Lucchi (1978), layered graded schists can be classified as arenaceous facies and as arenaceous-pelitic facies. These facies associations indicate deposition in middle- to

distal-submarine fan (Mutti and Ricci Lucchi, 1978).

The phyllite may represent two or three separate turbidite facies; arenaceous-pelitic; pelitic-arenaceous I; and pelitic-arenaceous II (Mutti and Ricci Lucchi, 1978). The occurrence of the phyllite suggests that these be included in the pelitic phases of the arenaceous-pelitic and pelitic-arenaceous I facies. Facies associations suggest distal submarine fan and abyssal-plane depositional environments.

Quartzite appears to represent two types of turbidite facies: arenaceous-conglomeratic facies is represented by pebble-gravel lithic rich units; arenaceous facies is represented by coarse-sand quartz-rich units (Mutti and Ricci Lucchi, 1978). Facies associations suggest deposition as channel-fill by grain flow in proximal- or middle-fan environment.

Provenance

Petrographic evidence suggests origins for detrital grains. Monocrystalline quartz grains that show trains of vacuoles, strain, and inclusions of muscovite, garnet, and orthoclase, are typical of quartz crystals of granitic origin (Bond and Devay, 1980). Polycrystalline quartz grains with unimodal granule size are characteristic of crystalline rock origin, e.g. granite. Volcanic rock fragments that contain relict feldspar and quartz

phenocrysts indicate a felsic volcanic-rock source. Silt sized detrital cores of tourmaline and garnet indicate a source for metamorphic sedimentary detritus.

Granitic or gneissic sources tend to produce clastic sediments which are deposited in terrestrial or near-shore environments (Condie, 1982). The Pinal Schist resembles a deposit which today is thought of as occurring in deep water, not necessarily near-shore, but certainly with a granitic or gneissic source. This supports the deep water and granitic/gneissic source interpretations of geochemistry and modal analysis.

Modal analyses allow use of the provenance diagrams of Dickinson and Suczek (1979) and Dickinson (1983) to provide constraints on the provenance of the Pinal sediments. Indications from QmPK, QFL, and QmFLt plots are that the Pinal sands have dual provenance. They appear to be mixed between recycled-orogen provenance (of collision orogen or of foreland uplift character) and mature craton interior (or continental block) provenance. Coarse grained sediments tend toward the recycled orogen classification. The diagrams concur in their indication that the provenance of the Pinal Schist is not similar to that of modern Pacific margin trench deposits.

If feldspar is added, as explained in the sedimentology section above, the indications of the provenance diagrams are changed. They then show primarily craton interior

source for graywackes and pelite, with only minor foreland uplift origin for lithic wackes. If preferential metamorphic destruction of detrital feldspar has taken place, the primary provenance of the Pinal Schist is the cratonic interior.

Sediment sources

Geochemistry constrains the sources of the Pinal Schist sediments. The plot of (La/Th)-Hf suggests that igneous rocks of granitic composition were the primary sediment sources for the Pinal Schist; not rocks of mafic to dacitic composition. Sediment sources are distinguished within the felsic rock field by the plot of CaO-Na2O-K2O (figure 4) as granitic, granodioritic, and quartz-monzonitic. The REE patterns of the Pinal Schist indicate that the main source of sediment was granitic continental crust.

Evidence from petrographic analyses constrains the types and proximity of sources of clastic grains for the Pinal Schist. A felsic plutonic source is indicated for monocrystalline and polycrystalline quartz grains that show trains of inclusions and inclusions, greater in size than the matrix, of muscovite, garnet, and feldspars. This source would have been far enough from the depositional basin for rounding of the plutonic quartz grains. A felsic volcanic source is indicated for felsic lithic volcanic grains. This source was sufficiently close to the depositional basin so that fine-grained felsic volcanics

were deposited before they could be preferentially destroyed by the effect of sediment transport (Harrell and Blatt, 1978). The evidence suggests a nearby source.

Sediment mixing

Petrographic evidence suggests that three classes of sediments are mixed in the Pinal Schist. These are granitic, quartz arenitic, and felsic volcanic. The evidence does not suggest input of mafic sediment.

Geochemical methods further constrain the mixing of sediments from different sources to produce the Pinal Schist. The ternary-oxide plot CaO-Al2O3-MgO indicates the maximum possible input of mafic material is 10 percent or less tholeiitic basalt. Binary oxide plots indicate that the composition of the Pinal Schist may be obtained by mixing various proportions of orthoquartzite, granite or granodiorite, and mafic rocks. The plot of K2O-Na2O indicates mixing of 10 to 86 percent orthoquartzite with 14 to 90 percent granite. The plot of Al2O3-K2O indicates mixing of 20 to 75 percent orthoquartzite with 25 to 80 percent granodiorite. The indication of Al2O3-Fe2O3T is 5 to 10 percent mafic rock plus 15 to 70 percent felsic rock plus 20 to 80 percent quartzite. The plot of Ca-Sr suggests that felsic, quartzitic, and mafic sources were present and that there may have been more than one felsic source. The plot of Rb-Sr indicates mixing of 10 to 90 percent granitic sediment with quartzitic sediment and excludes mafic

sediment.

To summarize, geochemical analyses indicate that the primary sediment source of the Pinal Schist is felsic, with granite through granodiorite compositions predominating. Results from geochemical analyses minimize tonalite-trondjhemite as a source. Mafic sources may be most similar to midocean-ridge basalt. Hypothetical mixing of quartzitic sediment, felsic sediment, and mafic or andesitic sediment is possible. The most consistent indication is that quartzitic and felsic sediment sources are together necessary and sufficient to produce the Pinal compositions, while mafic or andesitic sediment sources are not necessary and probably insignificant. Sediments could be mixed to produce the compositions of the Pinal Schist samples by using proportions ranging from 10 to 90 percent quartzitic sediment, from 10 to 90 percent felsic sediment, and less than 10 percent mafic sediment. More than one distinct source of felsic sediment may have been present.

TECTONIC INTERPRETATION OF THE PINAL SCHIST

Field evidence suggests a passive continental-slope or oceanic-basin environment. The evidence does not demand that this be an active plate margin; however, a rifted continental margin is possible. A passive continental margin or an intra-plate basin are both possible.

Modal analyses place better constraints on the tectonic environment of deposition of the schist. The tectonic environment cannot be a magmatic arc, but appears to be an immature foreland uplift or reactivated collisional orogen. Geochemistry also places some constraints on tectonic setting. Again, an inactive marginal basin is suggested, and the possibility of an active rift is not eliminated, but is only partially supported.

The Pinal Schist was deposited in a marginal oceanic basin. This basin was located close to a continental landmass that was uplifted due to crustal collision. No magmatic arc or island arc existed in the area of deposition. Predominant rocks exposed on the landmass were quartz arenites, granites, granodiorites, quartz-monzonites, and probably volcanic equivalents of the felsic rocks. These rocks contributed 90 to 100 percent of the sediment volume composing any particular deposit. Minor amounts of mafic and metamorphic rocks may have been exposed as well.

The tectonic model favored is that of a passive or rifted continental margin with probable big river drainage from the uplifted continental interior. The continent is thought to have been uplifted due to a previous collision.

Condie (1982a) proposes a tectonic model for the Southwest that explains observed features of the Southwestern Proterozoic from the Sierra Madre of Wyoming to west Texas. His model calls upon Phanerozoic-type plate tectonic processes, i.e. buoyancy driven subduction, and involves cyclical marginal basin closures and Andean-type orogenies associated with southwestward-migrating arcs. The place of the Pinal Schist in this model is uncertain because the Pinal Schist crops out ≈ 500 miles to the west of the area covered by the Condie model. However, the Pinal Schist itself appears to fit the model in certain ways.

The Pinal Schist was deposited by turbidity currents and grain flow as a submarine fan of a progradational submarine-slope sequence within a marginal basin. Proximal-fan channel sands, e.g. lithic-quartz wackes, were laid down by submarine-channel grain flows. Distal-fan turbidite sands, i.e. lithic wackes, were deposited as Bouma sequences interbedded with silts and pelites.

After deposition the proximal- and distal-fan deposits were brought into contact by tectonic foreshortening accompanied by isoclinal folding, transposition, or imbrication due to the closure of the ocean basin in which

the deposits accumulated. This has produced the observed reversals in grading of turbidite sands, which can be explained as overturned normal grading, rather than reverse-grading.

Tectonic closure of the basin that brought the proximal- and distal-turbidite deposits together was caused by a basin closure as described in Condie's (1982a) model. The sediment source for the submarine-fan deposits is the uplifted remnants of an Andean-type orogeny associated with the previous basin closure.

The hypothetical history of the deposition of the Pinal Schist follows. Subduction of oceanic crust caused collision of an immature, i.e. bi-modal, but strongly felsic, volcanic arc with a continental land mass toward the north. Collision resulted in an Andean-type orogeny that shed granitic and sedimentary detritus southward into a marginal basin. The sediments include mature sediments from the continental interior, granitic material, and a limited amount of felsic volcanic material. The immaturity of these sediments and their mode of deposition identify the sedimentary facies of the Pinal Schist as flysch. The flysch sediments were deposited in a submarine fan as channel sands by grain flow and as turbidity flows interbedded with pelagic pelites. The accumulated flysch was then tectonically foreshortened by the closure of the basin as a result of the collision with the continent of a

second arc system, probably from the south. The existence of this second arc, as well as the second, is questionable. The driving force behind tectonic movement is assumed to be buoyancy driven subduction. This implies that the Pinal Schist was deposited on a mafic oceanic crust. This crust must have been totally subducted leaving no evidence behind.

An alternate hypothesis involves rifting followed by accumulation of the Pinal Schist sediments on a passive rifted continental margin. Isoclinal folding of the sediments is accomplished by closure of the basin.

TABLE 1
MODAL ANALYSES

	PS-17	PS-19	PS-26	PS-28	PS-31	PS-40
Qm	19.3	15.4	31.0	20.7	24.8	20.4
Qp	14.2	16.0	26.5	17.4	18.8	14.6
Lv	1.4	1.2	3.9	7.7	0.4	2.6
Ls	0	0	0	0	0	0
K	0	0.1	1.0	0.4	0	0.9
P	0.2	2.9	0	0.4	0	0
Ma	49.5	53.9	21.5	44.4	42.7	54.4
Sr	6.8	6.4	3.7	9.4	6.4	3.5
Ch	0	0	0.2	0	0	0
Bi	5.1	3.2	0	2.9	6.4	3.7
Op	0	2.6	0.6	2.6	1.7	1.9
Ep	1.0	1.2	0.1	1.1	0.6	0.4
Tr	0.2	0	0	0.1	0.2	0
Zr	T	T	0	0.1	0	T

	PS-44	PS-50	PS-68	PS-69A	PS-70	PS-73
Qm	29.1	19.6	22.8	19.6	25.0	9.7
Qp	16.5	17.1	30.3	14.0	25.8	13.7
Lv	2.1	0	2.0	0.9	0.2	1.1
Ls	0	0	0	0	0	0
K	0.8	0	0.4	0.7	0.2	1.3
P	0.2	0.2	0	0.4	0.2	0
Ma	41.2	48.6	34.6	49.3	38.4	50.8
Sr	4.9	9.2	10.6	7.4	4.7	17.4
Ch	1.6	0	0.7	4.0	2.7	1.5
Bi	0	1.7	0	0	0	0
Op	2.5	1.5	0.4	3.3	1.5	2.9
Ep	2.0	1.9	1.1	1.5	1.7	1.1
Tr	0.1	T	0	0	0	T
Zr	0	0	0	0.4	0	0

TABLE 1 CONT.

	PS-79	PS-80	PS-87	PS-90!	PS-92	PS-96!
Qm	12.8	9.2	7.6	30.4	20.3	26.7
Qp	32.7	17.0	15.9	21.7	12.5	25.4
Lv	1.9	0	0.2	8.4	0.6	9.9
Ls	0	0	0	0	0	0
K	1.5	2.1	1.5	1.5	1.2	3.0
P	0	0	0.2	0.2	0.2	0.4
Ma	51.4	37.6	58.6	28.6	49.3	22.2
Sr	6.0	15.3	11.6	2.9	17.3	7.0
Ch	1.6	0.1	1.1	0.5	3.3	0
Bi	0	0	0	0	0	0
Op	1.9	2.8	2.0	0.1	2.0	0.8
Ep	0.1	2.3	2.0	T	3.1	T
Tr	T	0.1	T	T	0.1	0
Zr	0	0	T	0.1	0	T

	PS-96A#	PS-97	PS-100#	PS-102!	PS-108	PS-118#
Qm	5.8	24.6	12.1	27.8	20.8	3.0
Qp	12.0	23.5	7.9	32.9	17.4	4.4
Lv	0	0.9	0.6	0.9	1.4	0.2
Ls	0	0	0	0	0	0
K	0.2	1.0	0.5	2.2	5.0	T
P	0.4	0.2	0	0	0.6	0.8
Ma	50.2	40.1	66.2	39.7	45.7	61.4
Sr	28.4	5.5	7.7	4.4	6.2	29.6
Ch	0	1.6	3.0	0.3	0.9	0
Bi	1.8	0	0	0	0	1.0
Op	2.4	1.5	1.4	0.8	2.2	0.3
Ep	0.1	0.8	0.4	0.4	0.9	0.4
Tr	0	T	0.1	T	0.1	0
Zr	0	T	0	T	T	0

Qm, Qp, Lv, Ls, Kf, Pf = Dickinson and Suczek categories (see Table 5); T = Trace amount; observed but not counted. Ma = quartzo-feldspathic matrix; Sr = sericite in matrix Ch = chlorite in matrix; Bi = biotite in matrix; Op = opaques; Ep = epidote; Tr = tourmaline; Zr = zircon.
! = Pinal Schist Quartzites
= Pinal Schist Phyllites

TABLE 2
CHEMICAL ANALYSES

ELEMENT	PS-3	PS-10	PS-12	PS-17	PS-19
SiO2	78.94	78.97	79.33	79.31	79.42
TiO2	0.66	0.55	0.67	0.52	0.53
Al2O3	9.22	9.96	9.26	9.59	9.61
Fe2O3T	4.04	3.64	4.08	3.74	3.79
MgO	0.90	0.70	0.78	0.80	0.95
CaO	0.95	0.71	0.93	0.74	0.73
Na2O	2.30	1.81	1.93	1.87	1.62
K2O	2.21	2.15	2.20	2.20	2.21
MnO	0.05	0.05	0.05	0.05	0.04
P2O5	0.08	0.06	0.07	0.08	0.07
L.O.I.	0.69	1.11	1.19	0.97	0.97
Total	100.00	99.7	100.50	99.90	100.00
Rb	101	95.2	115	110	93.5
Sr	101	84.0	79.5	87.9	121
Cs	6.9	-	6.9	6.9	6.5
Ba	384	-	419	378	461
Y	43	37	33	33	32
Zr	421	314	289	282	293
Hf	15.6	-	9.5	8.3	8.8
Ta	1.1	-	1.0	1.1	2.6
Sc	9.3	-	10	7.8	6.6
Cr	99.5	-	132	100	68.3
Ni	22	13	18	23	12
Co	8.5	-	8.2	6.9	5.4
U	2.8	-	2.4	2.6	2.3
Th	19.1	-	13.9	13.9	13.5
La	36.2	-	28.5	33.9	32.7
Ce	79.2	-	63.1	66.1	66.3
Sm	6.5	-	5.6	6.2	5.9
Eu	1.2	-	1.3	1.0	1.3
Tb	1.0	-	0.87	0.88	1.1
Yb	4.3	-	4.3	2.9	2.9
Lu	0.78	-	0.75	.52	.50

Explanation on last page.

TABLE 2 CONT.

ELEMENT	PS-24	PS-26	PS-28	PS-31	PS-32
SiO2	74.64	84.73	82.20	82.14	80.84
TiO2	0.53	0.42	0.43	0.45	0.14
Al2O3	12.03	6.88	7.89	8.09	8.72
Fe2O3T	3.91	3.28	3.53	3.26	3.63
MgO	0.89	0.55	0.79	0.53	0.65
CaO	1.04	0.48	0.59	0.62	0.78
Na2O	2.41	1.37	1.20	1.53	1.51
K2O	2.67	1.69	2.14	1.72	2.31
MnO	0.05	0.04	0.05	0.04	0.05
P2O5	0.08	0.06	0.07	0.07	0.06
L.O.I.	1.24	0.75	1.00	0.70	-
Total	99.5	100.3	99.6	99.1	98.7
Rb	213	60.0	100	81.7	101
Sr	144	-	53	141	88
Cs	8.0	4.7	7.6	6.8	-
Ba	559	461	386	421	-
Y	22	-	31	41	28
Zr	234	191	216	192	274
Hf	7.0	8.7	7.6	7.2	-
Ta	1.2	0.9	0.7	0.9	-
Sc	10.6	1.4	7.8	7.8	-
Cr	11.9	63.5	92.1	69.9	-
Ni	29	19	20	16	19
Co	8.3	7.2	8.5	7.7	-
U	2.1	2.7	2.4	2.9	-
Th	11.2	13.1	10.2	14.4	-
La	31.0	27.4	23.8	28.7	-
Ce	50.2	52.2	56.3	65.1	-
Sm	5.6	5.1	4.6	5.3	-
Eu	1.2	0.65	1.0	0.94	-
Tb	1.2	1.2	0.73	0.68	-
Yb	4.6	3.0	3.1	2.9	-
Lu	0.89	0.48	0.51	0.53	-

Explanation on last page.

TABLE 2 CONT.

ELEMENT	PS-40	PS-50	PS-54	PS-69A	PS-69
SiO2	73.32	79.48	62.80	78.34	80.75
TiO2	0.61	0.53	0.64	0.54	0.51
Al2O3	13.25	9.20	19.49	10.45	9.09
Fe2O3T	4.67	4.02	6.12	3.99	3.79
MgO	1.01	0.75	1.17	0.88	0.86
CaO	0.44	0.71	0.60	0.37	0.35
Na2O	2.31	1.72	1.83	1.35	1.48
K2O	3.19	2.36	4.55	2.28	1.82
MnO	0.05	0.04	0.06	0.05	0.05
P2O5	0.10	0.07	0.08	0.07	0.07
L.O.I.	2.31	0.90	2.39	1.34	1.32
Total	100.25	99.77	99.71	99.65	100.11
Rb	148	108	244	104	82
Sr	95	71	118	68	65
Cs	9.4	7.4	14.9	-	5.5
Ba	483	424	797	-	221
Y	37	35	65	34	31
Zr	251	277	201	272	286
Hf	7.3	8.7	4.5	-	7.9
Ta	1.4	1.3	1.6	-	0.9
Sc	13.6	8.3	18.2	-	-
Cr	62.1	88.4	66.2	-	60
Ni	17	23	31	22	12
Co	11.7	9.0	8.2	-	5.7
U	2.7	3.4	3.9	-	3.3
Th	12.9	13.0	17.2	-	13.7
La	36.4	39.4	38.6	-	29.8
Ce	71.3	-	-	-	68.5
Sm	6.9	6.6	8.6	-	5.7
Eu	1.4	1.2	1.6	-	1.4
Tb	1.4	1.3	1.8	-	0.89
Yb	4.3	3.5	7.4	-	2.7
Lu	0.78	0.60	1.4	-	0.48

Explanation on last page.

TABLE 2 CONT.

ELEMENT	PS-70	PS-73	PS-77	PS-78	PS-80
SiO2	80.83	74.69	77.12	76.39	76.04
TiO2	0.52	0.50	0.46	0.43	0.44
Al2O3	8.82	11.72	11.23	11.31	11.39
Fe2O3T	3.86	3.95	3.44	3.95	3.27
MgO	0.56	0.80	0.67	0.75	0.62
CaO	0.44	0.91	0.89	0.60	0.76
Na2O	1.87	1.79	2.77	1.71	2.84
K2O	1.83	3.34	2.62	3.37	2.43
MnO	0.03	0.05	0.05	0.05	0.04
P2O5	0.06	0.08	0.07	0.07	0.06
L.O.I.	1.12	1.85	0.65	1.25	1.08
Total	99.90	99.67	99.96	99.88	98.96
Rb	87	164	121	138	116
Sr	63	68	127	73	94
Cs	-	-	7.4	6.1	-
Ba	-	-	470	803	-
Y	33	37	30	28	35
Zr	278	271	247	237	250
Hf	-	-	7.7	7.1	-
Ta	-	-	0.9	1.0	-
Sc	-	-	8.7	9.3	-
Cr	-	-	50	76	-
Ni	10	17	9	15	10
Co	-	-	6.8	4.4	-
U	-	-	3.5	3.6	-
Th	-	-	13.8	12.8	-
La	-	-	22.2	33.0	-
Ce	-	-	54.1	70.3	-
Sm	-	-	4.6	6.6	-
Eu	-	-	1.1	1.7	-
Tb	-	-	0.95	1.0	-
Yb	-	-	3.3	2.9	-
Lu	-	-	0.51	0.55	-

Explanation on last page.

TABLE 2 CONT.

ELEMENT	PS-83	PS-87	PS-90!	PS-92	PS-96A#
SiO2	74.17	75.32	88.73	77.87	75.32
TiO2	0.53	0.54	0.21	0.44	0.48
Al2O3	12.42	12.09	5.03	10.42	12.57
Fe2O3T	3.93	1.77	3.60	3.62	3.62
MgO	0.75	0.91	0.29	0.88	0.83
CaO	0.89	0.82	0.43	0.80	0.12
Na2O	2.31	2.46	1.14	2.05	0.82
K2O	3.29	2.59	0.92	2.11	3.97
MnO	0.05	0.06	0.04	0.07	0.03
P2O5	0.08	0.07	0.03	0.06	0.03
L.O.I.	1.42	1.40	1.02	1.48	2.14
Total	99.83	100.20	99.60	99.77	99.90
Rb	148	119	42.3	97.8	175
Sr	109	117	29.0	111	23
Cs	6.8	-	3.1	-	9.3
Ba	555	-	261	-	116
Y	34	36	24	33	35
Zr	291	309	150	220	254
Hf	9.3	-	4.6	-	7.3
Ta	1.1	-	1.0	-	0.7
Sc	10	-	3.0	-	-
Cr	10	-	30.2	-	≤13
Ni	14	20	4	18	22
Co	6.1	-	4.1	-	6.8
U	3.5	-	1.7	-	2.8
Th	16.5	-	8.0	-	12.3
La	28.6	-	22.9	-	37.9
Ce	68.2	-	-	-	-
Sm	5.7	-	4.2	-	6.7
Eu	1.1	-	0.9	-	1.8
Tb	0.92	-	0.71	-	1.4
Yb	1.3	-	2.1	-	4.0
Lu	0.54	-	0.37	-	0.77

Explanation on last page.

TABLE 2 CONT.

ELEMENTS	PS-96!	PS-97	PS-100#	PS-101#	PS-102!
SiO2	88.09	80.45	73.66	75.07	88.48
TiO2	0.26	0.50	0.59	0.56	0.24
Al2O3	6.39	8.69	12.40	12.64	5.36
Fe2O3T	2.19	3.62	4.69	4.19	1.99
MgO	0.19	0.65	1.11	1.13	0.29
CaO	0.11	0.90	0.78	0.40	0.59
Na2O	1.22	1.76	1.60	1.66	1.47
K2O	1.47	1.66	3.02	2.43	1.00
MnO	0.02	0.06	0.06	0.07	0.04
P2O5	0.04	0.07	0.09	0.07	0.03
L.O.I.	0.83	1.11	2.01	-	0.56
Total	100.83	99.46	100.00	98.23	100.00
Rb	62	78.3	145	101	38.1
Sr	24	136	104	80	87
Cs	-	6.3	-	8.4	2.2
Ba	-	395	-	473	169
Y	27	33	36	28	24
Zr	188	214	241	200	166
Hf	-	8.0	-	7.2	5.0
Ta	-	0.8	-	2.6	0.8
Sc	-	8.5	-	11.3	2.9
Cr	-	93.2	-	48.6	27
Ni	6	22	25	13	6
Co	-	8.5	-	<0.1	2.3
U	-	3.7	-	3.4	1.7
Th	-	13.1	-	14.0	7.0
La	-	27.9	-	43.2	20
Ce	-	68.5	-	-	40
Sm	-	5.1	-	7.1	3.6
Eu	-	0.89	-	1.2	0.59
Tb	-	0.90	-	1.1	0.61
Yb	-	2.3	-	3.8	1.9
Lu	-	0.59	-	0.70	0.33

Explanation on last page.

TABLE 2 CONT.

ELEMENT	PS-105	PS-112	PS-117	PS-118#	PS-122#
SiO2	74.05	78.19	79.84	71.17	72.23
TiO2	0.46	0.42	0.34	0.34	0.56
Al2O3	12.53	10.72	10.42	15.03	13.32
Fe2O3T	3.40	3.18	2.62	3.25	4.44
MgO	0.92	0.68	0.42	0.64	1.02
CaO	1.04	1.02	0.28	0.71	0.75
Na2O	2.24	2.57	2.56	2.24	2.63
K2O	3.16	2.29	2.28	4.72	2.90
MnO	0.05	0.05	0.01	0.07	0.06
P2O5	0.07	0.05	0.04	0.04	0.09
L.O.I.	1.54	0.74	0.80	1.29	1.37
Total	99.50	99.90	99.63	99.50	99.38
Rb	158	95.6	103	210	142
Sr	110	131	82	117	107
Cs	8.5	5.0	5.7	10.8	10
Ba	599	478	506	684	580
Y	32	30	30	40	24
Zr	220	231	167	229	248
Hf	7.1	6.5	7.1	6.7	8.1
Ta	1.0	1.0	0.7	2.0	1.3
Sc	1.6	6.9	1.1	10.0	2.0
Cr	14	41	46	25	<0.1
Ni	14	10	10	16	22
Co	4.5	7.1	2.7	6.3	11
U	3.1	3.0	2.1	4.1	3.4
Th	11	12	11	18	13
La	28	25	23	41	30
Ce	61	43	46	82	72
Sm	5.0	5.3	4.8	7.2	6.0
Eu	1.2	1.0	1.0	1.3	1.0
Tb	0.87	1.2	3.7	1.3	1.1
Yb	3.1	2.7	2.9	4.7	3.7
Lu	0.54	0.46	0.47	0.83	1.0

Explanation on last page.

TABLE 2 CONT.

ELEMENTS	PS-124*
SiO2	71.43
TiO2	0.24
Al2O3	15.87
Fe2O3T	2.48
MgO	0.78
CaO	2.24
Na2O	4.57
K2O	1.79
MnO	0.08
P2O5	0.14
L.O.I.	1.58
Total	101.21
Rb	70
Sr	-
Cs	5.0
Ba	690
Y	-
Zr	213
Hf	4.5
Ta	1.7
Sc	4.2
Cr	0.3
Ni	0
Co	0.3
U	2.3
Th	11
La	49
Ce	78
Sm	5.1
Eu	1.4
Tb	0.5
Yb	-
Lu	-

Total iron as Fe2O3T
Major elements in weight percent
Trace elements in parts per million
- = no determination
* = tonalitic felsic sill
! = quartzites
= phyllites

TABLE 3
CHEMICAL ANALYSES OF COARSE, MEDIUM, AND FINE GRAINED CLASTIC SEDIMENTS COMPARED TO AVERAGE PINAL SCHIST

ELEMENT	A	B	C	APS
SiO2	78.66	69.96	58.38	77.78
TiO2	0.25	0.59	0.65	0.48
Al2O3	4.78	10.52	15.47	10.62
Fe2O3	1.08		4.03	
Fe2O3T		3.47		3.71
FeO	0.30		2.46	
MgO	1.17	1.41	2.45	0.77
CaO	5.57	2.17	3.12	0.68
Na2O	0.45	1.51	1.31	1.90
K2O	1.32	2.30	3.25	2.52
MnO	Trace	0.06	Trace	0.05
P2O5	0.08	0.18	0.17	0.07
H2O+	1.33#	1.96	3.68	
H2O-	0.31	3.78	1.34	
LOI				1.24*
CO2	5.02	1.40	2.64	
SO3	0.07	0.03	0.65	
Cl	Trace	0.08	----	----
BaO	0.05	0.08	0.05	Trace
SrO	Trace	Trace	Trace	Trace
Total	100.41	$100.50	100.46	99.81

\# Includes organic matter.
$ Total includes ZrO2, 0.5; F, 0.07; S, 0.07; Cr2O3, 0.01; ZrO3, 0.0010; As2O5, 0.0004; PbO, 0.0002; less O=F2,S,0.12.
A. Sandstone, composite of 253 samples (after Pettijohn, 1963).
B. Mississippi River silt, composite of 235 samples (after Pettijohn, 1963).
C. Pelite, composite of 78 samples (after Pettijohn, 1963).
APS = Average Pinal Schist, average of 35 analyses (Table 1).
* APS = Loss on ignition.

TABLE 4
MEAN COMPOSITION OF PRINCIPAL SANDSTONE CLASSES
COMPARED TO AVERAGE PINAL SCHIST

ELEMENT	ORTHO 1 QUARTZITE	LITHIC 2 ARENITE	GRAY- 3 WACKE	ARKOSE 4	APS 5
SiO2	95.4	66.1	66.7	77.1	77.8
TiO2	0.2	0.3	0.6	0.3	0.5
Al2O3	1.1	8.1	13.5	8.7	10.6
Fe2O3	0.4	3.8	1.6	1.5	
Fe2O3T				>	3.71
FeO	0.2	1.4	3.5	0.7	
MgO	0.1	2.4	2.1	0.5	0.8
CaO	1.6	6.2	2.5	2.7	0.7
Na2O	0.1	0.9	2.9	1.5	1.9
K2O	0.2	1.3	2.0	2.8	2.5
MnO	---	0.1	0.1	0.2	0.05
P2O5	---	0.1	0.2	0.1	0.1
H2O+	0.3	3.6	2.4	0.9	
H2O-	---	0.7	0.6	---	
LOI				> #	1.2
CO2	* 1.1	5.0	0.3	3.0	
SO3	---	---	0.1	---	
C	---	---	0.1	---	---
Total	100.7	100.0	100.4	100.0	99.8

1. Total, 26 analyses (after Pettijohn, 1963).
* Estimated from CaO.
2. Total, 20 analyses (after Pettijohn, 1963).
3. Total, 61 analyses (after Pettijohn, 1963).
4. Total, 32 analyses (after Pettijohn, 1963).
5. APS = Average Pinal Schist, total 35 analyses.
\# APS = Loss on Ignition

TABLE 5
DEFINITION OF GRAIN POPULATIONS FOR TRIANGULAR COMPOSITIONAL DIAGRAMS

TRIANGULAR DIAGRAM	UPPERMOST POLE	LOWER LEFT POLE	LOWER RIGHT POLE
QFL	Q	F	L
	Quartzose grains (= Qm + Qp)	Feldspar grains (= P + K)	Unstable aphanitic lithic (= Lv + Ls)
QmFLt	Qm	F	Lt
	Monocrystalline quartz grains	(same as above)	Total aphanitic lithic fragments (= L + Qp)
QmPK	Qm	P	K
	(same as above)	Plagioclase grains	K-feldspar grains
QpLvLs	Qp	Lv	Ls
	Polycrystalline quartzose lithic fragments (chert quartzite,etc)	Volcanic and metavolcanic lithic fragments (inc. hypabyssal)	sedimentary and metasedimentary litnic fragments (argillite, pelite, hornfels, slate)

After Dickinson,1982.

TABLE 6
NEUTRON ACTIVATION INSTRUMENTAL PARAMETERS

RADIO-NUCLIDE	PEAK ENERGY(KeV)	COOLING TIME(DAYS)	COUNTING TIME(SECONDS)	CHONDRITE VALUE
Sm153	103.2	4	5000	0.181
Np-239(U)	277.6	4	5000	
La-140	487.0	4	5000	0.330
Na-24	1368.4	4	5000	
Lu-177	208.8	7	8000	0.034
Np-239	277.6	7	8000	
Yb-175	282.6	7	8000	0.200
Tb-160	298.6	7	8000	0.047
Yb-175	396.1	7	8000	0.200
Eu-157	121.8	28	12000	0.069
Ce-140	145.5	28	12000	0.880
Yb-169	177.2	28	12000	0.200
Eu-152	216.0	28	12000	0.069
Ta-182	222.1	28	12000	
Tb-160	298.6	28	12000	0.047
Pa-233(Th)	311.8	28	12000	
Cr-51	320.1	28	12000	
Hf-181	482.2	28	12000	
Ba-131	496.3	28	12000	
Eu-152	779.1	28	12000	0.069
Cs-134	795.8	28	12000	
Tb-160	879.3	28	12000	0.047
Sc-46	889.3	28	12000	
Tb-160	1178.1	28	12000	0.047
Co-60	1332.5	28	12000	
Eu-152	1408.1	28	12000	0.069

TABLE 7
ELEMENT CONCENTRATIONS FOR INTERLAB ROCK STANDARDS
USED IN NEUTRON ACTIVATION ANALYSIS

ELEMENT	LOSP		BLCR		HI31
SiO2	75.90		53.50		58.80
TiO2	0.20		0.89		0.88
Al2O3	12.03		18.10		16.70
Fe2O3T	1.81		7.62		6.47
MgO	0.07		4.85		4.21
CaO	0.93		8.39		6.50
Na2O	3.49		3.57		3.11
K2O	4.83		1.32		2.88
Sc	5.7		32		23
Cr	2.7		130		34
Co	0.6		30		13
Cs	2.0		2.5		0.5
Ba	960		370		772
Hf	11		4.3		---
Ta	1.9		0.5		---
Th	2.4		4.0		6.8
U	4.2		1.5		0.5
La	70		12		33
Ce	160		28		67
Sm	17		4.0		7.5
Eu	2.4		1.3		1.8
Tb	3.1		0.8		0.85
Yb	11	3.5		3.3	
Lu	1.8		0.6		0.56

Oxides in weight percent.
Trace elements in parts per million.

TABLE 8
SET-UP FOR X-RAY FLUORESCENCE ANALYSIS

ELEMENT	PEAK	Kv / Ma	CRYSTAL	COLLIMATOR
Si	K	45 / 55	RX4	FINE
Al	K	45 / 55	PET	COARSE
Fe	K	45 / 55	LiF(200)	FINE
Mg	K	45 / 55	TAP	COARSE
Ca	K	45 / 55	LiF(200)	COARSE
Na	K	45 / 55	TAP	FINE
K	K	45 / 55	LiF(200)	COARSE
Ti	K	45 / 55	LiF(200)	COARSE
Mn	K	45 / 55	LiF(200)	COARSE
P	K	45 / 55	LiF(200)	COARSE
Rb	K	40 / 60	LiF(220)	COARSE
Sr	K	40 / 60	Lif(200)	COARSE
Zr	K	40 / 60	LiF(200)	COARSE
Y	K	40 / 60	LiF(200)	COARSE
Nb	K	40 / 60	LiF(200)	COARSE

TABLE 9
SYMBOLS USED IN FIGURES

SYMBOL(S)	EXPLANATION
ORTH, OQ	Orthoquartzites
GR.FD.	Granitic Field
GRA	Granites
GRAN	Granodiorites
QM	Quartz-monzonite
T.TR.,TT	Tonalite-Trondhjemites
CAB	Calc-alkaline Basalts
R.T.	Rift Tholeiites
MORB	Mid-ocean Ridge Basalts
CC	Continental Crust
A, ARK	Arkose
SA, SAK	Subarkose
QA	Quartz Arenites
LA	Lithic Arenite
SLA	Sublithic Arenite
SS	Sandstones
GRY, GW	Graywackes
AW	Arkosic Wacke
QW	Quartz Wacke
LGW	Lithic Graywacke
SGW	Subgraywacke
PGY	Precambrian Graywackes
PMGY	Paleozoic and Mesozoic graywackes
▲	Pinal Schist Quartzites
▼	Pinal Schist Phyllites
●	Pinal Schist Schists
□	Pinal Schist Tonalitic Sill

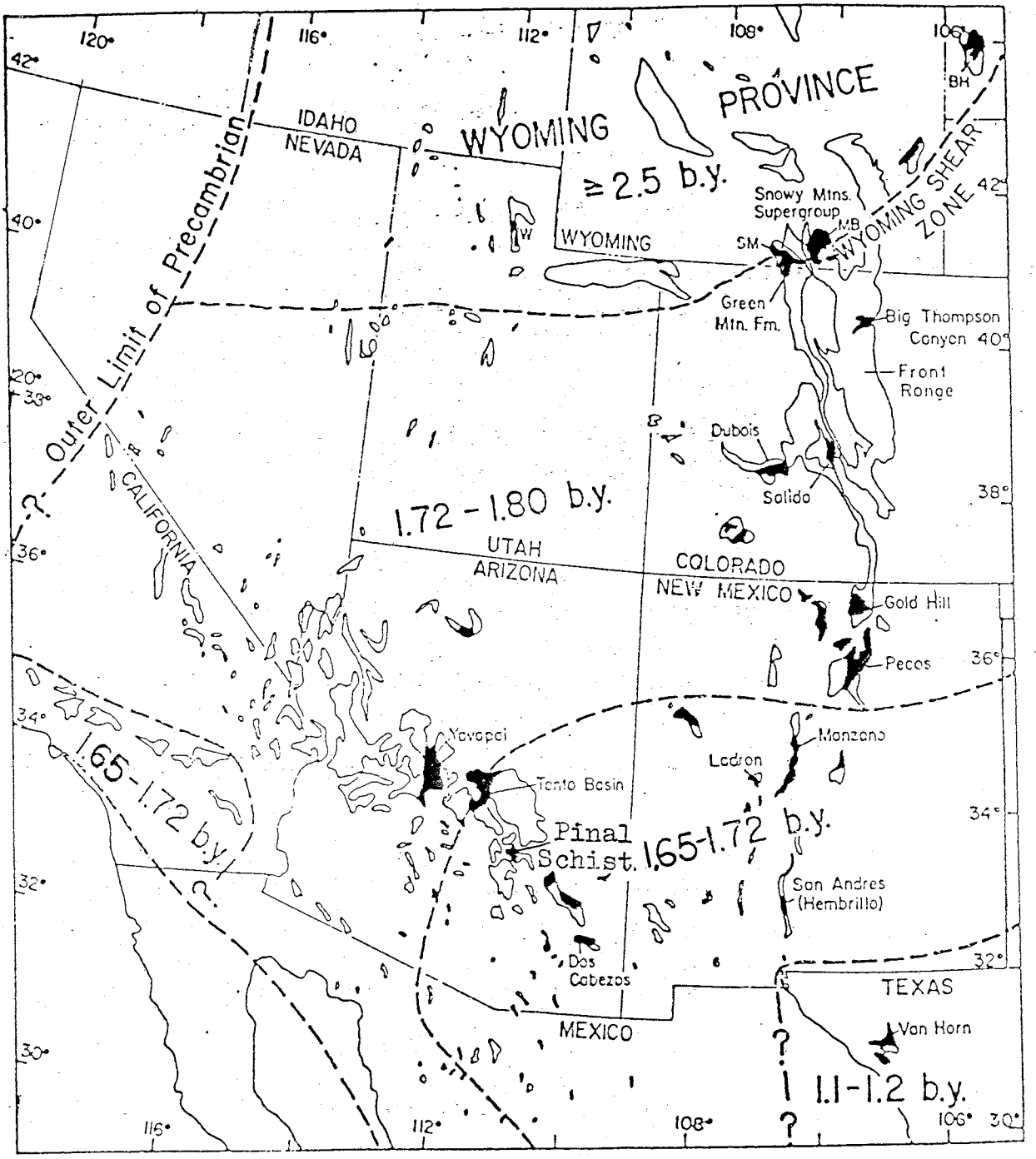

Figure 1. Regional map of the southwestern United States showing Precambrian age provinces and locatiion of the Pinal Schist in the study area (modified after Condie, 1982).

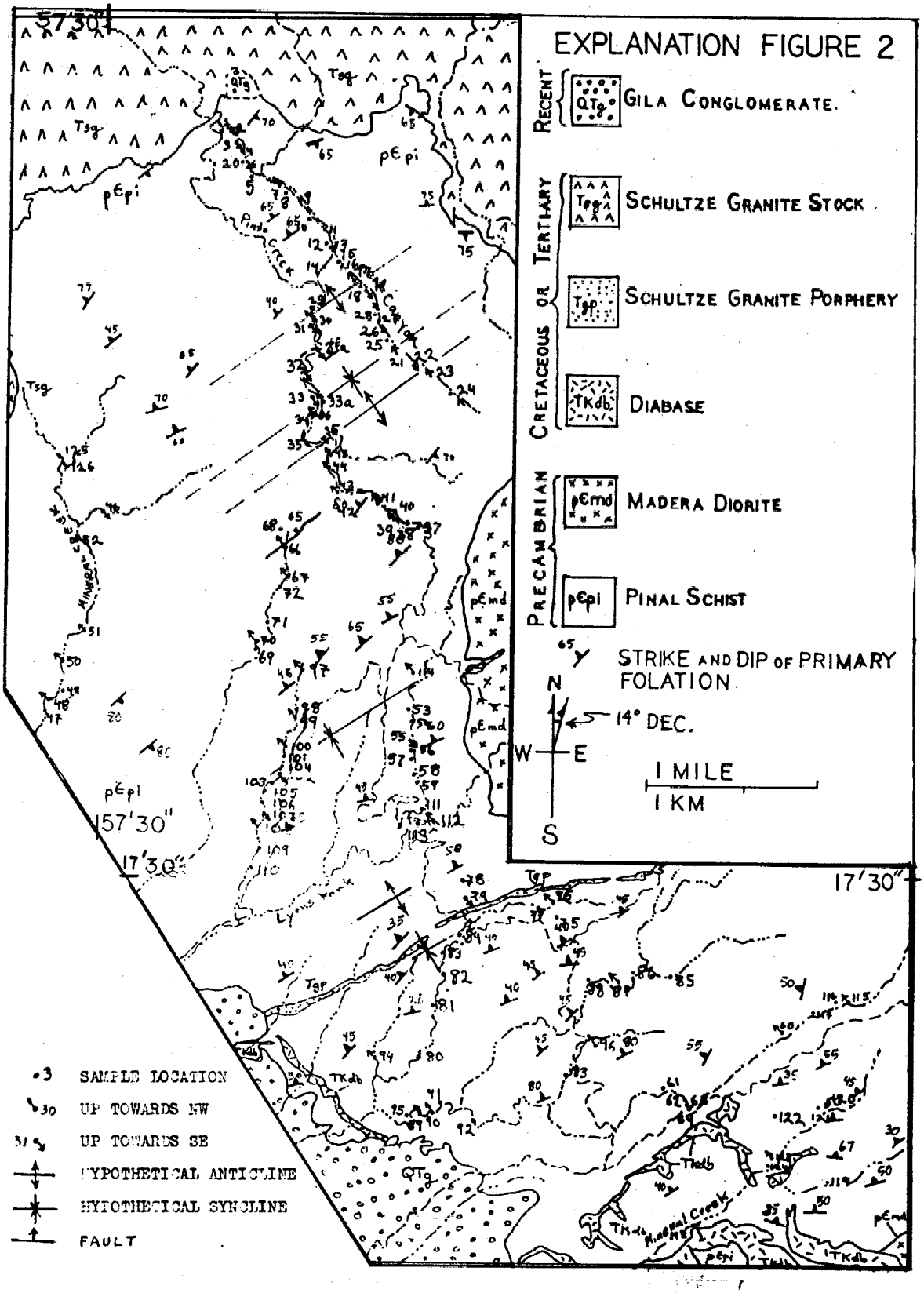

Figure 2. Geologic map of the study area (modified after Peterson, 1958). Overlay: sample locations; direction of stratigraphic up-section; locations of mapped fault and tonalitic sills.

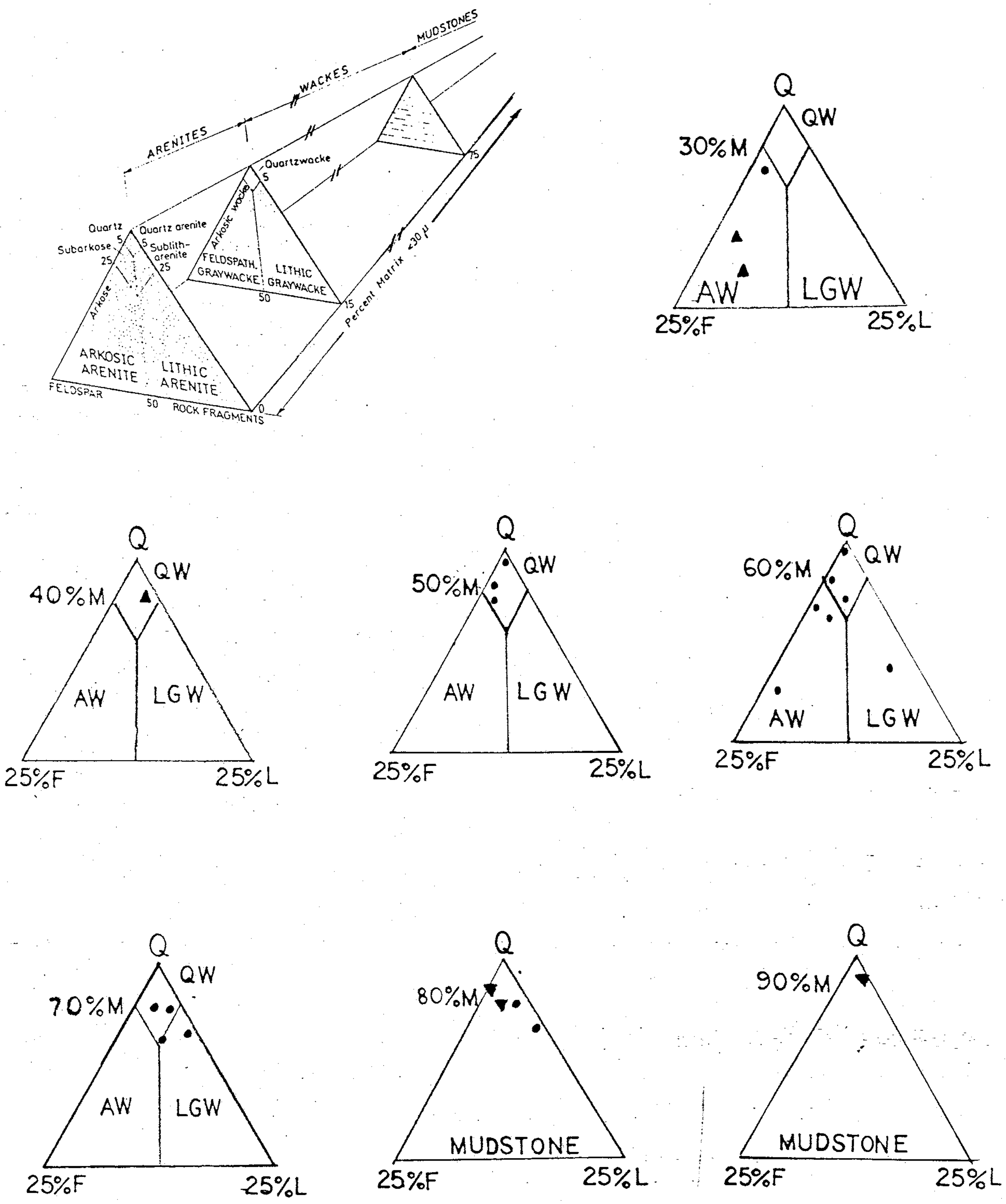

Figure 3. Sedimentary classification (After Pettijohn, et al., 1973). See Table 9 for symbols used in figures. M = Matrix +/- 5%.

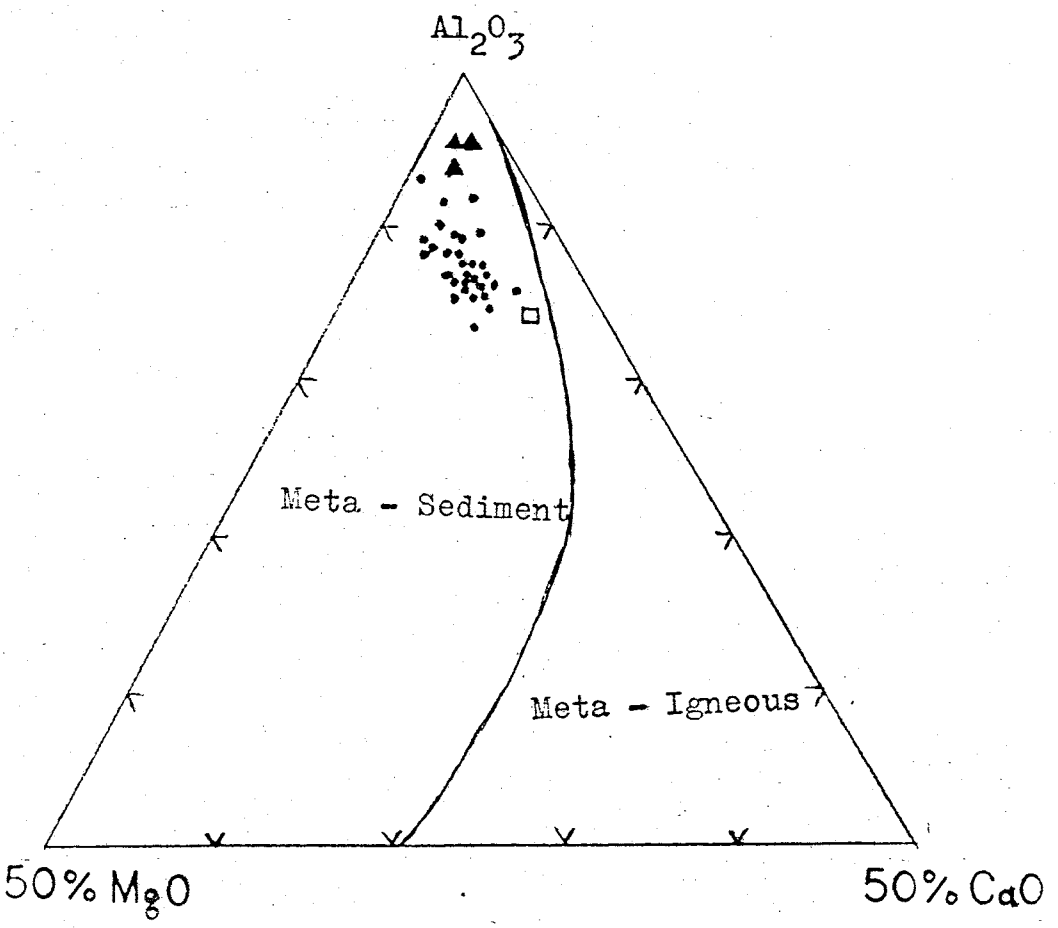

Figure 4. CaO-Al2O3-MgO diagram (fields after Leyreloup, et al., 1977). See Table 9 for symbols used in figures.

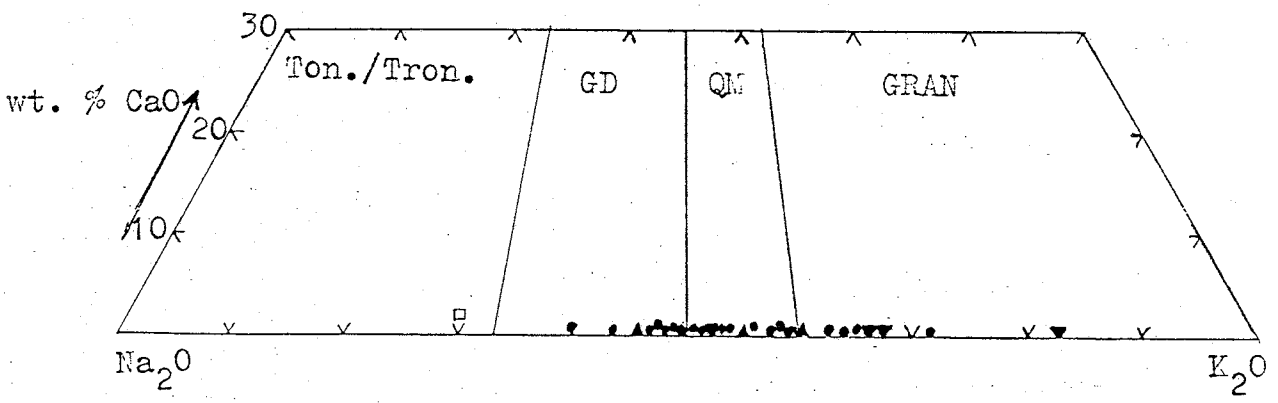

Figure 5. CaO-Na2O-K2O diagram (fields after Condie, 1979). See Table 9 for symbols used in figures.

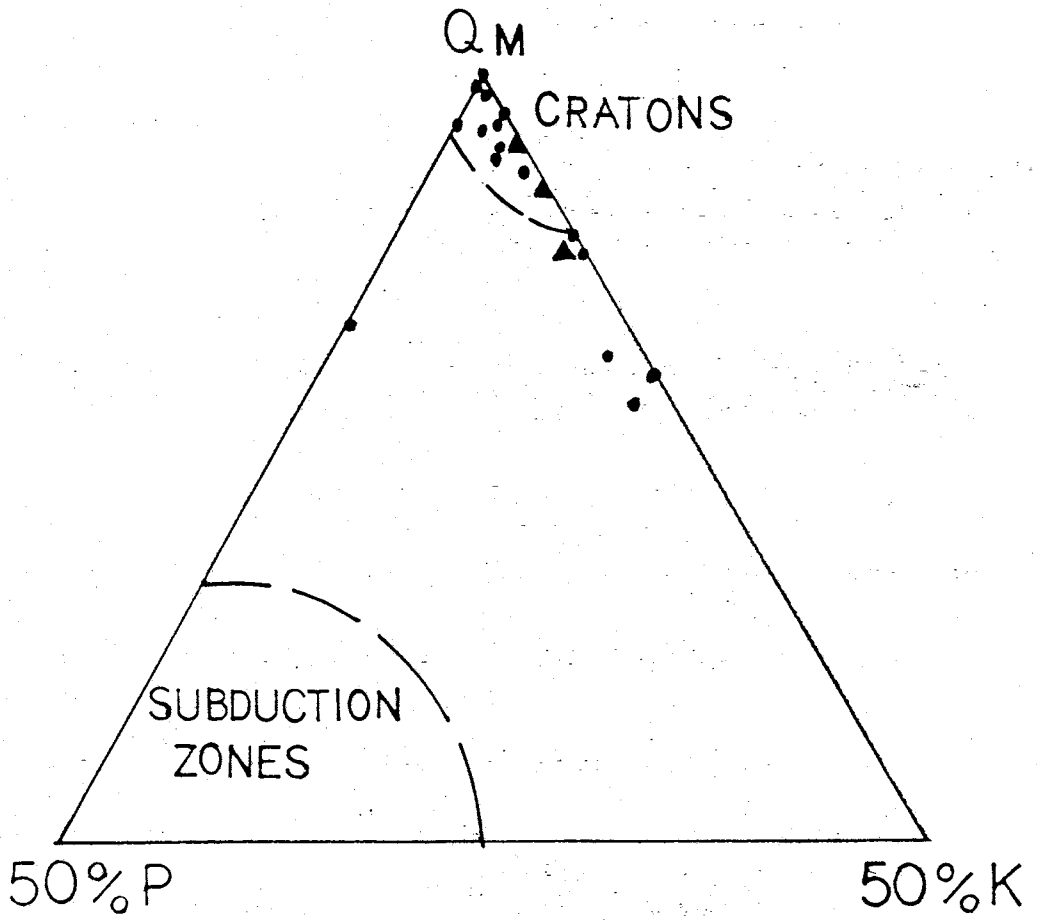

Figure 6. QmPK diagram (modified after Dickinson and Suczek, 1980). See Table 9 for symbols used in figures.
Qm = monocrystalline quartz grains
P = plagioclase grains
K = K-feldspar grains

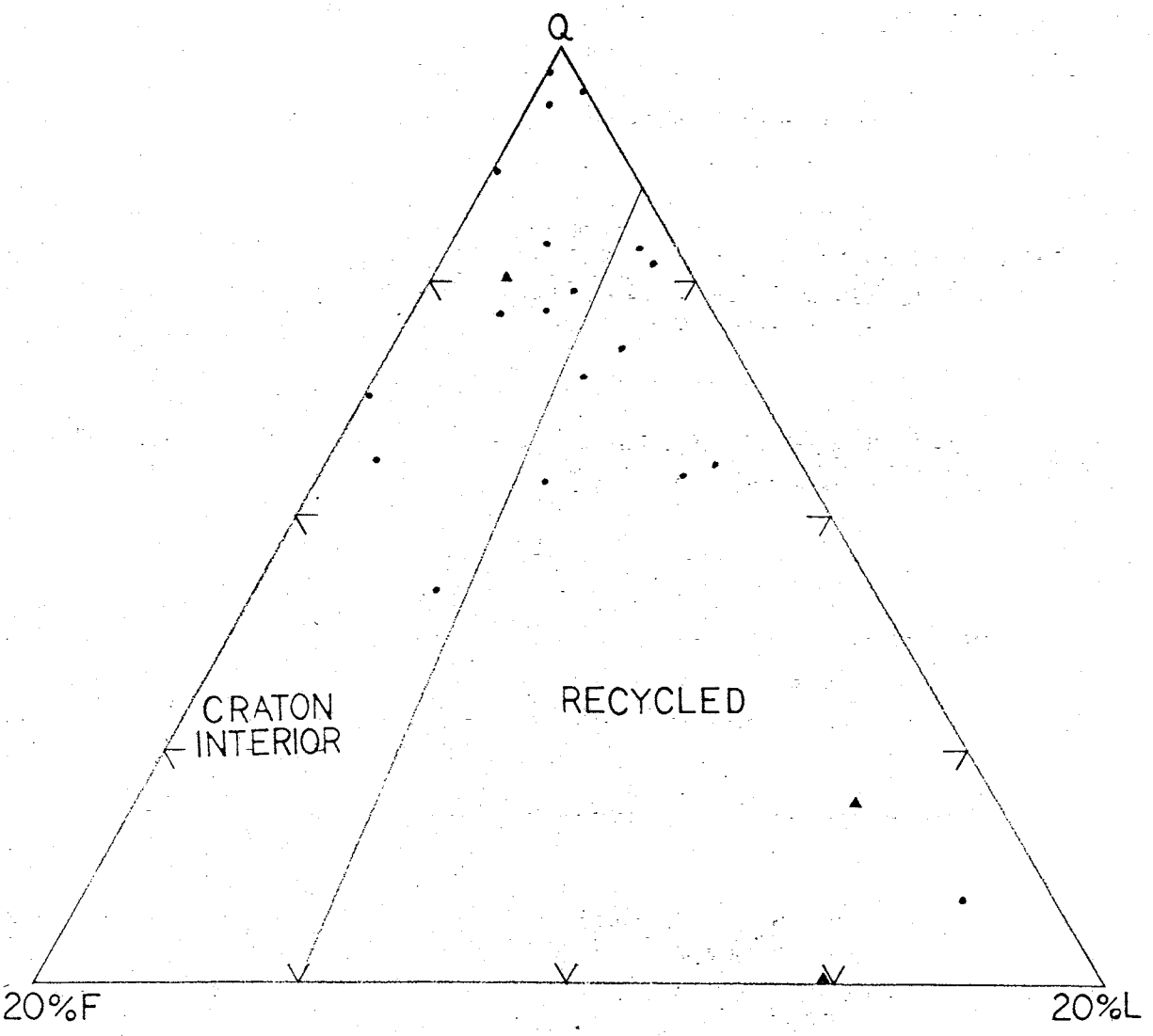

Figure 7. QFL diagram (after Dickinson, 1983).
See Table 9 for symbols used in figures.
Q = all quartz grains
F = all feldspar grains
L = all lithic grains except polycrystalline quartz

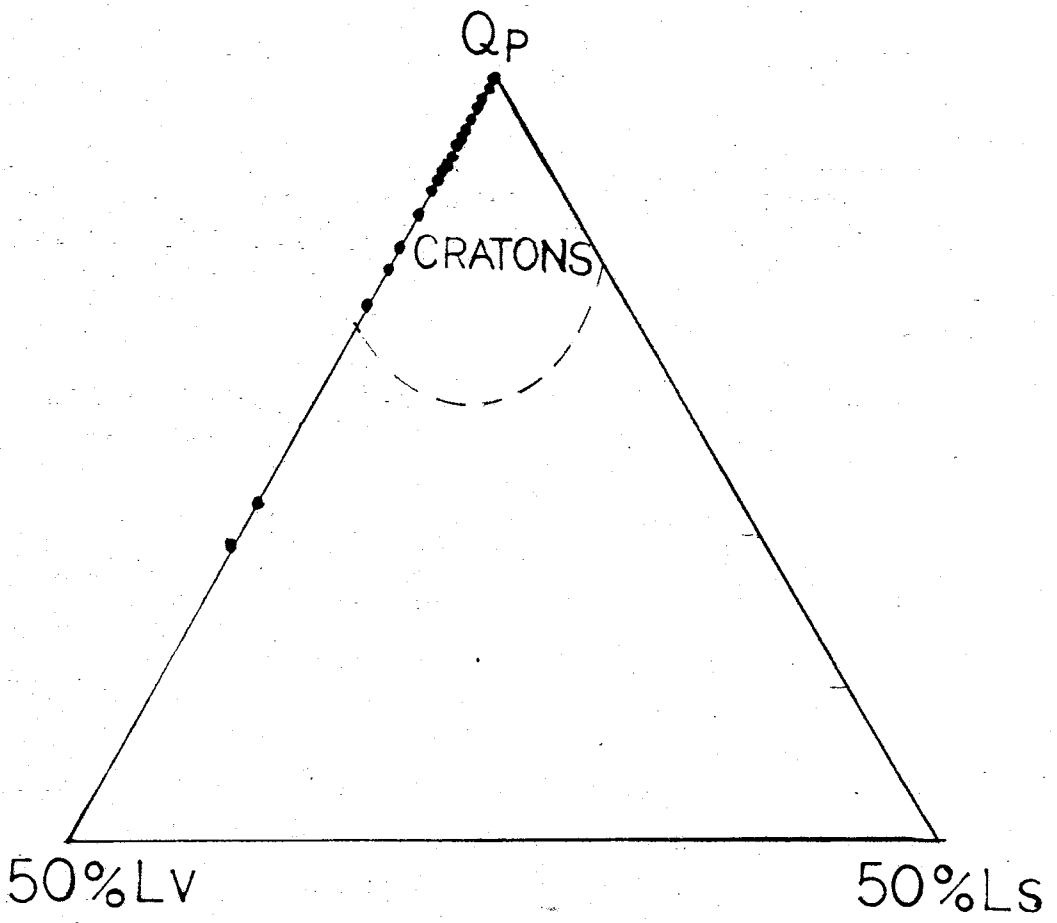

Figure 8. QpLvLs diagram (modified after Dickinson and Suczek, 1980). See Table 9 for symbols used in figures.
Qp = all polycrystalline quartz
Lv = all volcanic lithic grains
Ls = all sedimentary lithic grains

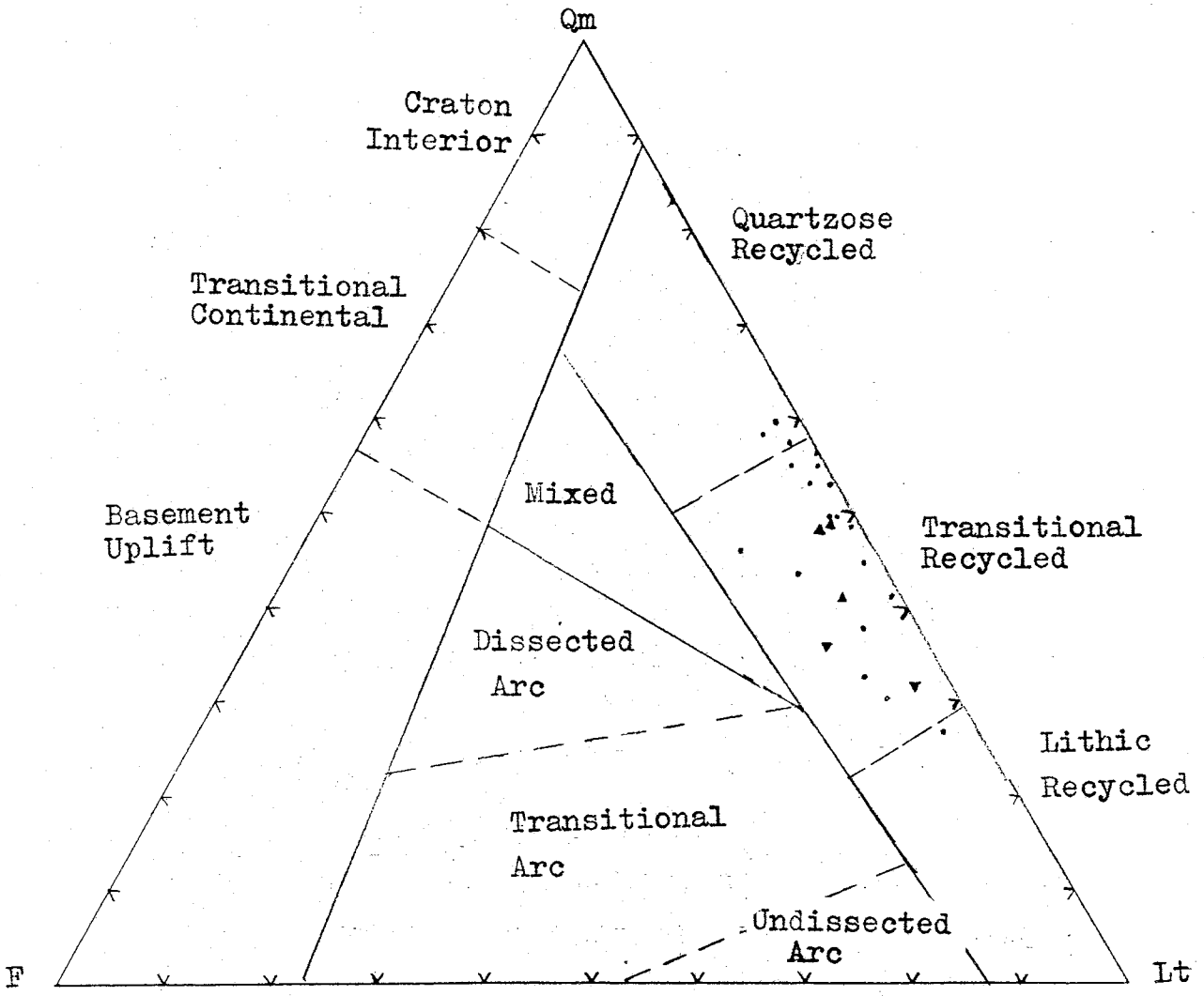

Figure 9. QmFLt diagram (after Dickinson, 1983).
See Table 9 for symbols used in figures.
Qm = all monocrystalline quartz grains
F = all feldspar grains
Lt = all lithic grains

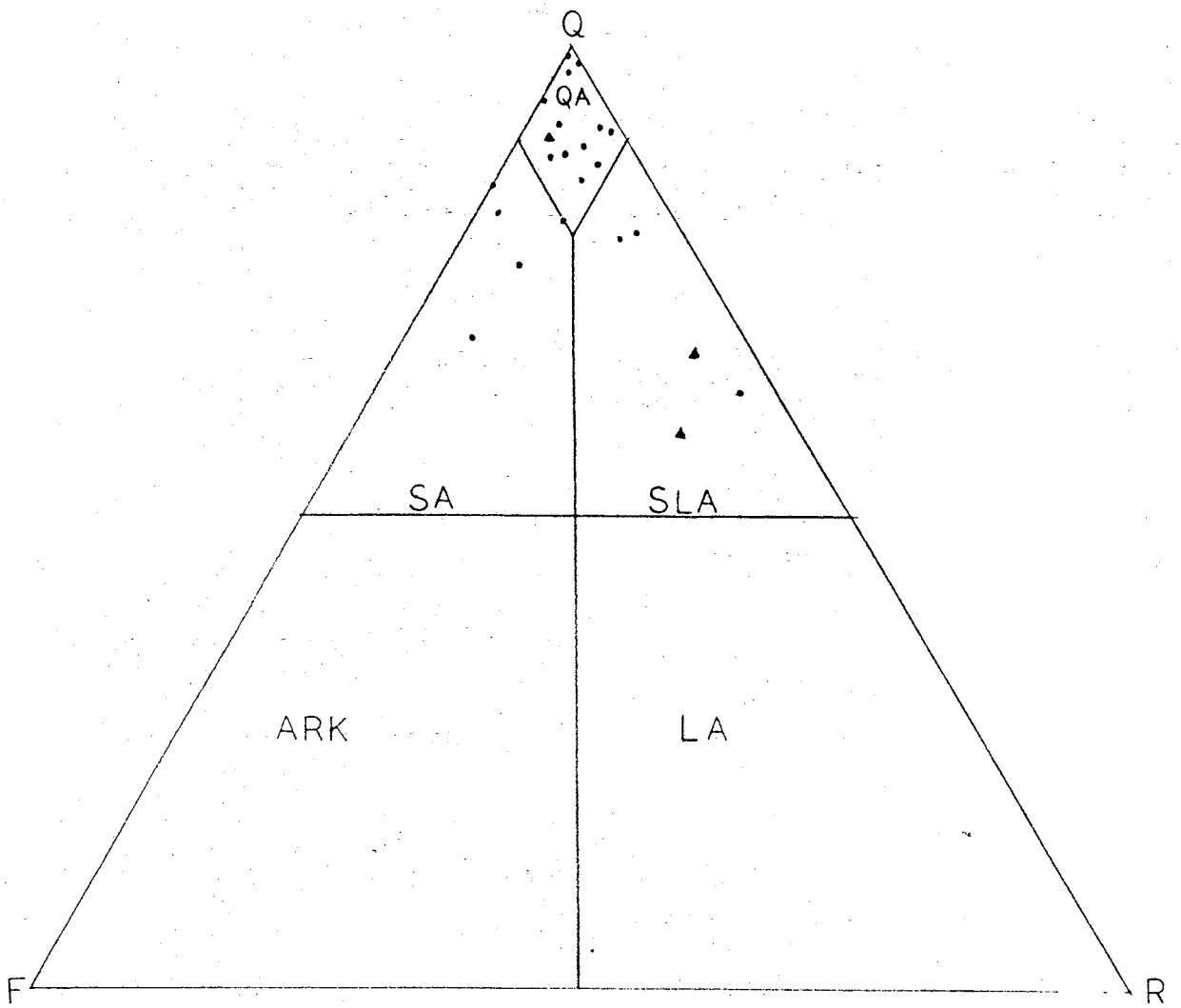

Figure 10. QFR diagram (modified after Folk, 1974).
See Table 9 for symbols used in figures.
Q = all quartz grains
F = all feldspar grains
R = all rock fragments

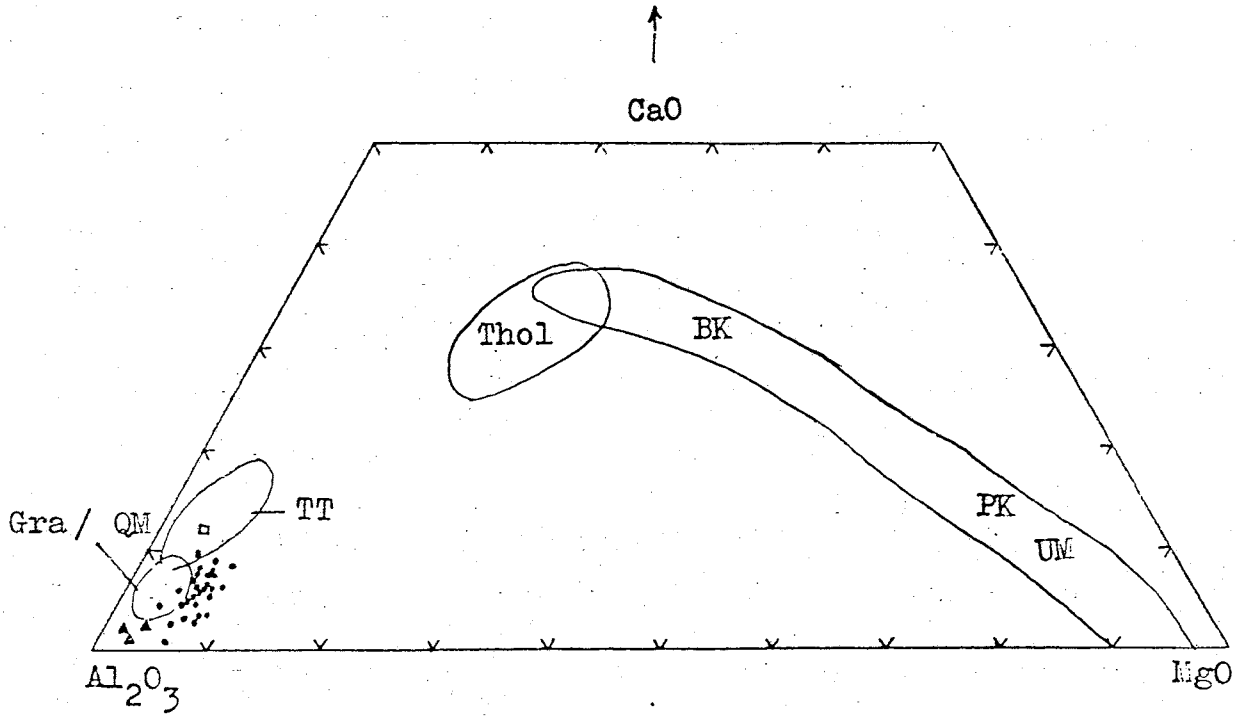

Figure 11. CaO-Al2O3-MgO diagram (fields after Bavinton and Taylor, 1980). See Table 9 for symbols used in figures.

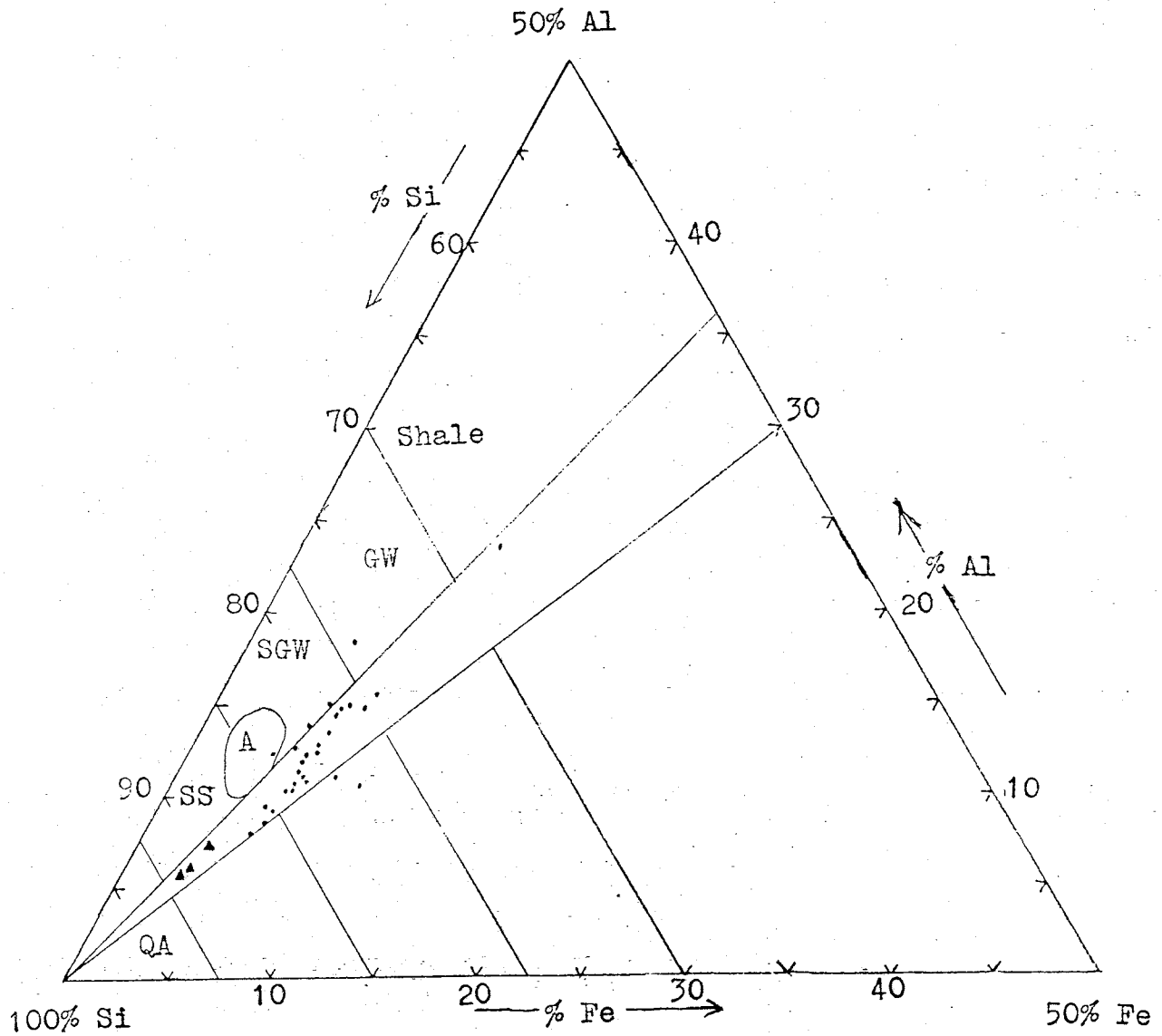

Figure 12. Al-Si-Fe diagram (fields after Moore and Dennon, 1970). See Table 9 for symbols used in figures.

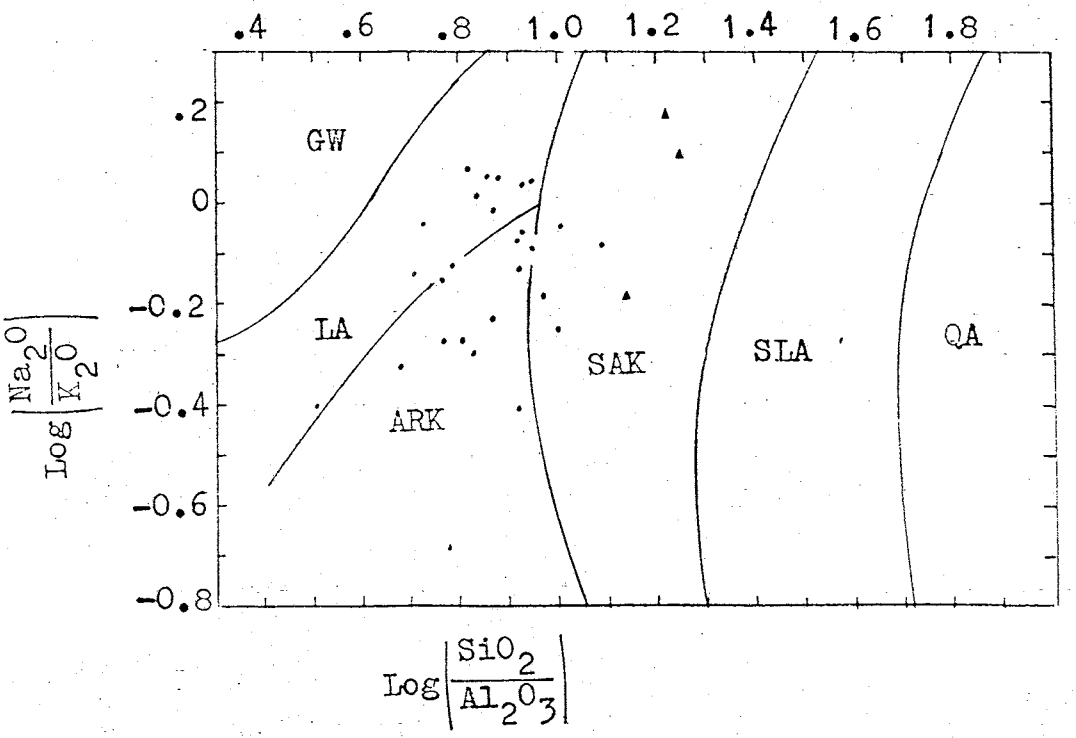

Figure 13. log(Na2O/K2O)-log(SiO2/Al2O3) diagram (fields after Pettijohn, 1963). See Table 9 for symbols used in figures.

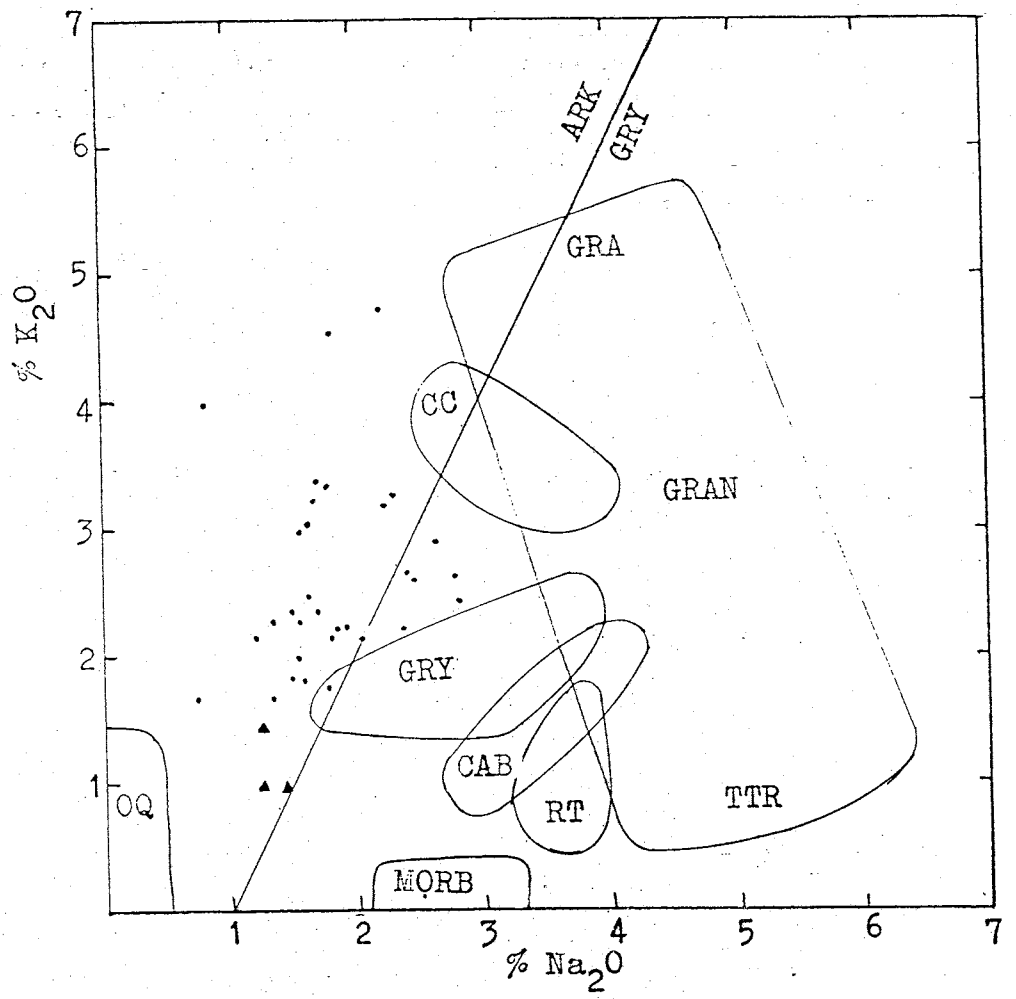

Figure 14. K2O-NaO diagram (modified after Pettijohn, 1963, McLemore, 1980, and fields after Martell, 1982). See Table 9 for symbols used in figures.

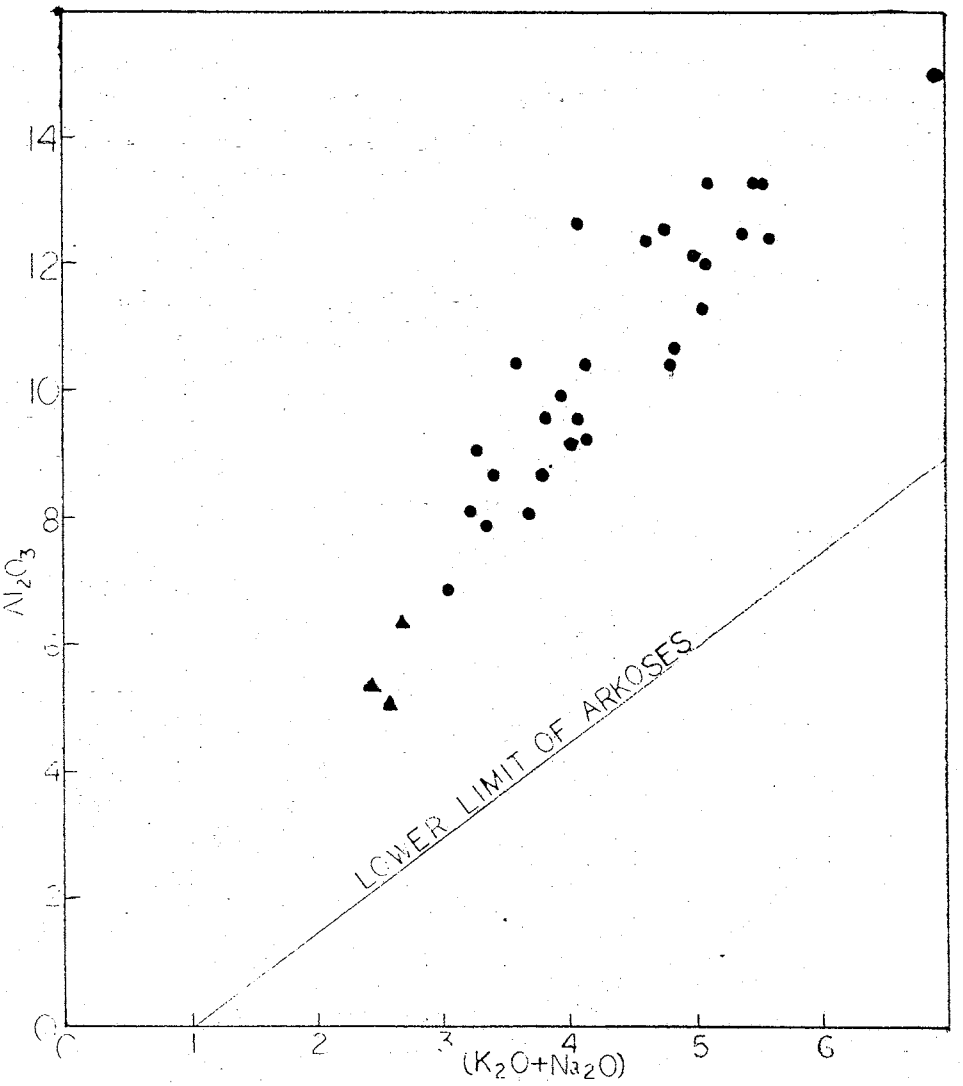

Figure 15. (K2O+Na2O)-Al2O3 diagram (modified after Pettijohn, 1963). See Table 9 for symbols used in figures.

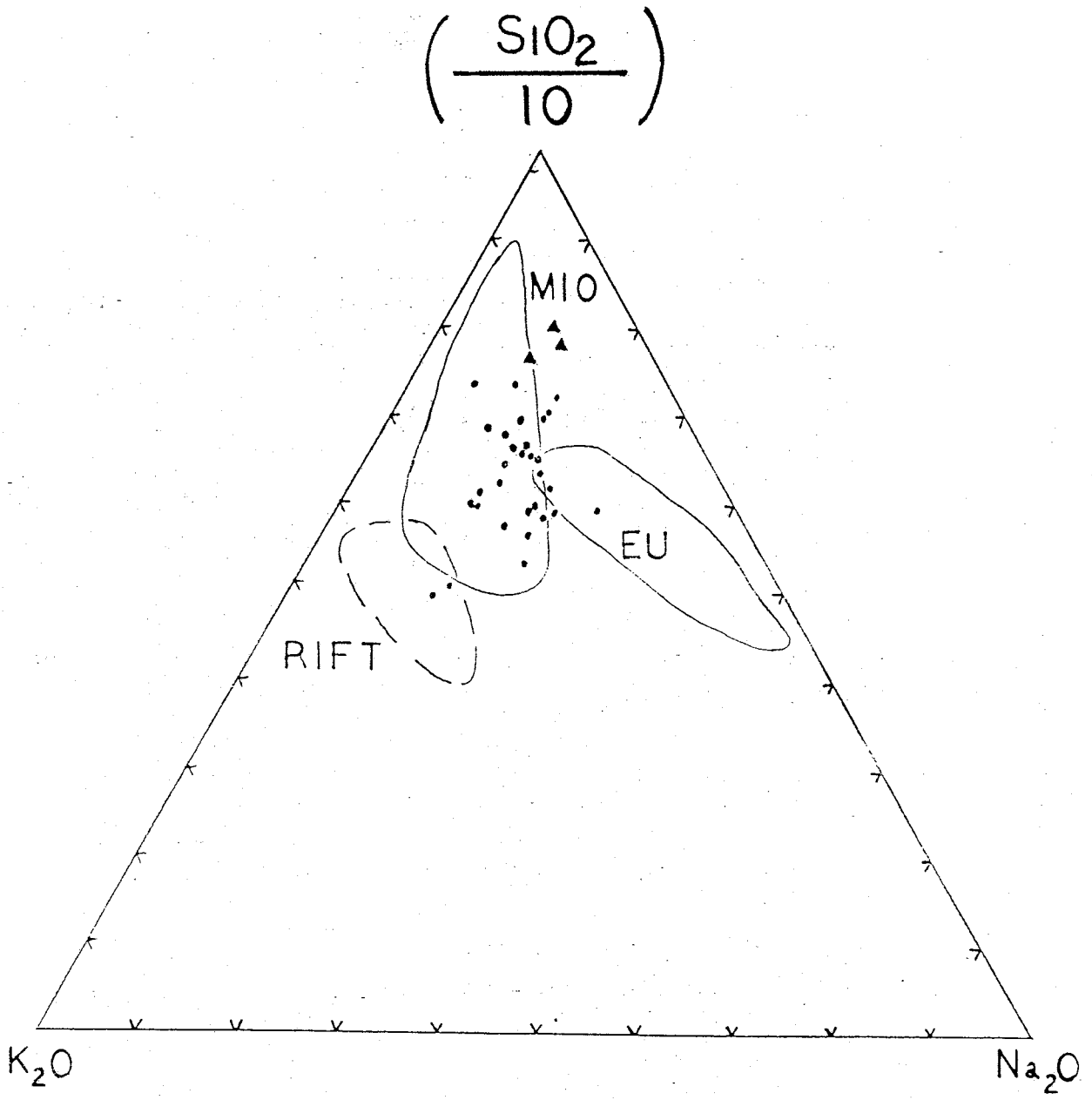

Figure 16. (SiO2/10)-K2O-Na2O diagram (after Schwab, 1973, and fields after McLemore, 1980).
Mio = sandstones of miogeosynclinal origin
Eu = sandstones of eugeosynclinal origin
Rift = sandstones of rift origin
See Table 9 for symbols used in figures.

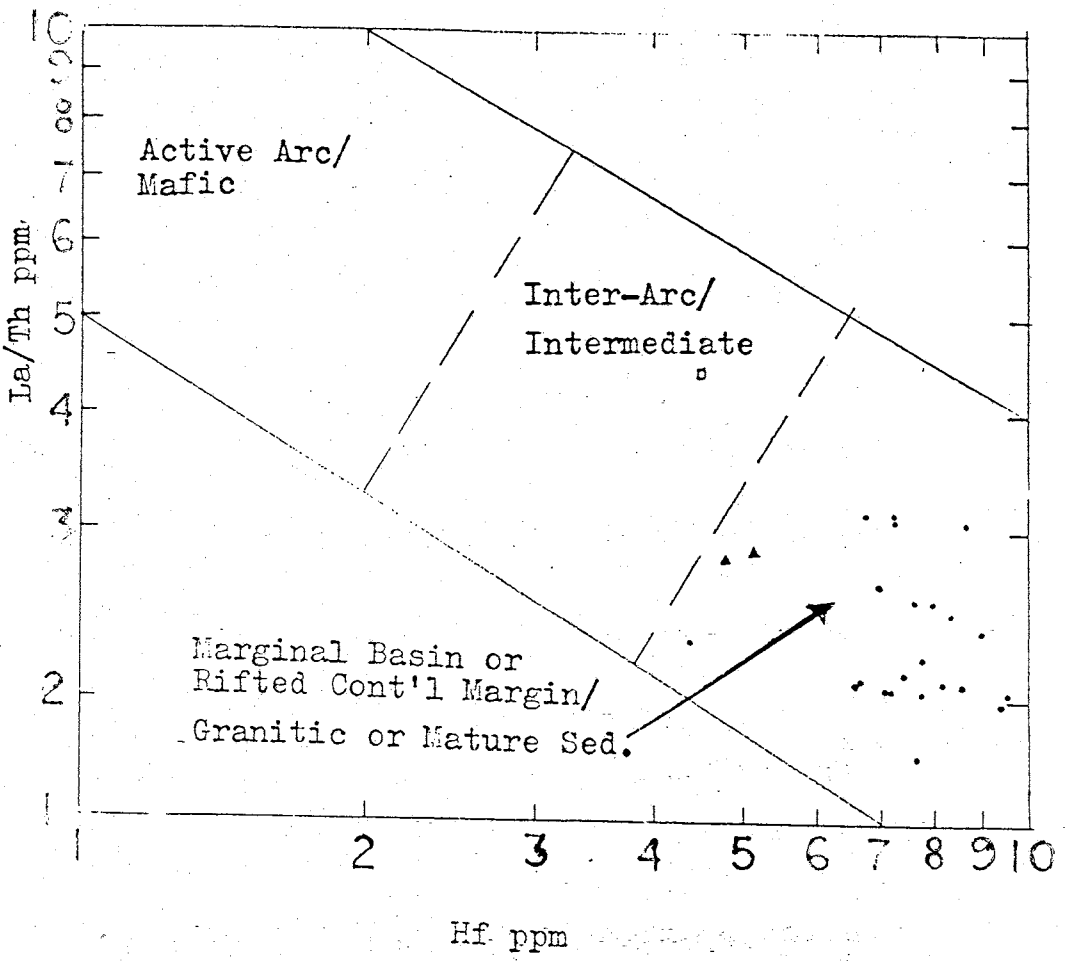

Figure 17. (La/Th)-Hf (ppm) diagram (modified after Bathia and Taylor, 1981). See Table 9 for symbols used in figures.

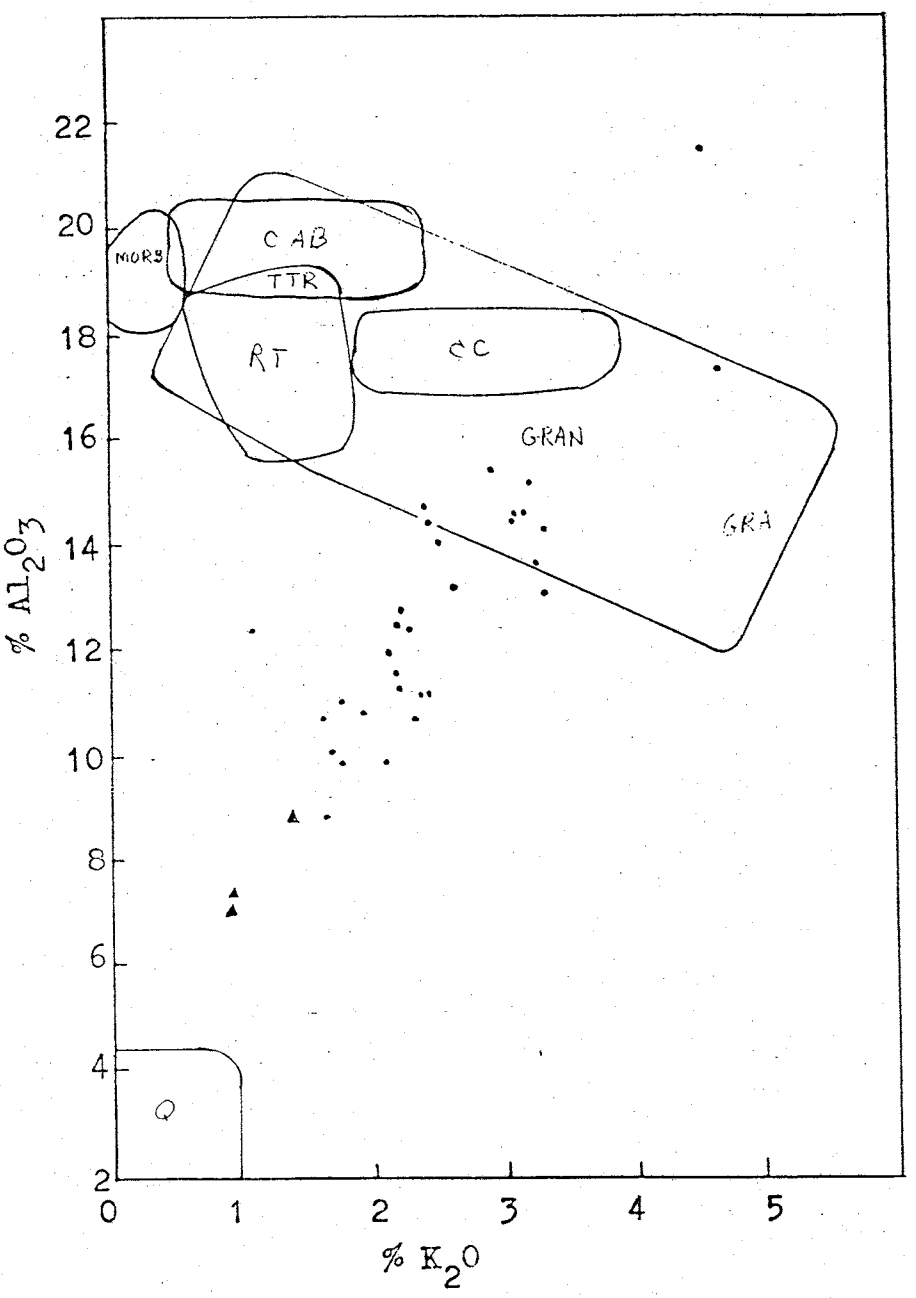

Figure 18. Al2O3-K2O diagram (fields after Martell,1982). See Table 9 for symbols used in figures.

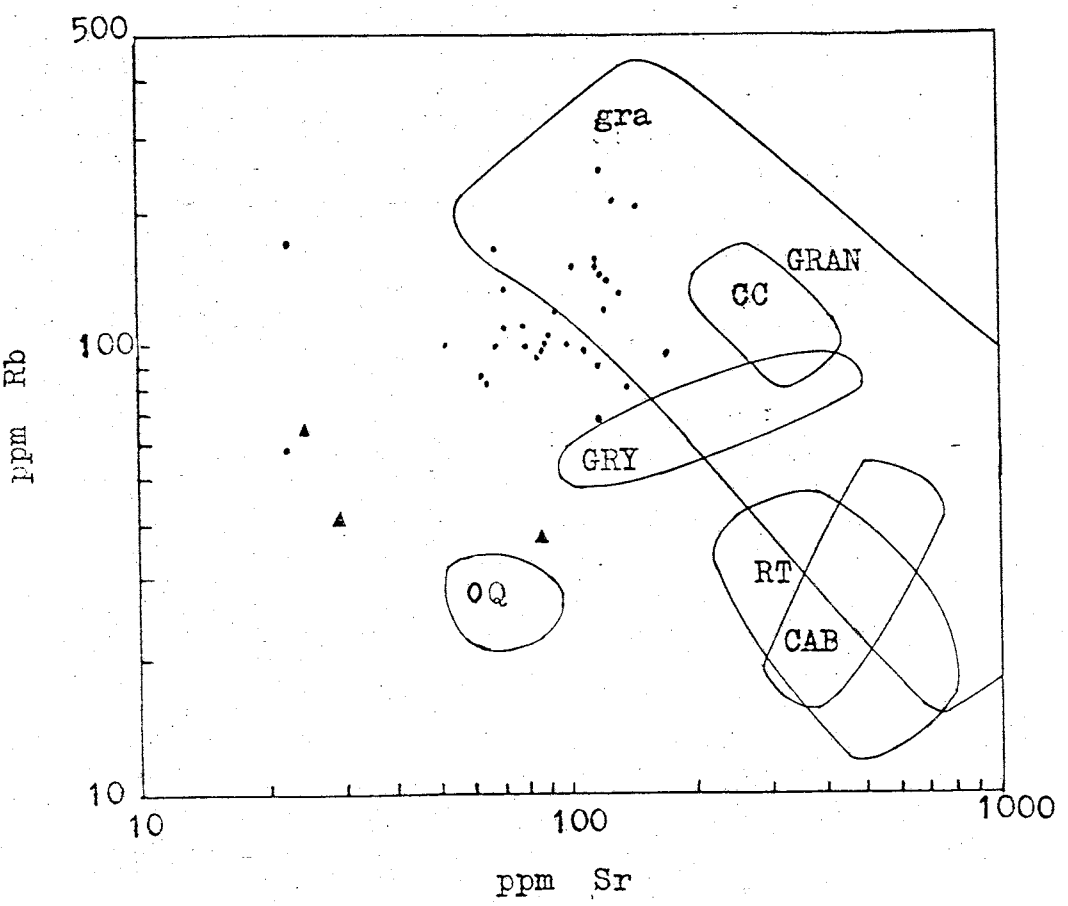

Figure 19. Rb-Sr (ppm) diagram (fields after Martell, 1982). See Table 9 for symbols used in figures.

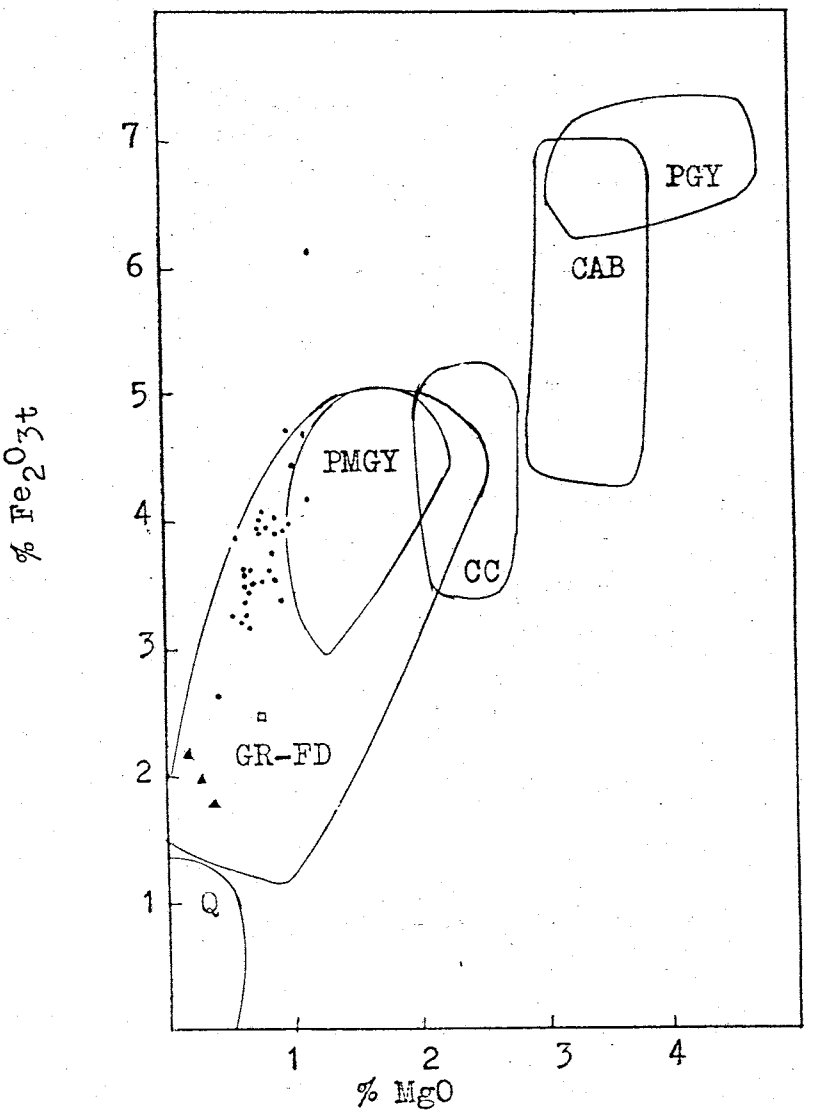

Figure 20. Fe2O3T-MgO diagram (fields after Martell, 1982). See Table 9 for symbols used in figures.

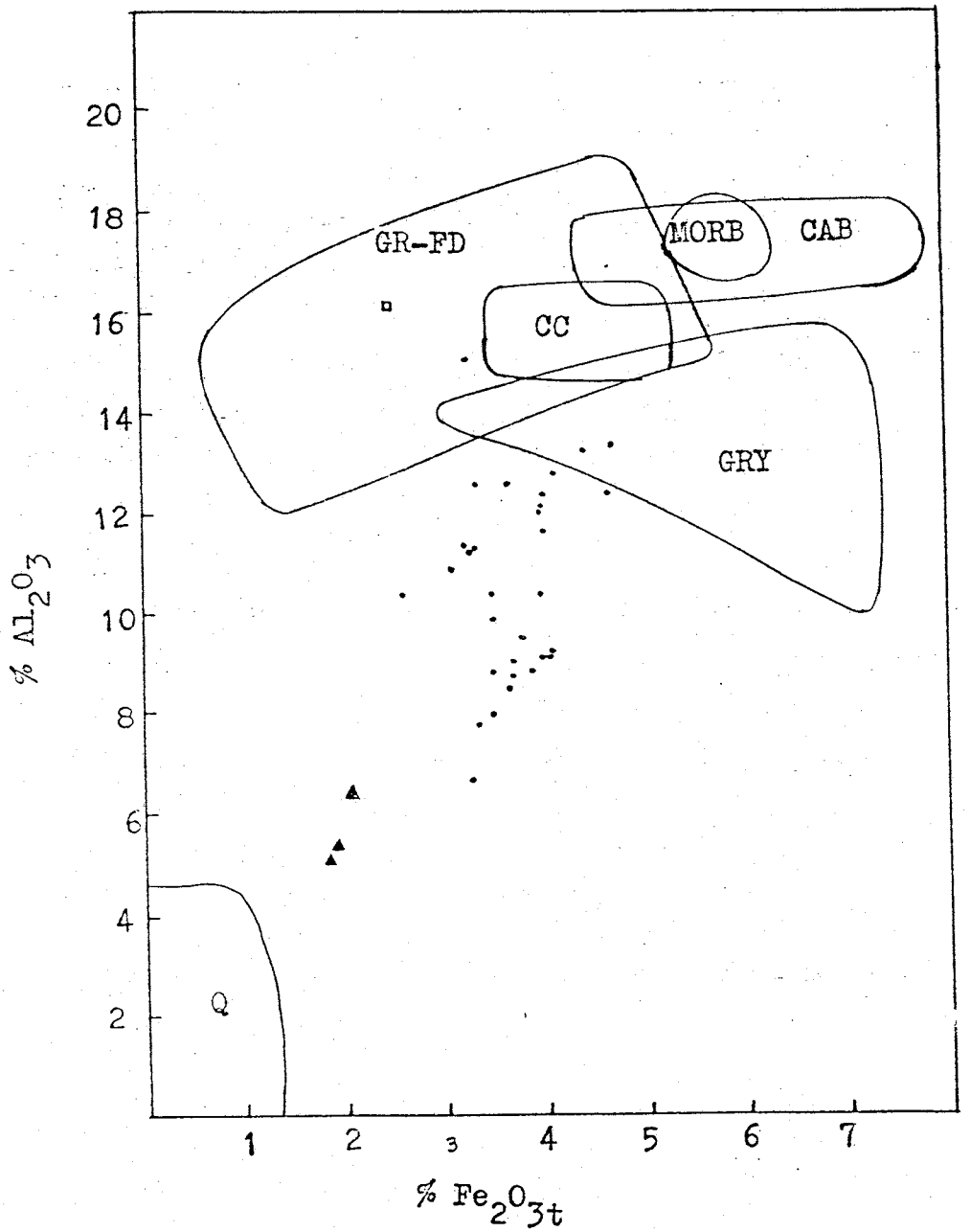

Figure 21. Al2O3-Fe2O3T diagram (fields after Martel, 1982). See Table 9 for symbols used in figures.

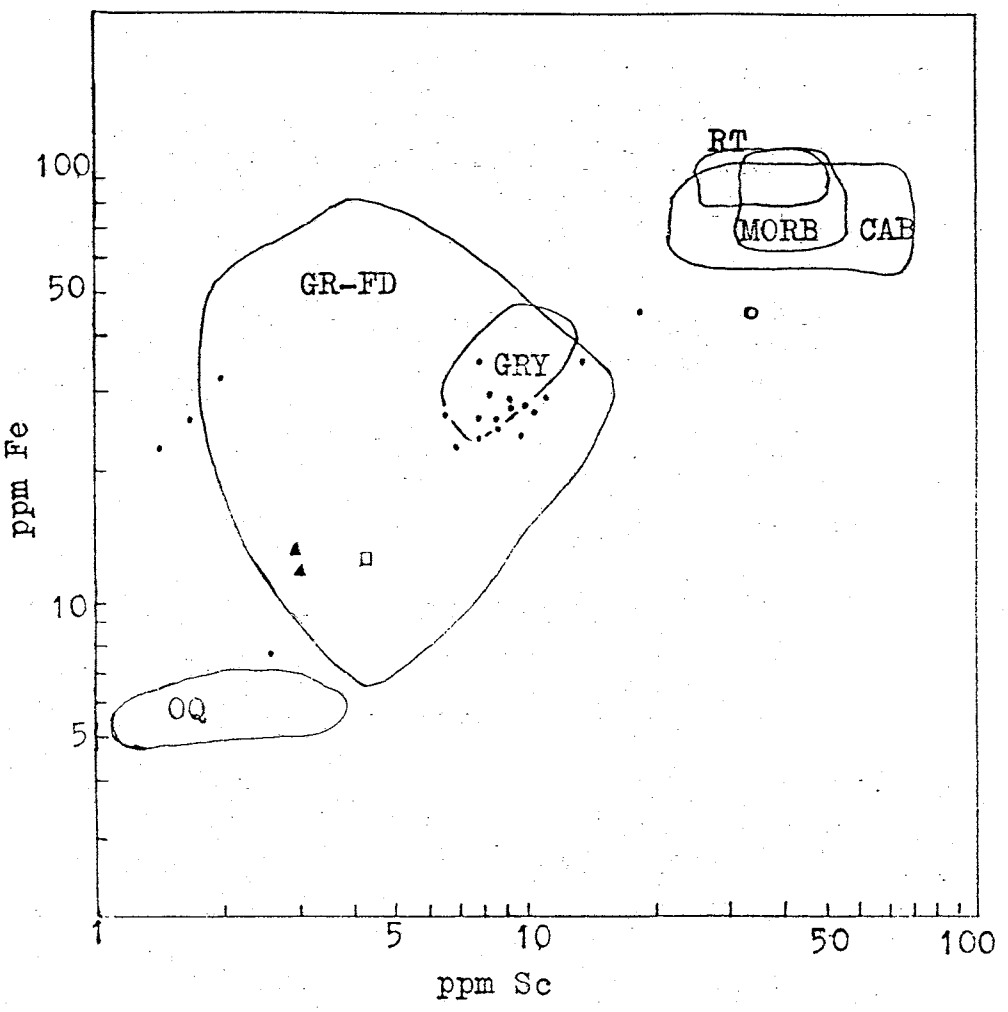

Figure 22. Fe-Sc (ppm) diagram (fields after Martell, 1982). See Table 9 for symbols used in figures.

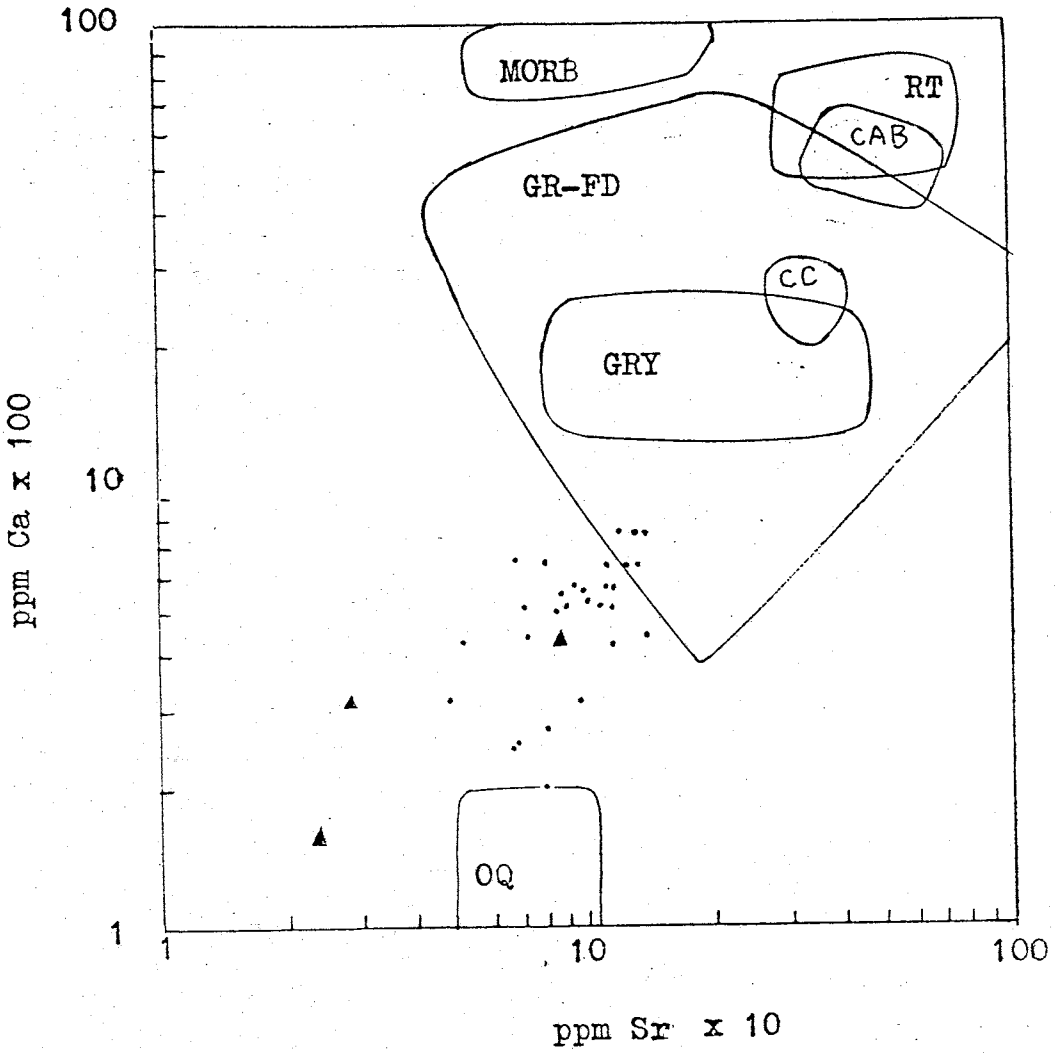

Figure 23. Ca-Sr (ppm) diagram (fields after Martell, 1982). See Table 9 for symbols used in figures.

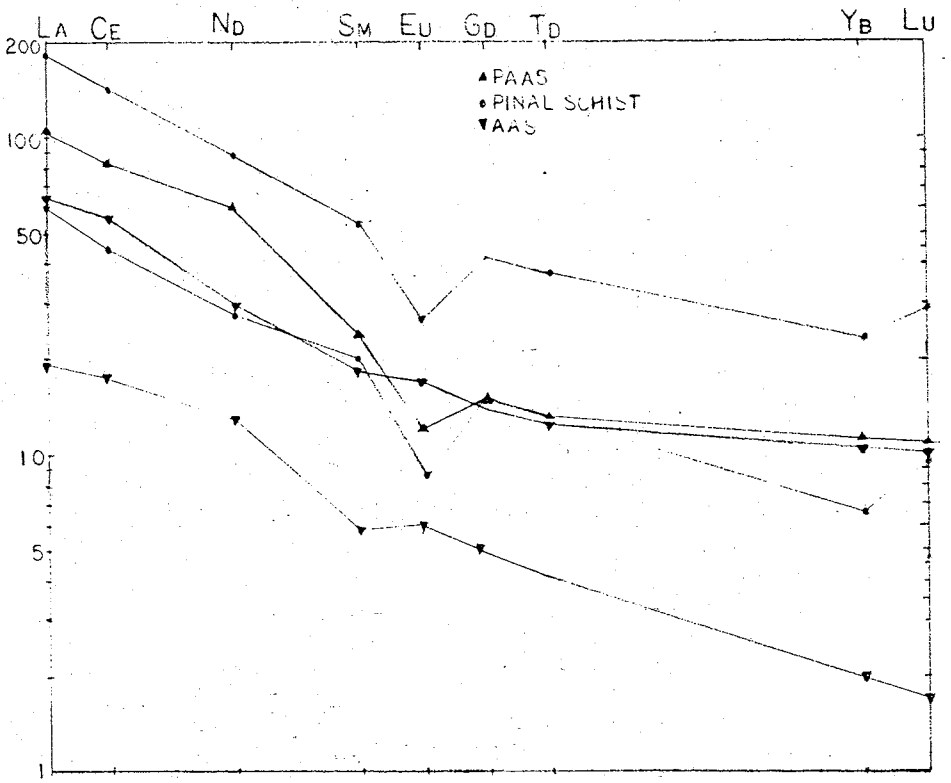

Figure 24. Rare-earth element envelope of Pinal Schist compared to envelope of average Archean sediment (AAS) and to average post-Archean Austrialian sediment (APASS) (AAS and APASS after Taylor and McLennan, 1980).

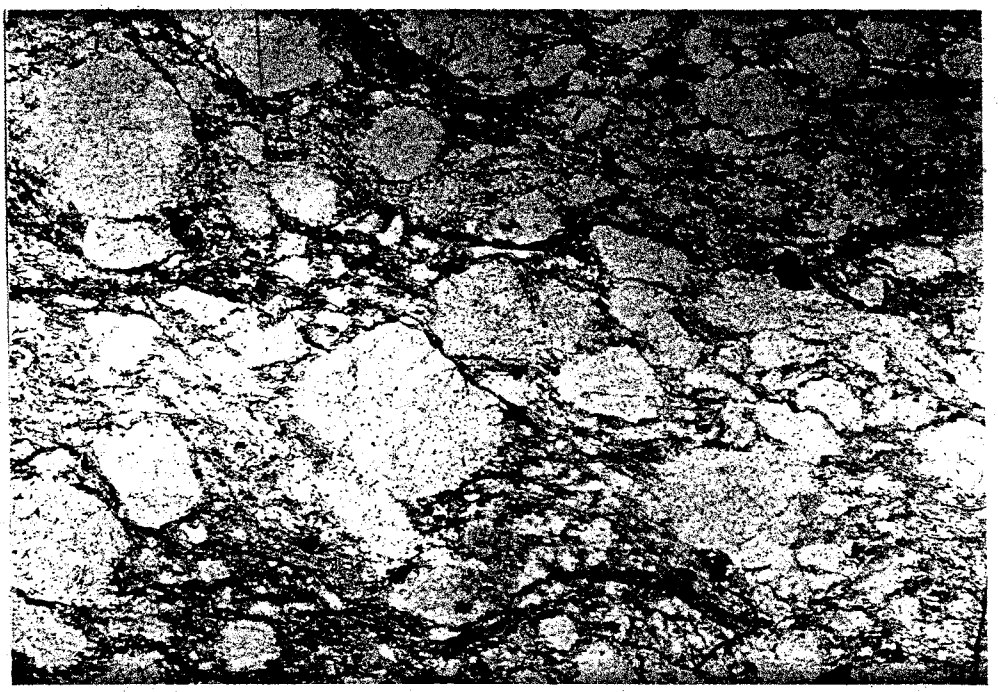

1MM

1MM

Plate 1. Chlorite-biotite-sericite-quartz schist, showing bimodal grainsize and poor sorting, sub-angular to sub-rounded, sub-spherical to elongate grains, and fine grain matrix. Plane-polar light.

Plate 2. Same as Plate 1, except cross-polar light. Note micro-graphitic intergrowth of quartz and feldspar in fine-sand-sized detrital grain (center).

Plate 3. Tourmaline crystal showing sub-spherical, well-rounded, silt-sized detrital core; matrix is sericite and opaques. Looking down c-axis detrital core is pale-brown, overgrowth is blue. Plane-polar light.

Plate 4. Tourmaline crystal showing spherical, well-rounded, silt-sized detrital core; matrix is quartz, sericite, and chlorite. Oriented perpendicular to c-axis and shown in plane-polar light at minimum absorption. At maximum absorption detrital core is brown and overgrowth is blue-green.

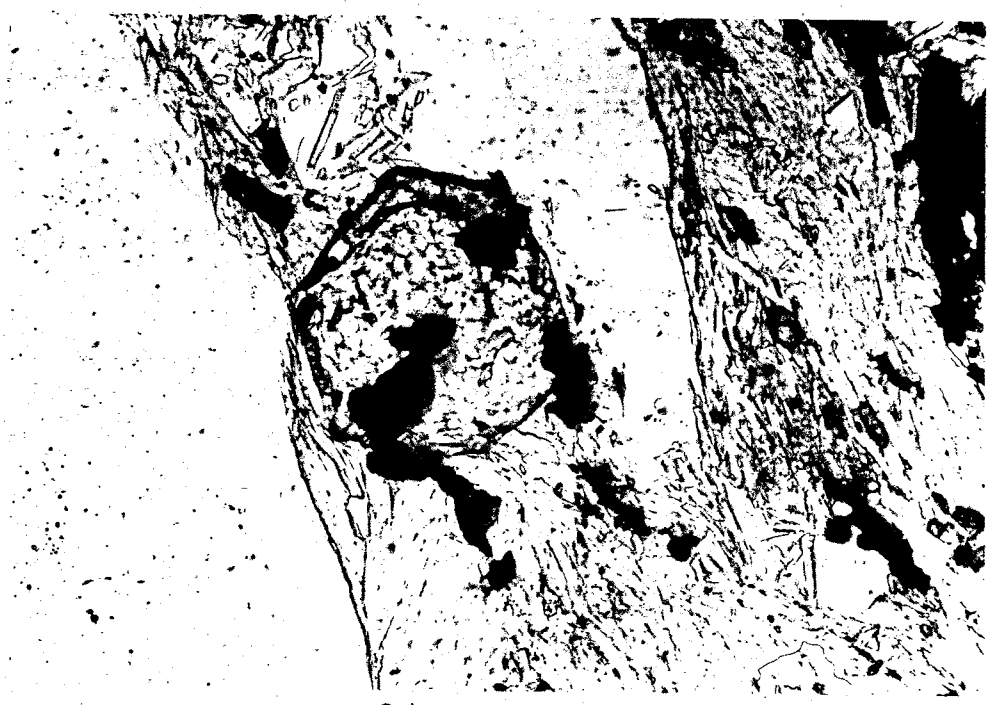

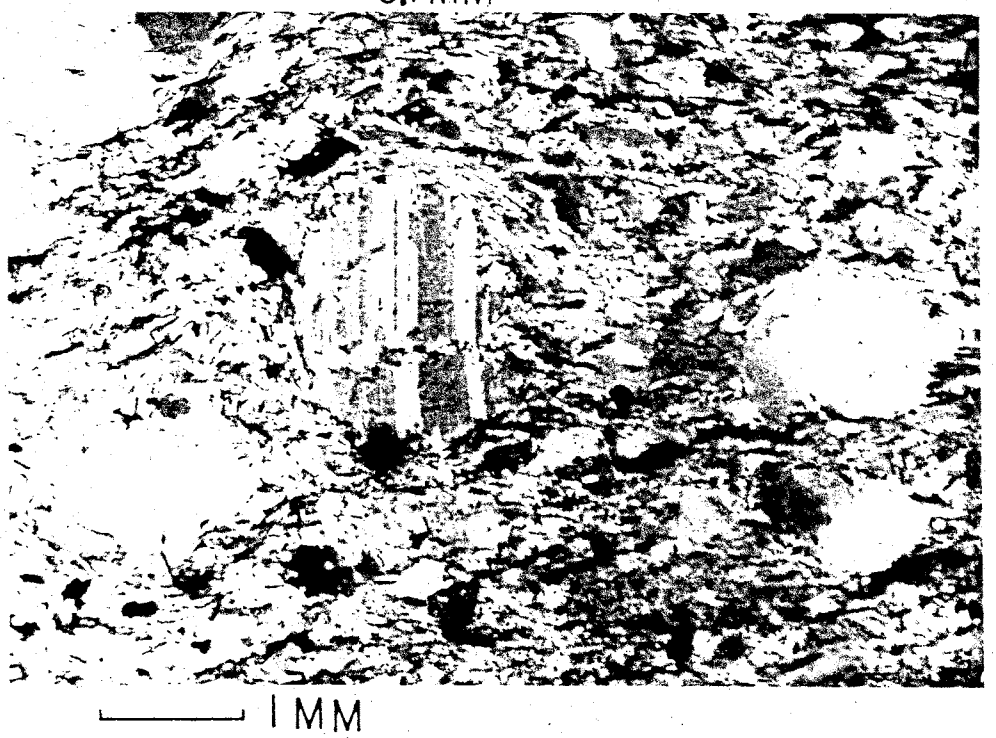

Plate 5. Garnet crystal showing rounded, sub-spherical, silt-sized detrital core; in a matrix of quartz and sericite. Plane-polar light.

Plate 6. Fine-sand-sized, rounded, subspherical detrital plagioclase grain; matrix is quartz, sericite, chlorite. Cross-polar light.

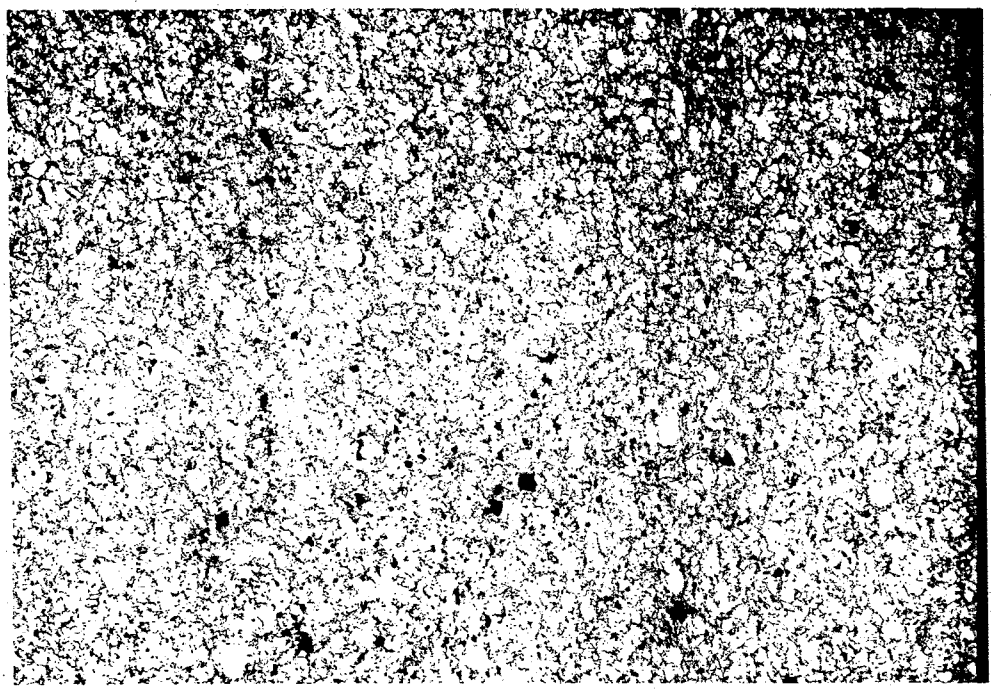

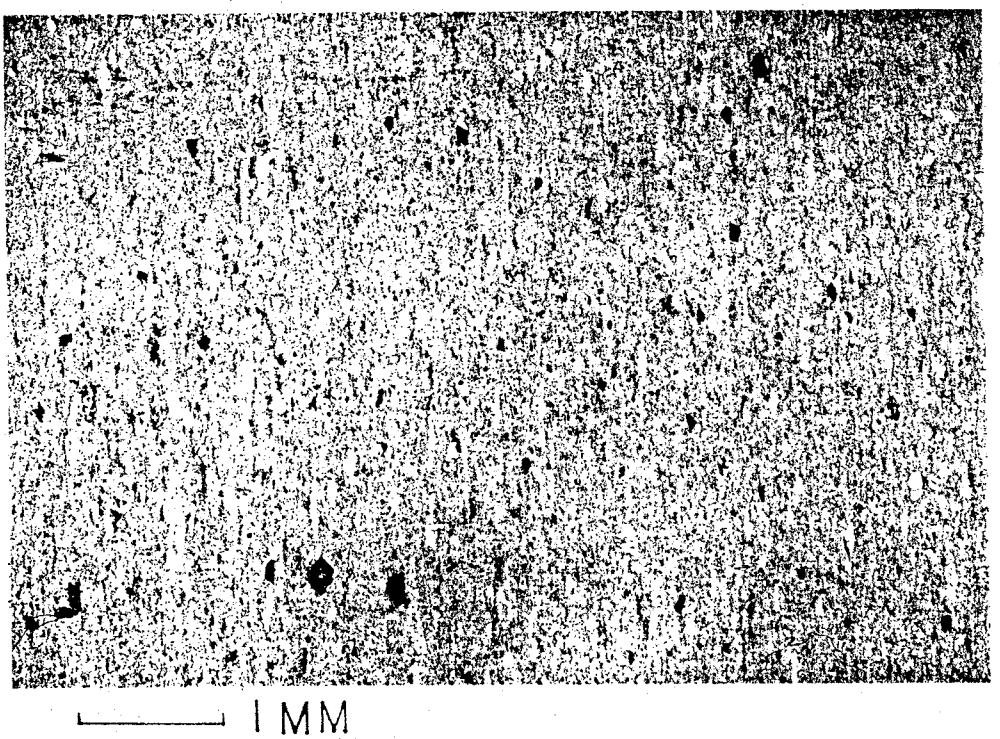

Plate 7. Laminated fine-grain phyllite shows foliation, fine-sand- and silt-sized clasts of quartz, cross-foliation, and segregation of dark and light minerals. Plane-polar light.

Plate 8.Very fine-grain phyllite shows foliation and silt-sized relic clasts. Plane-polar light.

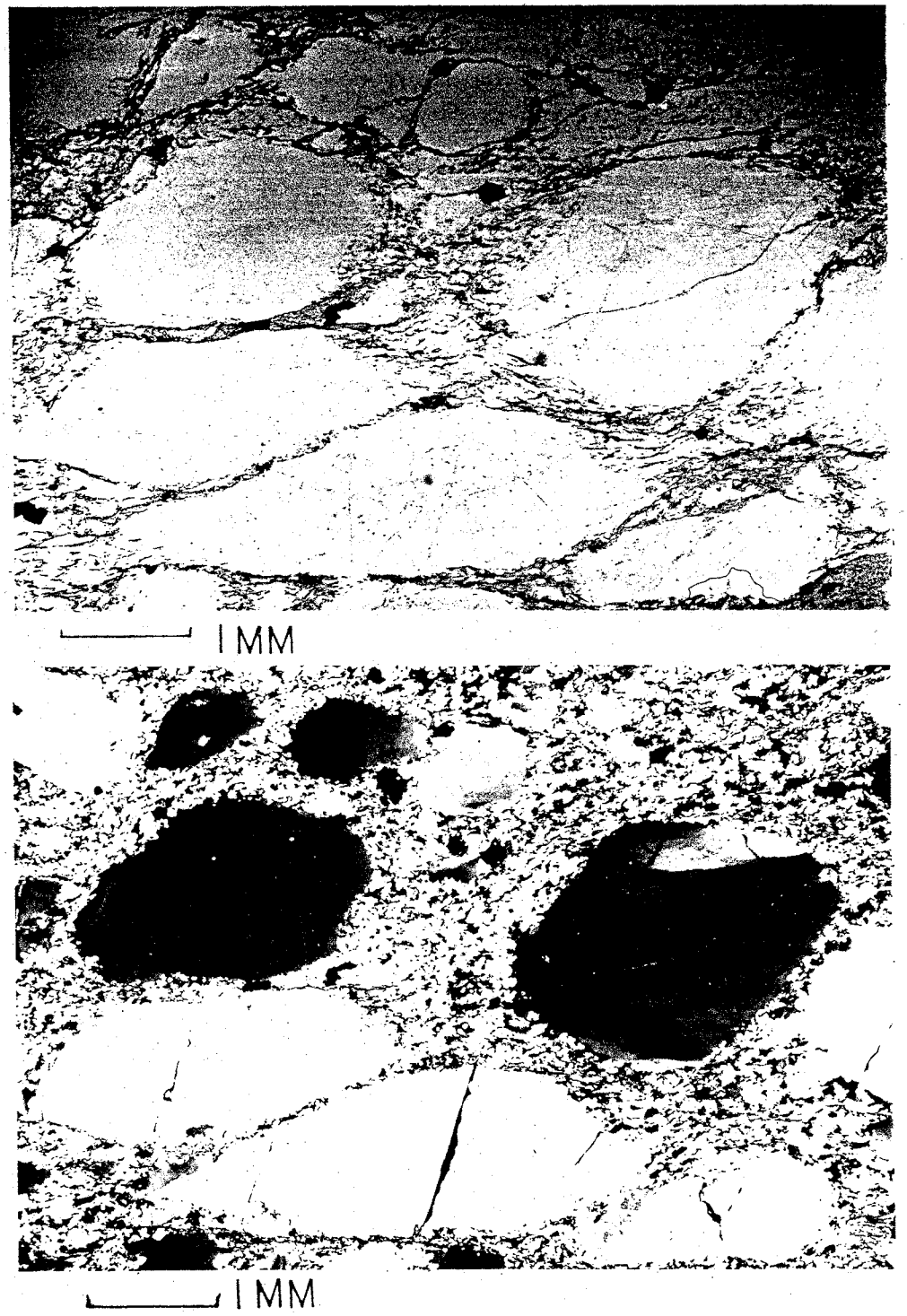

Plate 9. Coarse-sand- to medium-sand-sized, well-rounded, elongate monocrystalline quartz clasts showing inclusions and fractures; matrix is recrystallized quartz and sericite. Note recrystallized rock fragment in upper right-hand corner. Plane-polar light

Plate 10. Same as Plate 9, except cross-polar light. Note undulatory extinction in monocrystalline quartz, and how well rock fragment blends in to matrix.

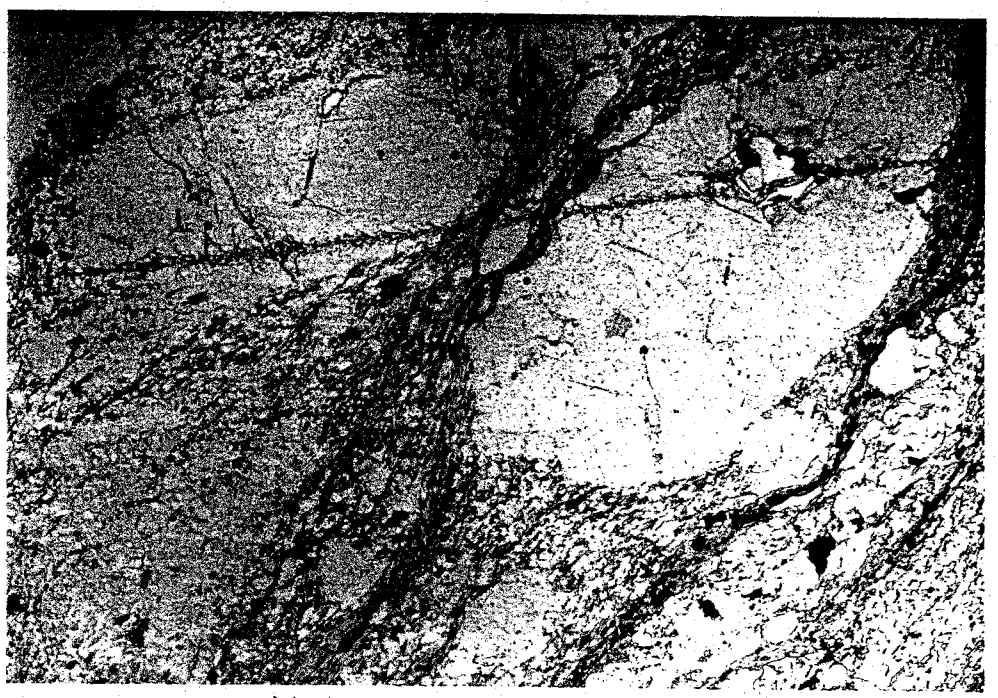

1MM

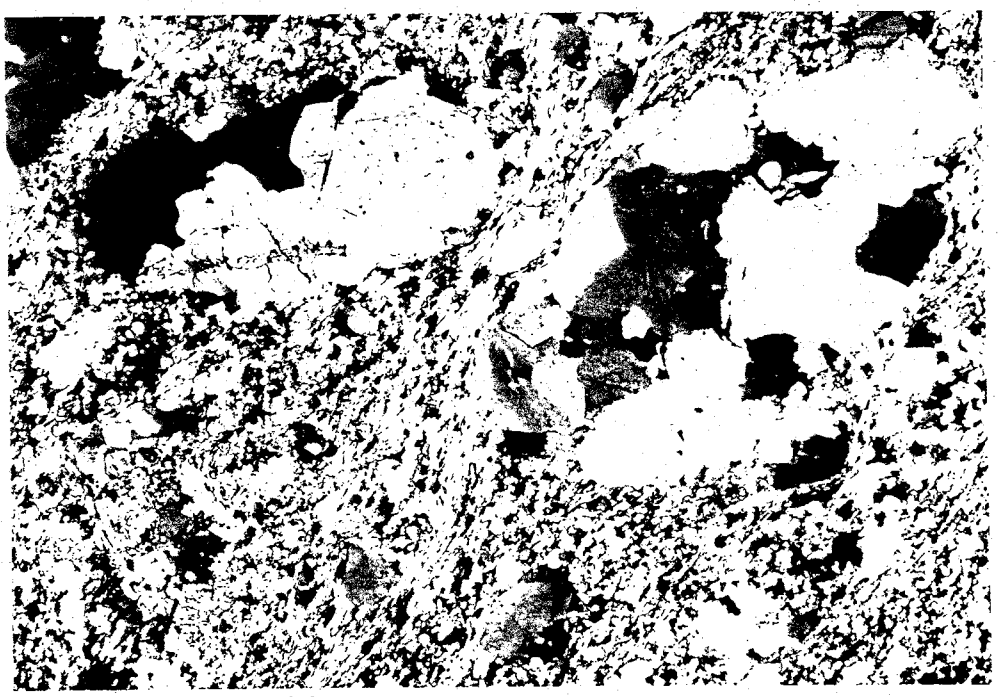

1MM

Plate 11. Coarse-sand-sized, well-rounded, elongate, coarsely-polycrystalline quartz grains; matrix is quartz, sericite, and chlorite. Diagonal line is a scratch on the rock thin-section surface.

Plate 12. Same as Plate 11, except cross-polar light. Note widely divergent domains of individual crystals.

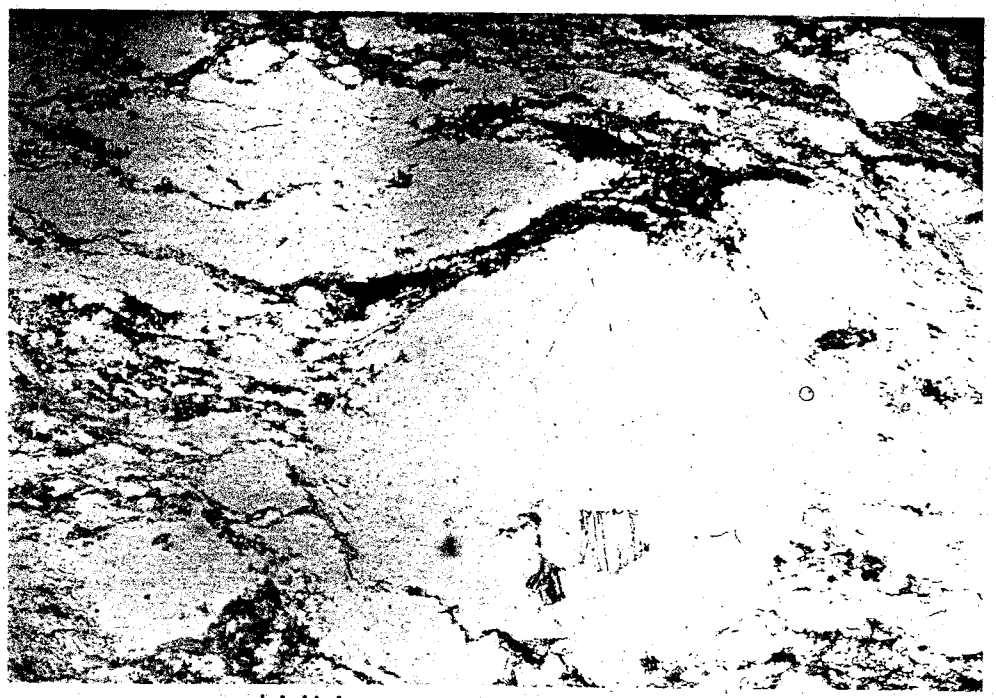

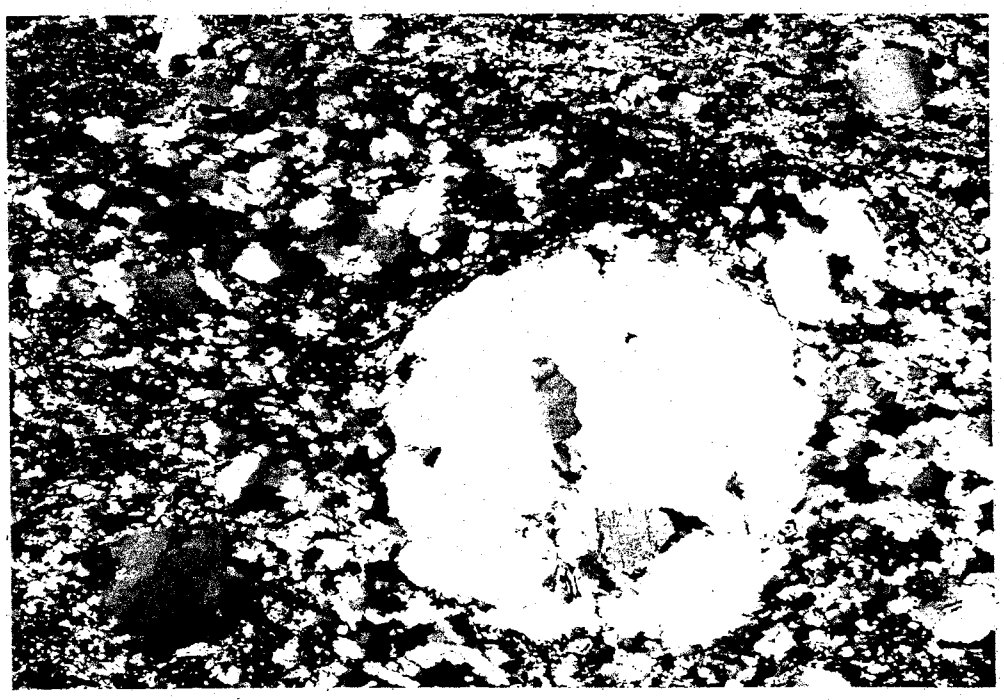

Plate 13. Well-rounded, medium-sand-sized, spherical, monocrystalline quartz grain showing inclusion of muscovite. Note spindle-shaped polycrystalline quartz grain in upper left-hand corner. Plane-polar light.

Plate 14. Same as Plate 13 except cross-polar light. Note finely-polycrystalline quartz grains, and recrystallization of matrix.

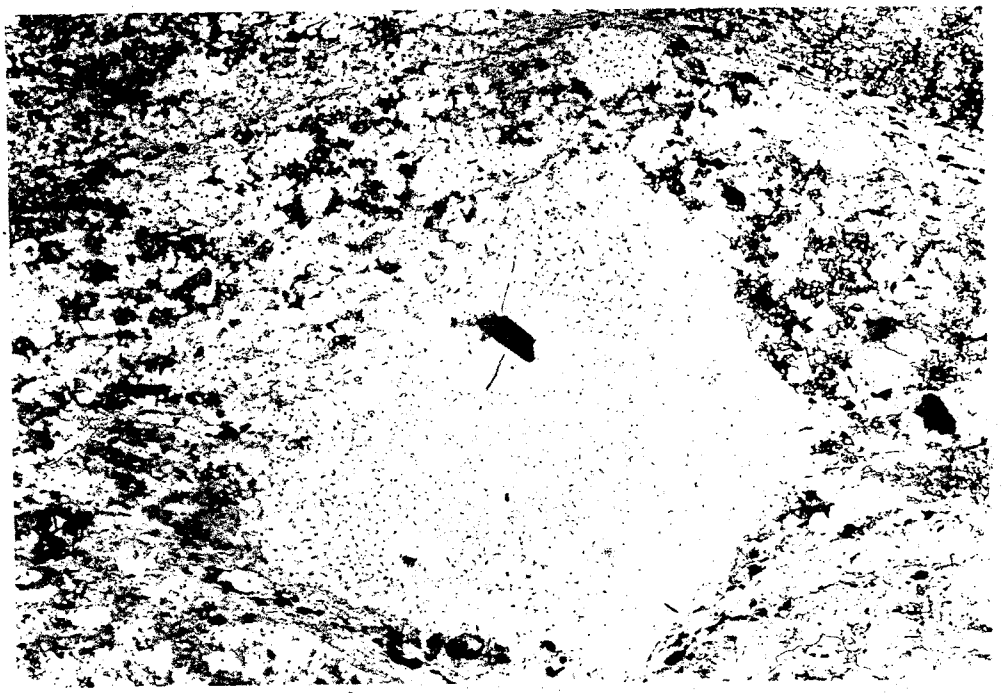

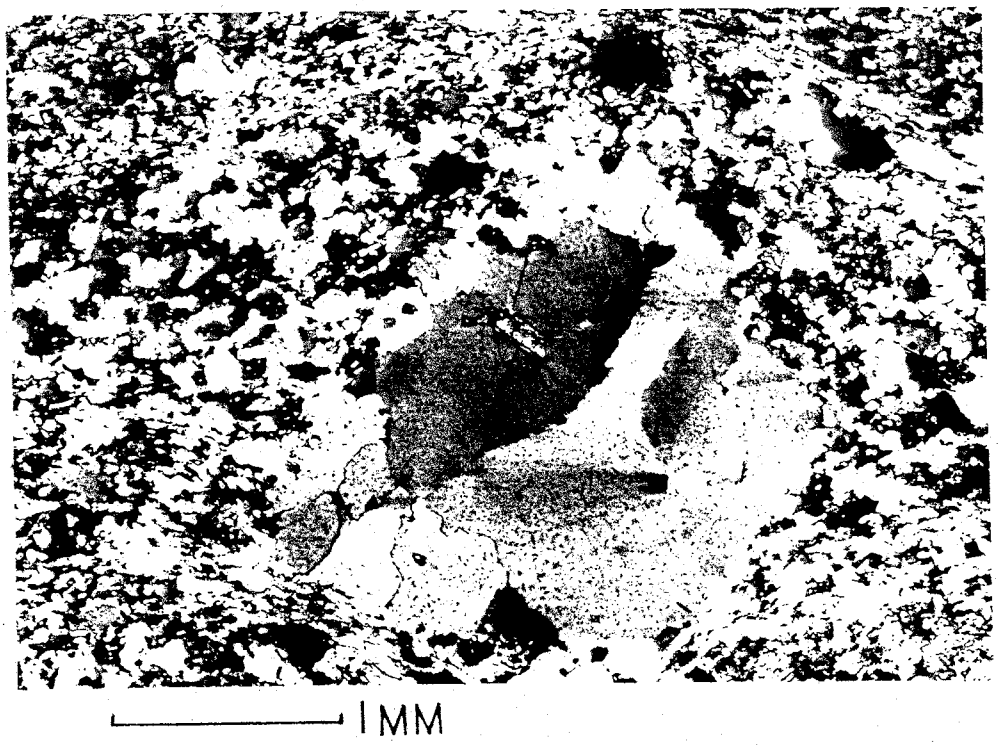

Plate 15. Sub-angular, blocky, medium-sand-sized, coarsely-polycrystalline quartz grain showing rutile inclusion. Note lithic grain deformed around upper half of quartz grain. Plane-polar light.

Plate 16. Same as 15 except cross-polar light; note recrystallization of lithic grain.

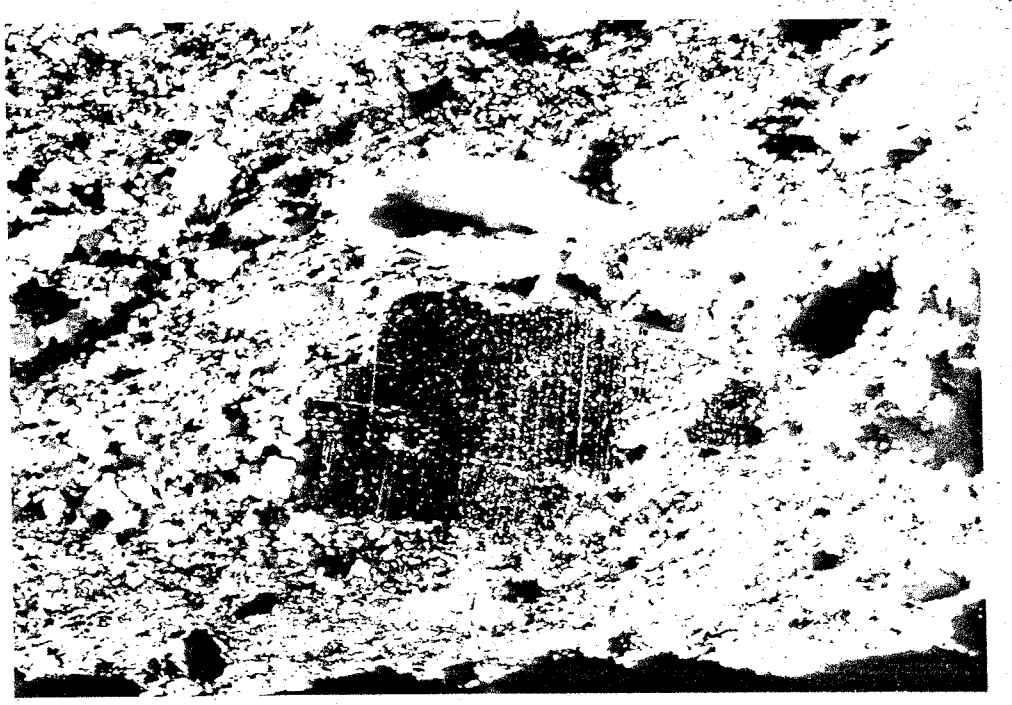

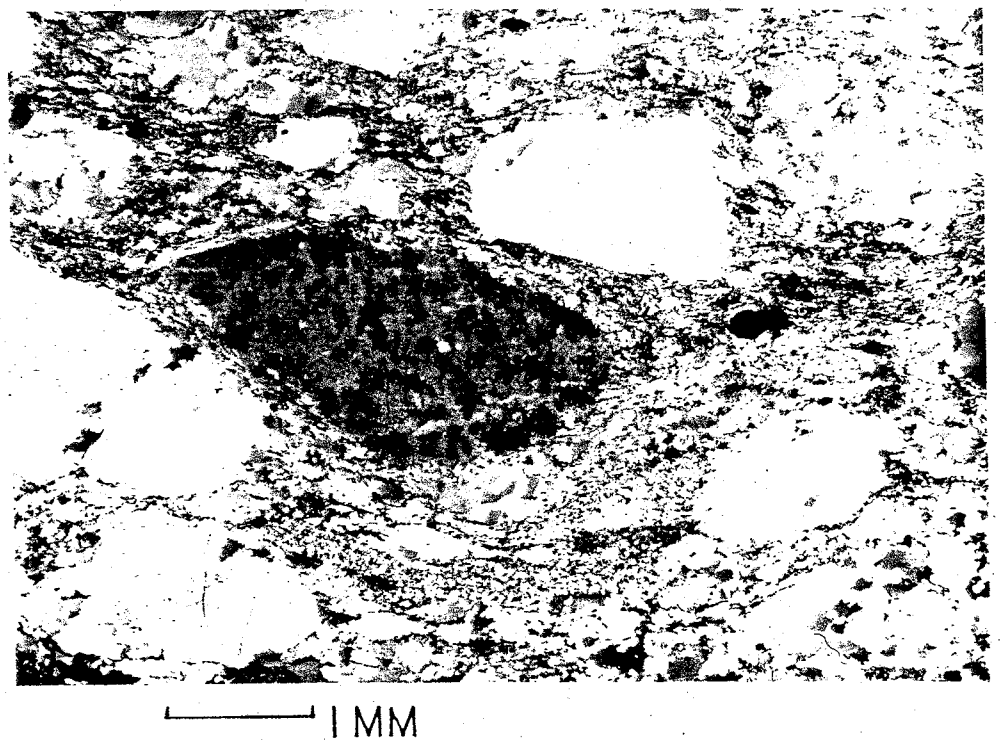

Plate 17. Sub-angular, blocky, fine-sand-sized, detrital plagioclase. Note twinning and alteration. Cross-polar light.

Plate 18. Elongate, rounded, med-sand-sized, detrital potassium-feldspar; note exsolution patterns. Also note fine-sand-sized monocrystalline and polycrystalline quartz grains. Cross-polar light.

Plate 19. Lithic grains, monocrystalline and polycrystalline quartz. Note minute (0.004mm) feldspar crystal in largest lithic grain (above circular shaped bubble), deformation of lithic grain around quartz grains, very fine grain size of lithic grain matrix. Also note well rounded, coarse-sand to fine-sand-sized quartz. Plane-polar light.

Plate 20. Same as Plate 19 except cross-polar light. Note twinning of feldspar phenocryst and of sub-angular, fine-sand-sized plagioclase grains, also monocrystalline and polycrystalline quartz.

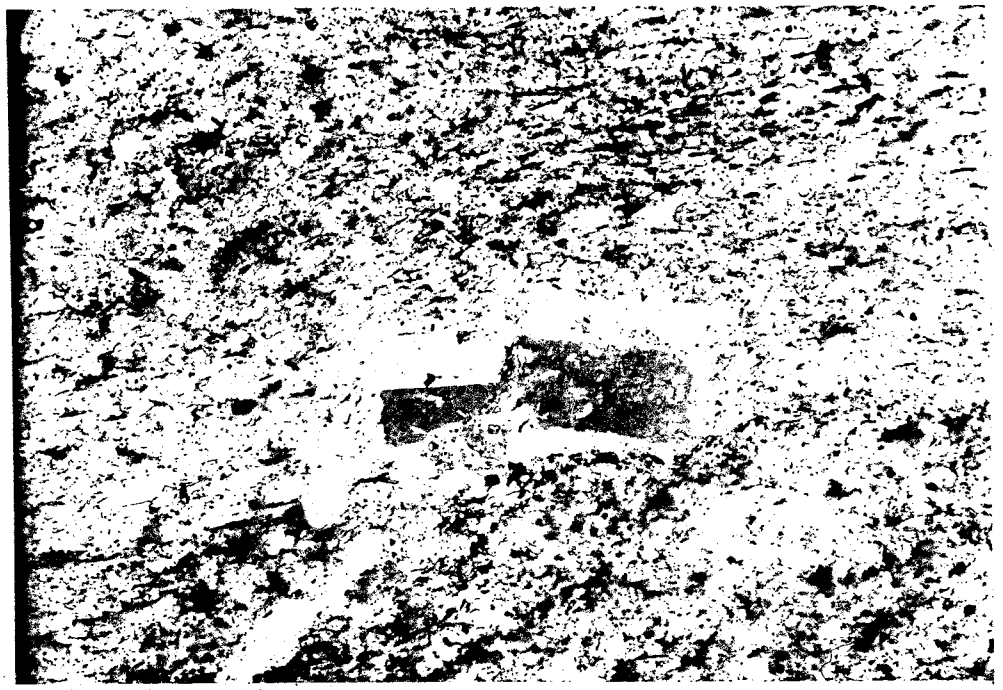

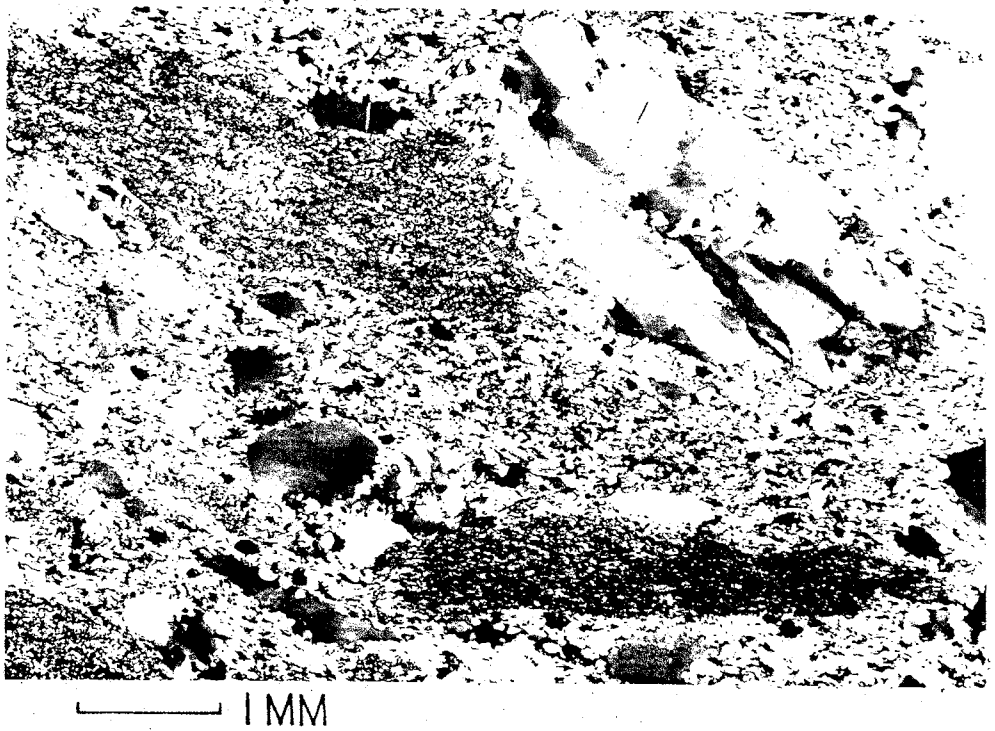

Plate 21. Detail of feldspar phenocryst in large lithic fragment shown in Plates 18 and 19, note twinning, extremely-fine grain matrix. Cross-polar light.

Plate 22. Coarse-sand sized, rounded, elongate, lithic grains showing K-feldspar staining. Note well-rounded, elongate, monocrystalline and polycrystalline quartz. Cross-polar light.

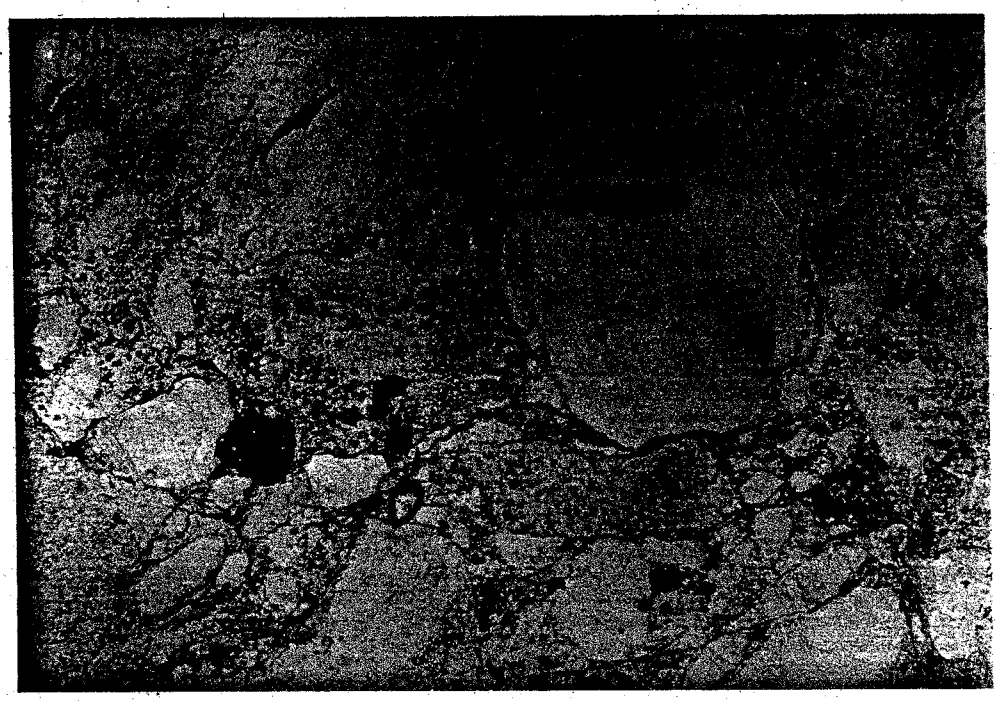

1 MM

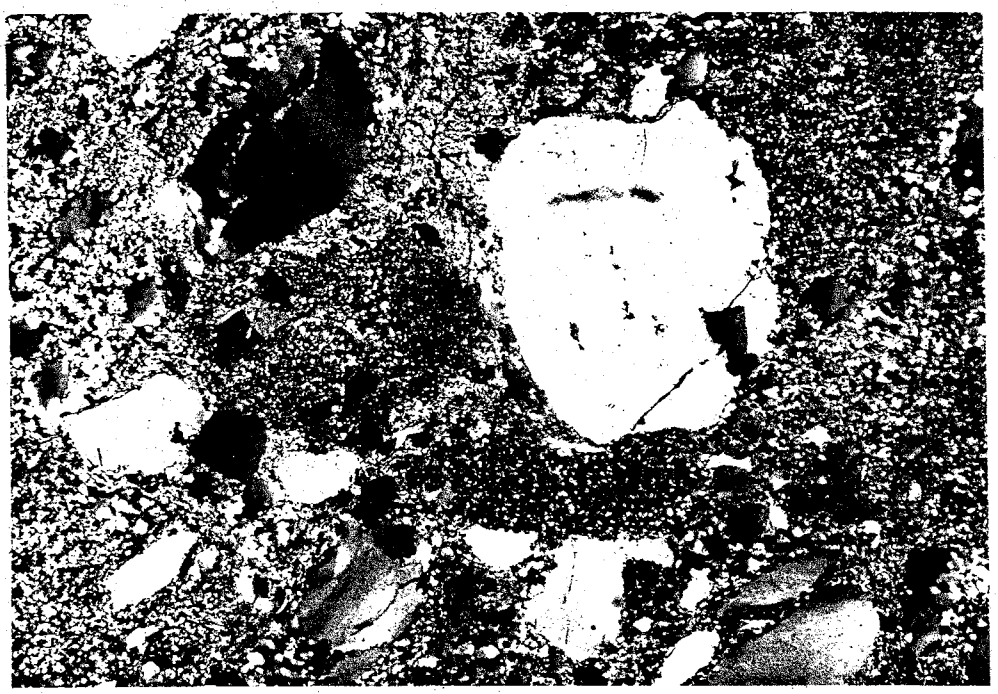

1 MM

Plate 23. Quartzite showing detrital monocrystalline quartz, detrital opaque, lithic grains, and sub-rounded zircon. Note poor sorting, sub-angular to sub-rounded grains, inclusion in largest quartz grain, and definition of lithic fragments in plane-polar light.

Plate 24. Same as 22 except cross-polar light. Note lithic grain enclosing feldspar phenocryst to left of large quartz grain; phenocryst (above rounded opaque) shows twinning. Also note undulose extinction of quartz.

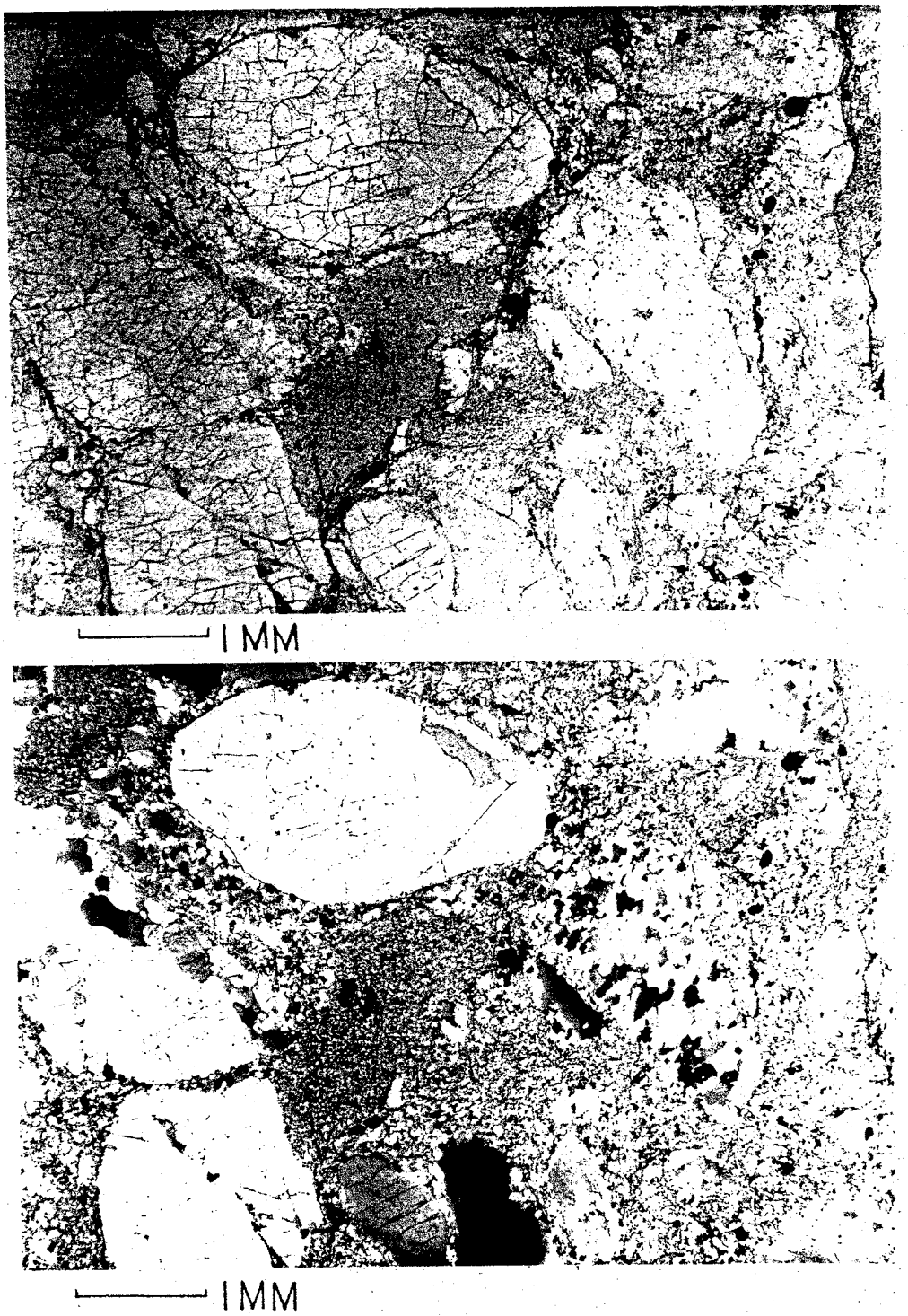

Plate 25. Quartzite shows monocrystalline and polycrystalline quartz, lithic fragments, and untwinned, slightly-altered plagioclase. Quartz is coarse-sand and medium-sand-sized, elongate, well-rounded to sub-angular and shows recrystallization. Lithic grain shows quartz phenocryst. Plagioclase is fine-sand-sized rounded and shows cloudy alteration. Plane-polar light.

Plate 26. Same as Plate 23 except cross-polar light. Note extinction of polycrystalline quartz.

REFERENCES

Abbey, S., 1980, Studies in "Standard Samples" for use in the General Analyses of Silicate Rocks and Minerals Part 6: 1979 Edition of "Usable" Values. Can. Geol. Surv. Pap. 80-14: 1-30.

Bavinton, O. A., and Taylor, S R., 1980, Rare-earth-element geochemistry of Archean metasedimentary rocks from Kambalda, western Australia; Geochemica et Cosmochemica Acta V. 44: 639-648.

Bhatia, M. R. and Taylor, S. R., 1981, Trace-element Geochemistry and Sedimentary Provinces: a Study from the Tasman Geosyncline, Australia. Chem. Geol., 33: 115-125.

Blatt, H., Middleton, G., Murray, R., 1972, Origin of Sedimentary Rocks: Prentice-Hall, Inc., Englewood, N. J.

Bond, G. C. and Devay, J. C., 1980, Pre-upper Devonian quartzose sandstones in the Shoo Fly Formation northern California - petrology, provenance, and implications for regional tectonics, Journal of Geol., 88: 285-308.

Bouma, A. H., 1962, Sedimentology of some flysch deposits. Elsevier, Amsterdam, 168 pp.

Brown, E. H., Babcock, R. S., Clark, M. D., and Livingston,D. E., 1979, Geology of the older Precambrian rocks of the Grand Canyon Part I. Petrology and structure of the Vishnu Complex. Precambrian Research, V. 8, p. 219-241.

Condie, K. C., 1982a, Plate-tectonics Model for Proterozoic Continental Accretion in the Southwestern United States. Geology, 10: 37-42.

----------1982b, Early and Middle Proterozoic Supracrustal Succesions and their Tectonic Settings. American Journal of Science, V.282: 341-357.

Condie, K. C. and Budding, A. J., 1979, Geology and geochemistry of Precambrian rocks, central and south-central New Mexico. New Mexico Bur. of Mines and Mineral Resources, Mem. 35, 58 pp.

Cooper, J. R., and Silver, L. T., 1964, Geology and ore deposits of the Dragoon quadrangle, Cochise County Arizona: U.S. Geol. Survey Prof. Paper 416, 196 p.

Damon, P. E., Livingston, D. E., and Erickson, R. C.,

1962, New K-Ar Dates for the Precambrian of Pinal, Yavapai, and Coconino Counties, Arizona. New Mexico Geological Society Guidebook, 13th Field Conference: 56-57.

Deer, W. A., Howie, R. A., and Zussman, J., 1966, An introduction to the rock forming minerals. Longman Group Ltd., Lond.

Dickinson, W. R. 1974, Plate Tectonics and Sedimentation. In Tectonics and Sedimentation. W. R. Dickinson, Ed. S. E. P. M. Spec. Pub. No. 22: 1-27.

----------1982, Compositions of Sandstones in Circum-Pacific Subduction Complexes and Fore-Arc Basins. The American Association of Petroleum Geologists Bulletin, V.66, No.2: 121-137.

Dickinson, W. R., Beard, L. S., Brakenridge, G. R., Evjavec, J. L., Ferguson, R. C., Inman, K. F., Knepp, R. A., Lindberg, F. A., and Ryberg, P. T., 1983, Provenance of North American Phanerozoic sandstones in relation to tectonic setting, Geo. Soc. Am. Bull., V. 94, p. 222-235.

Dickinson, W. R. and Suczek, C. A., 1979, Plate Tectonics and Sandstone Compositions. A. A. P. G. Bull. 63: 2164- 2182.

Folk, R. L., 1974, Petrology of sedimentary rocks, Hemphill's, Austin, Tx., p. 120-125.

Harrell, J. and Blatt, H., 1978, Polycrystallinity: effect on the durability of detrital quartz. Journal of Sed. Pet., 48: 25-30.

Henry, D. J., 1982, Tourmaline as a petrogenetic indicator in staurolite grade metapellitic rocks. Geo. Soc. Am. Abstracts with Programs, p. 513.

Kroner, A., 1980, Precambrian plate tectonics. In Precambrian Plate Tectonics, Kroner, A., ed., Elsevier Pub. Co., Amsterdam, p.57-90.

Kuenen, Ph. H., 1958, Problems concerning source and transportation of flysch sediments. Geologie en Mijnbouw (n. sr.), 20e Jaarg., p.329-339.

Lanphere, M. A., 1968, Geochronology of the Yavapai Series of central Arizona, Canadian Journal of Earth Sciences, 5: 757-762.

Leyreloup, A., Dupuy, C., and Andriambololona,R., 1977,

Contributions to Mineralogy and Petrology, V.62: 283-300.

Livingston, D. E., and Damon, P. E., 1968, Precambrian ages in central Arizona and northern Sonora. Canadian Journal of Earth Sciences, V. 5: 763-772.

Livingston, D. E., 1969(a), Geochronology of older Precambrian rocks in Gila County, Arizona. Unpublished doctoral dissertation, University of Arizona, Tucson, Arizona: 180-214.

----------1969(b), Chronology and initial strontium isotope ratios of older Precambrian rocks in the Gila County region, Arizona. Geo. Soc. Am. Abstracts with Programs for 1969, Part 7, p. 136.

Martell, C., 1982, Petrology and geochemistry of a progressively metamorphosed sedimentary formation in Big Thompson Canyon, Larimer County, Colorado. Masters thesis, New Mexico Institute of Mining and Technology, Socorro, New Mexico, p. 1-68, fig. 1,6-22.

McLemore, V. T., 1980, Geology of the Precambrian Rocks of the Lemitar Mountains, Socorro County, New Mexico. Masters thesis, New Mexico Institute of Mining and Technology, Socorro, New Mexico, p. 5-26.

McLennan, S. M., Nance, W. B. and Taylor, S. R., 1980, Rare Earth Element-Thorium Correlations in Sedimentary Rocks, and the Composition of the Continental Crust. Geochemica et Cosmochemica Acta 44: 1833-1839.

McLennan, S. M. and Taylor, S. R., 1980, Th and U in Sedimentary Rocks: Crustal Evolution and Sedimentary Recycling. Nature 285: 621-285.

Moore, B. R. and Dennen, W. H., 1970, A geochemical trend in silicon-aluminum-iron ratios and the classification of clastic sediments. Journal of Sedimentary Petrology, V. 40: 1147-1152.

Mutti, E. and Ricci Lucchi, F., 1978, Turbidites of the Northern Apennines: an introduction to facies analysis. International Geology Review, V. 20, No. 2, p. 125-166.

Pettijohn, F. J., 1963, Chemical composition of sandstones - excluding carbonate and volcanic sands. U. S. Geol. Survey Prof. Paper 440-S: S1-S19.

Pettijohn, F.J., Potter, P. E., and Siever, R. A., 1973, Sand and Sandstone. Springer-Verlag, p. 25-67.

149-260.

Peterson, N. P., 1954, Geology of the Globe quadrangle Arizona: U. S. Geol. Survey Quad. Map GQ-41.

---------- 1961, Geology and Ore Deposits, Globe-Miami District, Arizona. Geol. Surv. Prof. Pap. 342: 8-64.

---------- 1963, Geology of the Pinal Ranch Quadrangle, Arizona. Geological Survey Bulletin 1141-H: H1-H18.

Ransome, F. L., 1903, Geology of the Globe copper district, Arizona: U. S. Geol. Survey Geol. Atlas, Folio 111.

---------- 1904, Description of the Globe quadrangle (Arizona): U. S. Geol. Survey Geol. Atlas,

---------- 1919, Copper Deposits of Ray and Miami Arizona. U. S. G. S. P. P. 115: 32-37.

Schmidt, E. A., 1967, Geology of the Mineral Mountain Quadrangle. Unpublished Masters Thesis, University of Arizona, Tucson, Arizona: 7-84.

Schwab, F. L., 1975, Framework Mineralogy and Chemical Composition of Continental Margin Type Sandstone. Geology, V. 3: 487-490.

Shanmugam, G. and Moiola, R. J., 1982, Eustatic control of turbidites. Geology, V.10, p. 231-235.

Silver, L. T., 1978, Precambrian Formations and Precambrian History in Cochise County, Southeastern Arizona. New Mexico Geological Society Guidebook, 29th Field Conference, Land of Cochise, p. 157-163.

Silver, L. T., Anderson, C. A., Crittenden, M., Robertson, J. M., 1977, Chronostratigraphic elements of the Precambrian rocks of the southwestern and far western United States. Geo. Soc. Am. Abstracts with Programs, p. 1176.

Steiger, R. H. and Jager, E., 1977, Subcommision on Geochronology: convention on the use of decay constants in geo- and cosmochemistry. Earth and Planetary Science Letters, V.36, p. 359-362.

Taylor, S. R. and McLennan, S. M., 1980. The rare element evidence in Precambrian sedimentary rocks: implications for crustal evolution. In Precambrian

Plate Tectonics, Kroner, A., ed., Elsevier Pub. Co., Amsterdam, p. 527-548.

APPENDIX A
COLLECTION AND PREPARATION OF SAMPLES

Collection of samples

The nighest priority in the field was to obtain good samples for geochemical and petrological analyses and to sample a representative population of the rock in any particular area. Representative samples of exceptionaly different character were also collected. Samples collected were fresn in appearance and free of viens and alteration. Areas of outcrop that showed extremes of veining, alteration, and ore-type mineralization were not sampled except where warranted due to exceptional character.

Particular attention was paid to indications of relict sedimentary features such as crossbedding, graded beds, turbidite-like bed sequences, flute-casts, etc.

Sample preparation

Selected samples were reduced to powder by standard methods using a jaw-crusher, rotary-mill, vibratory splitter, ceramic hand mortar, and an automatic agate mortar and pestle. The agate grinder was used to avoid tungsten contamination from the tungsten-carbide high-speed grinder which had been in use previously. From 10 to 40 grams of fine powder of each sample were produced in this manner. Up to this point preparation for neutron activation and X-ray fluorescence were identical and simultaneous. Larger portions of coarser grain samples were used to assure correct average composition.

APPENDIX B

Neutron Activation Analyses

Samples were analyzed by neutron activation according to the parameters given in Table 6. Polyethelene vials were loaded with 0.5 gram amounts of each sampled and sealed. At the same time, 0.5 gram portions of three interlab standard rock sample powders placed in vials following the same procedures. Oxide and trace element concentrations used for the standards are given in Table 7. The samples were shipped to the Sandia Laboratory nuclear reactor where they were irradiated with thermal neutrons.

During analyses samples were placed in an apparatus which held them steady and with less than 1% deviation from sample to sample. Powder that showed a tendency to stick to the sides of the polyethelene vials was tamped down by tapping the bottom of each vial several times. The analyzing crystal was lithium-doped germanium (Ge(Li)), cooled by liquid nitrogen. Output from the crystal was digitized and stored on magnetic discs. The computer setup used to control data input, storage, retrieval, and analyses was the ND-6600 system supplied with software by Nuclear Data Inc. Data analyses was facilitated by use of a CRT display that allowed the analyst to examine and manipulate parameters for determination of peak-areas, and thus ensure the most accurate analyses possible.

APPENDIX C

X-ray fluorescence analyses

Analyses by X-ray fluorescence was performed to obtain major-element data and some trace elements that were at the time difficult or unreliable to obtain using NAA methods. Two separate analyses were done to obtain major and trace elements by XRF. Major elements were analyzed in the form of fused disks, while trace elements were analyzed as pressed-powder pellets.

Fused disks for major element analyses were made by fusing a measured quantity of powdered rock with a flux to make an X-ray opaque glass disk containing a dilute solid solution of sample. The flux used was Spectroflux which is a powdered lithium-borate glass. The sample and powder were measured to within 0.0001 gram tolerance, quantities were recored and corrected, and the samples were fused. The samples were fused in a platinum crucible with a platinum lid at approximately 900 degrees centigrade for five to fifteen minutes. Disks were formed and quenched to glass by pressing in a preheated mechanically linked platten and mold.

Major elements analyzed included Si, Al, Fe, Mg, Ca, Na, K, Ti, Mn, and P. Analyses was performed on a Rigaku XRF spectrometer using computer control. A program based on silicate analyses by Norrish and Hutton was used to convert the raw counting data to a form giving oxide precents of the elements. Concentrations of minor elements used are given in Table 7 (Abbey, 1980). Trace elements analyzed were Rb, Sr, Y, Zr, Ni. Analytical conditions for major and minor elements are given in Table 8.

APPENDIX D

Modal Analyses

Modal analyses of selected thin sections was performed. Categories were established for point counting using Dickinson and Suczek's (1980) detrital mode categories as a basis (Table 5) . Detrital grains larger than 00.05 mm in diameter were counted using a standard point counting stage and counter. Six basic categories of detrital grains were counted, and seven other categories were counted as well.

Method

Point counts were done with a microscope equipped with a point counting stage and register. Results are tabulated according to several categories (TABLE 1). Counts were made of detrital grains in the following categories:

Qm: monocrystalline quartz grains.

Qp:polycrystalline quartz grains of quartz-arenite, quartzite, and chert.

;Ls: lithic grains of sedimentary or metasedimentary origin excluding quartzite and chert.

Lv: lithic grains of volcanic origin.

K: potassium feldspar grains.

P: plagioclase feldspar grains.

Counts are also kept of the following non-Dickinson and Suczek categories:

Ma: matrix of primarily quartzo-feldspathic character.

Sr: matrix of primarily sericitic character.

Ch: chlorite in the matrix

Bi: biotite in the matrix

Op: opaque grains and matrix.

Ep: epidote as grains and matrix.

Zr: zircon grains

Tr: tourmaline grains

Interpretation of the nature of individual grains is difficult. One inherent difficulty is distinguishing certain grain categories (e. g., chert from fine-grained volcanics) that often resemble each other very closely but must be classed within different categories in the Dickinson and Suczek system. Another is the fact that most grains have been subjected to a certain amount of recrystallization. In some cases, recrystallization has progressed so far that grain boundaries are all but indistinguishable from matrix. In fact, some grains grade into matrix with no obvious boundary at all. In most cases, grain boundaries were best defined using plane-polar light and low magnification.

All quartz grains that were one continuous crystal were counted as monocrystalline quartz (Qm). In some cases, single - crystalline quartz grains have inclusions of muscovite and feldspar. These grains were counted in their entirety as monocrystalline. All quartz grains made up of more than one quartz crystal are counted as polycrystalline quartz (Qp). This includes polycrystalline quartz of igneous origin, metamorphic origin, sedimentary-quartzite grains, and chert. Potassium and plagioclase feldspars were distinguished from each other by staining, twinning, and alteration. Quartz was distinguished from feldspar by optical methods. Lithic grains were divided into two categories, lithic-volcanic (Lv) and lithic-sedimentary (Ls). Lithic-volcanic grains are distinguished by fine grain quartzo-feldspathic crystal matrix, prolate shape, and presence of quartz and feldspar phenocrysts. The lithic-sedimentary category includes all fine-grained sedimentary and metasedimentary rocks. These were not found in the Pinal Schist.

To date, no completely reliable system for resolving the problem of distinguishing various grain types has been developed. For this reason, there is a certain amount of uncertainty associated with results from the point counting process. Certain grains posed more problems than others, particularly those with poorly defined boundaries and those that resembled both chert and lithic material. Probably no more than 70 percent of these problem grains were identified correctly; however, most grains were not so difficult to distinguish. Uncertainty varies for each point-counted slide. Some sections showed few apparent effects of metamorphic deformation, while others showed more pronounced effects. In most cases, sections which that showed severe deformation were omitted from the point-counting process; however, slides showing moderate deformation were used. The overall uncertainty in distinguishing grains from matrix may be as great as 2 or 3 counts out of 100 in the less deformed rocks, and as great as 4 to 6 counts out of 100 in the more deformed rocks. Difficulty in categorizing lithic grain

types, especially chert vs. fine-grained lithics, was greater in the more deformed rocks and especially so in finer grained rocks. Uncertainty in categorizing lithic grain types may be as high as 10 or 15 per 100 lithic grain counts. Certain diagrams are less sensitive than others to the effects of counting uncertainty.

Evaluation of tectonic provenance by modal analyses

The Dickinson and Suczek (1980) technique is to divide framework grain types into categories which are plotted against each other on triangular diagrams. The groupings grain types fall into when they are plotted form characteristic patterns. These diagrams allow tectonic setting to be distinguished with consistency for modern sediments. The grain types and the different groupings used appear in Table (5).

Some of the provenance diagrams of Dickinson (1983) and Dickinson and Suczek (1980) nullify the effects of possible misidentification as discussed above. Of the four diagrams, QpLvLs is the most suspect because lithic grains are the hardest to classify. The plot of QmPK should be fairly reliable except for the effects of preferential feldspar destruction and the inconsistent staining of thin sections. QFL resolves the problem of distinguishing Lv grains from Ls grains, but combines Qm grains with Qp grains, which allows confusion between chert (Qp) and fine-grained felsic volcanics (Lv). Only QmFLt resolves the problems of feldspar (F = P + K), lithic origin (L = Lv + Ls), and chert vs. felsic lithic volcanics (Lt = L + Qp).

In addition, modal analyses data was used to assign sedimentary-rock names to the various rock types. By plotting framework-grain frequencies against the proportion of matrix in each rock, sedimentary rock names were assigned to the rocks. In addition, sandstone classification schemes using detrital-framework grain modes were used.

Sedimentary rock classification

The sedimentary rock classification scheme used is after Pettijohn, et al., (1973). Detrital framework grains and matrix content assign sedimentary names to rocks. In this scheme Q is all monocrystalline and polycrystalline quartz grains, F is all feldspar, and R is all lithic fragments. These three are plotted at the points of a triangular diagram. The diagram is extended in three dimensions to include matrix content as a fourth component (Figure 7a). From 0 to 15 percent matrix, all rocks are classified as sandstones or arenites. From 15 to 70 percent matrix, all rocks are classified as wacke-stones, and from 70 to 100 percent matrix, all rocks are classified as

pelite.

To use this scheme, Qm is added to Qp to get Q, K is added to P to get F, and Lv is added to Ls to get R. Q, F, and R represent the total framework detrital grains. Ma, Sr, Ch, Bi, Op, and Ep are added to get total matrix. Percentages of framework grains are then plotted by projection onto triangular diagrams at particular percentages of matrix. Samples witnin +/- 5 percent matrix are plotted by projection onto plots at 45 percent (Figure 8(b)), 55 percent (Figure 8(c)), 65 percent (Figure 8(d)), 75 percent (Figure 8(e)), and 85 percent matrix (Figure 8(f)).

Sandstone classification

Folk (1974) plots total quartz (monocrystalline quartz plus polycrystalline quartz minus chert) against feldspar (plagioclase plus k-spar plus gneiss and granite) against rock fragments (volcanic lithics plus sedimentary lithics plus chert). Note that this is essentially identical to Dickinson and Suczek's QFL diagram, since identifiable chert in the Pinal Schist is minimal.

APPENDIX E
Brief Petrographic Descriptions of the Analysed Samples

PS-3 Schist. Dark-gray, fine-grained rock with two foliations. Graded beds 45cm to 80cm thick fine toward SE, possible relict crossbedding and scour marks. Relict sand grains are poorly-sorted, fine to medium sand-sized, rounded, sub-spherical quartz.

PS-10 Schist. Light-gray, medium-grained rock, which is foliated, lineated, and massive (no grading). Relict sand grains are poorly-sorted, medium sand-sized, sub-rounded, elliptical quartz.

PS-17 Schist. Medium-gray, coarse-grained rock, which is foliated and massive. Relict sand grains are poorly-sorted, medium to coarse sand-sized, medium-rounded, and elliptical. Rock is composed of quartz sand (35%), lithic sand (1.4%), feldspar sand (0.4%), and has a fine grain matrix of quartz and feldspar (50%), sericite (6.8%), biotite (5.1%), and epidote (1.0%), tourmaline and zircon are present as trace minerals (<1%).

PS-19 Schist. Light-brown-gray, coarse to fine-grained rock which is foliated and shows grading cycles, fining from coarse to fine sand towards SE. Apparent relict crossbedding in fine-sand near tops of beds. Relict sand grains are poorly-sorted, coarse to fine sand-sized, sub-rounded to sub-angular, and elliptical to sub-spherical. Rock is composed of quartz sand (31.4%), lithic sand (1.2%), feldspar sand (3.0%), and has a fine grain matrix of quartz and feldspar (54%), sericite (6.4%0, biotite (3.2%), opaque minerals (2.6%), and epidote (1.2%), zircon occurs as a trace mineral (<1%), and there is possible detrital epidote.

PS-24 Schist. Blue-gray, poorly-foliated, fine to coarse-grained rock, which is a 2m thick graded bed, grading coarse to fine towards NW. Relict sand is very pooly-sorted, coarse to fine-sand sized, sub-rounded, and elliptical to sub-spherical.

PS-26 Schist. Pale-gray, coarse-grained rock which is foliated and massive. Relict sand is poorly-sorted, very coarse sand-sized, sub-angular, and sub-spherical. Blue quartz, white chert, feldspar, and fine-grained lithic fragments visible in hand sample. Erosive contact with much finer grain layer indicates up is toward SE. Rock is composed of quartz sand (57.5%), lithic sand (3.9%), feldspar sand (1.0%), and fine-grained matrix of quartz (21.5%), sericite (3.7%), chlorite (<1%), opaques (<1%), and epidote (<1%).

PS-28 Schist. Blue-gray, coarse-grained rock which is foliated and graded. Grading is coarse to fine-sand fining towards NW. Relict sand is very poorly-sorted, medium to coarse sand-sized, sub-angular to sub-rounded, and elliptical to sub-spherical. Rock is composed of quartz sand (38.1%), lithic sand (7.7%), feldspar sand (<1%), and fine-grained matrix of quartz (44.4%), sericite (9.4%), biotite (2.9%), opaques (2.6%), and epidote (1.1%), tourmaline and zircon occur as trace minerals.

PS-31 Schist. Dark-gray, coarse-grained, rock which is layered, foliated, and graded. Grading is medium to fine-grain fining toward SE. Relict sand is very poorly-sorted, medium to fine sand-sized, rounded, and spherical. Fine- grained upper layer is graded fine-sand to coarse-silt and shows laminations 1-2cm thick. There is secondary foliation in the upper layer at an angle to primary bedding and foliation which resembles crossbedding. This rock assemblage appears to represent a well-preserved turbidite bed. Rock sample is quartz sand (42.6%), lithic sand (<1%), and fine-grained matrix of quartz (42.7%), sericite (6.4%), biotite (6.4%), opaques (1.7%), epidote (<1%), and traces of tourmaline.

PS-32 Schist. Pale-gray, medium-grained rock which is poorly-foliated and graded. Grading is medium to fine-grain fining toward SE. There is possible relict crossbedding in finest layers. Relict sand is poorly-sorted, medium to fine sand-sized, rounded, and elliptical. Both blue quartz and chert are visible in hand sample.

PS-40 Schist. Mottled pale-gray, medium-grained rock which is massive and foliated. Relict sand is poorly-sorted, medium to fine sand-sized, sub-rounded, sub-spherical. Detrital tourmaline is present. Rock is composed of quartz sand (35.0%), lithic sand (2.6%), feldspar sand (<1%), and fine grain matrix of quartz (54.4%), sericite (3.5%), biotite (3.7%), opaques (1.9%), and epidote (<1%), and traces of zircon.

PS-44 Schist. Pale-yellowish-gray, coarse-grained rock which is non-foliated and graded. Grading is coarse to fine-grain finning towards NW. Relict sand grains are poorly-sorted, coarse to medium sand-sized, well-rounded, and sub-spherical. Rock is composed of quartz sand (45.6%), lithic sand (2.1%), feldspar sand (1.0%), and fine-grain matrix of quartz (41.2%), sericite (4.9%), chlorite (1.6%), opaques (2.5%), and epidote (2.0%), and traces of tourmaline.

PS-50 Schist. Pale blue-gray, fine grained rock which is foliated and massive. Relict sand grains are poorly sorted, coarse to medium sand-sized, rounded, and elliptical. Rock

is composed of quartz sand (36.7%), feldspar sand (<1%), and fine-grain matrix of quartz (48.6%), sericite (9.2%), biotite (1.7%), opaques (1.5%), and epidote (1.9%), with traces of tourmaline.

PS-54 Hornfels-schist. Mottled blue-gray, fine-grained rock which is foliated and massive. extensive quartz banding and veining in outcrop. Relict sand grains obliterated by recrystallization. rock is composed of idiomorphic quartz, muscovite, and biotite, with traces of tourmaline.

PS-69A Schist. Pale-gray, medium-grained rock which is foliated and graded. Grading is medium to fine-grain fining towards NW. Relict sand grains are medium to fine sand-sized, poorly-sorted, sub-rounded, sub-spherical. appears to represent bottom (Tb) layer of well preserved turbidite bed of which PS-69 represents the top layer. Rock is composed of quartz sand (33.6%), lithic sand (<1%), feldspar sand (1.1%), and fine-grain matrix of quartz (49.3%), sericite (7.4%), chlorite (4.0%), opaques (3.3%), and epidote (1.5%), with traces of zircon.

PS-69 Phyllite. Pale greenish-gray, very-fine-grained rock which is strongly foliated, is lineated, and has vien quartz. No relict sand. Appears to show relict crossbedding. Probably represents uppermost layer of a turbidite bed (E or D).

PS-70 Schist. Pale-gray, medium-grained rock which is pooly-foliated and shows grading. Grading is medium to fine-grain fining towards NW. Relict sand grains are coarse to medium sand sized, poorly-sorted, sub-rounded, and sub-spherical. Rock is composed of quartz sand (XX%), lithic sand (<1%), feldspar sand (<1%), and fine grained matrix of quartz (XX%), sericite (XX%), chlorite (2.7%), opaques (1.5%), and epidote (1.7%).

PS-77 Schist. Pale-gray, coarse-grained rock which is a non-foliated, 2m thick, massive layer. Relict sand grains are coarse to fine sand sized, very poorly-sorted (bi-modal), sub-rounded, and sub-spherical.

PS-78 Sericite-schist. Gray, fine-grained rock which is poorly-foliated and massive. Relict sand grains are not present.

PS-80 Schist. Pale-gray, medium-grained rock which is foliated and massive. Relict sand grains are poorly-sorted, medium to fine sand-sized, sub-angular, and sub-spherical. Rock is composed of quartz sand (26.2%), feldspar sand (2.1%), and fine-grain matrix of quartz (37.6%), sericite (15.3%), chlorite (<1%), opaques (2.8%), and epidote (2.3%), with traces of tourmaline.

PS-83 Schist. Pale-gray, medium-grained, rock which is foliated and massive. Relict sand grains are poorly-sorted, medium to fine sand-sized, sub-rounded, and sub-spherical.

PS-87 Schist. Pale-gray, medium-grained rock which is poorly-foliated and shows grading and lamination. Grading is coarse to fine-grain fining towards NW. Relict sand grains are poorly-sorted, coarse to fine sand-sized, sub-rounded, and sub-spherical. Rock is composed of quartz sand (22.5%), lithic sand (<1%), feldspar sand (1.7%), and fine-grain matrix of quartz (58.6%), sericite (11.6%), chlorite (1.1%), opaques (2.0%), and epidote (2.0%), with traces of tourmaline and zircon.

PS-90 Quartzite. Gray, very coarse-grained rock which is non-foliated, is lineated by elongate grains, and graded. Grading is granule-gravel to coarse sand-sized fining towards NW. Relict detrital grains are medium-well sorted, granule to coarse sand-sized, well-rounded, strongly prolate with sub-spherical cross-sections. Quartz, lithics, and feldspar all visible in hand sample. Bed is 2.5m thick, pinches laterally over 10-22m. Rock is composed of quartz sand and gravel (52.1%), lithic sand and gravel (8.4%), feldspar sand (1.7%), and fine-grain matrix of quartz (28.6%), sericite (2.9%), chlorite (<1%), opaques (<1%), and traces of epidote, tourmaline, and zircon.

PS-92 Schist. Gray, medium-grained, rock which is poorly-foliated and massive. relict sand grains are poorly-sorted, coarse to fine sand-sized, sub-rounded, sub-spherical. Rock is composed of quartz sand (32.8%), lithic sand (<1%), feldspar sand (1.4%), and fine-grain matrix of quartz (49.3%), sericite (17.3%), chlorite (3.3%), opaques (2.0%), epidote (3.1%), and traces of tourmaline.

PS-96A Schist. Light-gray, fine-grained rock which is laminated, foliated, and graded. Grading is fine to very-fine sand-size fining towards NW. Laminations are 0.5-1cm. Layer is 10cm thick, snows relict crossbedding and appears to represent middle or upper layer of a turbidite bed (PS-96). Relict sand is well-sorted, fine to coarse silt-sized, rounded, and spherical. Rock is composed of quartz sand (17.8%), feldspar sand (<1%), and fine-grain matrix of quartz (50.2%), sericite (28.4%), biotite (1.8%), opaques (2.4%), and traces of epidote.

PS-96 Quartzite. Pale pinkish-gray, very coarse-grained rock which is non-foliated, lineated by elongated grains, and shows grading. Distinct coarse to fine grading cycles, 1-2.5m thick repeat, fining towards Nw. Cycles consist of massive lower beds, graded middle beds, and laminated or crossbedded upper layers (PS-96A). Lineation strongly suggests relict crossbedding of lower graded layers. These

cycles appear to represent well preserved turbidite beds. Relict sand grains are granule to medium sand-sized, poorly sorted, sub-angular to sub-rounded, prolate with sup-spherical cross-sections. Rock is composed of quartz sand (62.1%), lithic sand (9.9%), feldspar sand (3.4%), and fine grain matrix of quartz (22.2%), sericite (7.0%), opaques (<1%), and traces of epidote and zircon.

PS-97 Schist. Blue-gray, coarse-grained rock which is poorly-foliated and graded. Grading is coarse to medium-grain, fining towards NW. Relict sand grains are poorly sorted, medium to coarse sand-sized, sub-angular to sub-rounded, and sub-spherical. Rock is composed of quartz sand (48.1%), lithic sand (<1%), feldspar sand (1.2%), and fine-grain matrix of quartz (40.1%), sericite (5.5%), chlorite (1.6%), opaques (1.5%), epidote (<1%), and traces of tourmaline and zircon.

PS-100 Schist. Gray, medium-grained rock which is foliated and graded. grading is medium to fine-grain, fining towards NW. Relict sand grains are medium-sorted, well-rounded, and spherical. Rock is composed of quartz sand (20.0%), lithic sand (<1%), feldspar sand (2.2%), and fine-grain matrix of quartz (66.2%), sericite (7.7%), chlorite (3.0%), opaques (1.4%), and epidote (<1%), and traces of tourmaline.

PS-102 Quartzite. Gray, very coarse-grained rock which is foliated and graded. Grading is from granule to fine sand-size, fining towards SE. Relict detrital grains are poorly sorted, granule to fine sand-sized, sub-rounded, and sub-spherical. rock is composed of quartz sand (60.7%), lithic sand (<1%), feldspar sand (2.2%), and fine-grain matrix of quartz (39.7%), sericite (4.4%), chlorite (<1%), opaques (<1%), epidote (<1%), and traces of tourmaline, zircon, and garnet.

PS-101 Phyllite. Blue-gray, very fine-grained rock which is well-foliated, laminated, and lineated by kink-fold axes. Relict detrital grains are well sorted, very-fine sand-sized to silt-sized, rounded, elliptical.

PS-105 Schist. Medium-gray, fine-grained rock which is foliated and massive. Relict sand grains are poorly-sorted, medium to fine sand-sized, sub-angular to sub-rounded, and sub-spherical.

PS-112Schist. Blue-gray, medium-grained rock which is foliated and graded. grading is coarse to medium-grain, fining towards NW. Relict sand grains are poorly-sorted, coarse to fine sand-sized, rounded, elliptical.

PS-117 Schist. Pale-gray, coarse-grained rock which is poorly-foliated and massive. Relict sand grains are very

poorly-sorted, well-rounded, and elliptical to spherical.

PS-118 Phyllite. Gray, very fine-grained rock which is foliated, massive, and laminated. Laminations are 5-15mm. Relict detrital grains are well-sorted, silt-sized, rounded, and elliptical to sub-spherical. Rock is composed of quartz silt (7.4%), lithic silt (<1%), feldspar silt (<1%), and very fine-grained matrix of quartz (61.4%), sericite (29.6%), biotite (1.0%), opaques (<1%), and epidote (>1%).

PS-122 Phyllite. Gray, fine grained rock which is well-foliated, massive and laminated. Laminations are 5-15mm. Relict detrital grains are poorly sorted, fine-sand to silt-sized, sub-rounded, and elliptical to sub-spherical.

PS-124 Tonalitic schist. White to pale-green with pink spots, coarse-grained rock which is foliated and massive. Relict phenocrysts of plagioclase (~25%, An 22) and quartz (~25%) are present, with oblate clots of chlorite (~10%) and epidote (~10%), in a fine-grained groundmass of quartz (~10%), sericite (~10%), opaques(~5%), and carbonate (~5%), with traces of allanite.

This thesis is accepted on behalf of the faculty of the Institute by the following committee:

Adviser

Date